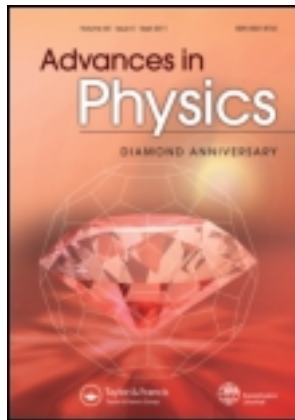


This article was downloaded by: [Cornell University]

On: 08 June 2012, At: 02:47

Publisher: Taylor & Francis

Informa Ltd Registered in England and Wales Registered Number: 1072954 Registered office: Mortimer House, 37-41 Mortimer Street, London W1T 3JH, UK



Advances in Physics

Publication details, including instructions for authors and subscription information:

<http://www.tandfonline.com/loi/tadp20>

The Fermi gas model of one-dimensional conductors

J. Sólyom ^a

^a Central Research Institute for Physics, H-1525, Budapest, P.O. Box 49, Hungary

Available online: 28 Jul 2006

To cite this article: J. Sólyom (1979): The Fermi gas model of one-dimensional conductors, *Advances in Physics*, 28:2, 201-303

To link to this article: <http://dx.doi.org/10.1080/00018737900101375>

PLEASE SCROLL DOWN FOR ARTICLE

Full terms and conditions of use: <http://www.tandfonline.com/page/terms-and-conditions>

This article may be used for research, teaching, and private study purposes. Any substantial or systematic reproduction, redistribution, reselling, loan, sub-licensing, systematic supply, or distribution in any form to anyone is expressly forbidden.

The publisher does not give any warranty express or implied or make any representation that the contents will be complete or accurate or up to date. The accuracy of any instructions, formulae, and drug doses should be independently verified with primary sources. The publisher shall not be liable for any loss, actions, claims, proceedings, demand, or costs or damages whatsoever or howsoever caused arising directly or indirectly in connection with or arising out of the use of this material.

The Fermi gas model of one-dimensional conductors

By J. SÓLYOM

Central Research Institute for Physics,
H-1525 Budapest, P.O. Box 49, Hungary

[Received 5 September 1978]

ABSTRACT

The Fermi gas model of one-dimensional conductors is reviewed. The exact solutions known for particular values of the coupling constants in a single chain problem (Tomonaga model, Luther-Emery model) are discussed. Renormalization group arguments are used to extend these solutions to arbitrary values of the couplings. The instabilities and possible ground states are studied by investigating the behaviour of the response functions. The relationship between this model and others is discussed and is used to obtain further information about the behaviour of the system. The model is generalized to a set of coupled chains to describe quasi-one-dimensional systems. The crossover from one-dimensional to three-dimensional behaviour and the type of ordering are discussed.

CONTENTS

	PAGE
§ 1. INTRODUCTION	202
§ 2. THE MODEL.	204
§ 3. PERTURBATIONAL TREATMENT OF THE MODEL.	208
§ 4. RENORMALIZATION GROUP TREATMENT.	211
4.1. Poor man's scaling.	212
4.2. Multiplicative renormalization generated by cut-off scaling.	214
4.3. Determination of the response functions.	222
§ 5. EXACT SOLUTION OF THE TOMONAGA-LUTTINGER MODEL.	226
5.1. Green's function in the Tomonaga-Luttinger model.	227
5.2. Response functions of the Tomonaga-Luttinger model.	231
5.3. Boson representation of the Tomonaga-Luttinger Hamiltonian.	236
§ 6. THE LUTHER-EMERY SOLUTION OF THE BACKWARD SCATTERING PROBLEM.	240
6.1. Calculation of the energy spectrum on the Luther-Emery line.	240
6.2. Response functions of the Luther-Emery model.	244
§ 7. SCALING TO THE EXACTLY SOLUBLE MODELS.	247
§ 8. PHYSICAL PROPERTIES OF THE MODEL.	251
8.1. Phase diagram of the Fermi gas model.	251
8.2. Uniform susceptibility, compressibility and specific heat.	255
8.3. Temperature dependence of the conductivity.	256
§ 9. DIFFERENT CHOICES OF THE CUT-OFF.	257
9.1. Scaling theories with two cut-offs.	258
9.2. Relationship between the physical cut-offs and the cut-off of the bosonized Hamiltonian.	259
§ 10. SOLUTION OF THE MODEL BELOW THE LUTHER-EMERY LINE.	260
§ 11. RELATIONSHIP BETWEEN THE FERMI GAS MODEL AND OTHER MODELS.	266
11.1. The two-dimensional Coulomb gas.	267
11.2. Spin models.	270
11.3. Field-theoretical models.	277
11.4. The Hubbard model.	279
11.5. Summary of the relationships between the various models.	281

§ 12. SYSTEM OF WEAKLY COUPLED CHAINS.	283
12.1. Chains coupled by inter-chain forward scattering.	286
12.2. Chains coupled by inter-chain backward scattering.	288
12.3. Simultaneous treatment of backward and forward scattering.	293
12.4. Crossover from 1-d to 3-d behaviour.	295
12.5. The effect of inter-chain hopping.	296
12.6. Quasi-1-d fermion model with strong on-site interaction.	298
§ 13. CONCLUDING REMARKS.	299
ACKNOWLEDGMENTS.	300
REFERENCES.	301

§ 1. INTRODUCTION

Chemists have long been aware that many organic crystals are highly anisotropic due to the stacking of the molecules into loosely coupled chains. The anisotropy can be characterized by the ratio of the conductivities measured parallel and perpendicular to the chain direction, which can be as large as 10^3 . Elementary considerations can explain—at least partly—this large value. The building blocks of these crystals are usually large flat molecules lying rather closely to each other in one direction, thus forming chains which are nearly perpendicular to the plane of the molecules. The overlap of the wave-functions in the direction of the chain allows the electrons to move easily along the chains. Since adjacent chains are some distance away, there is less probability of inter-chain hopping, and thus the motion of electrons is almost one-dimensional (1-d).

Physicists realized only relatively recently that these systems have many interesting and unusual properties, which are due to the quasi-one-dimensional (quasi-1-d) nature of these materials. It is well known that the behaviour of 1-d systems differs in many respects from that of 2-d and 3-d systems. By studying the properties of 1-d conductors, it became possible for the first time to observe the peculiar dimensionality effects. During the past few years, two different classes of quasi-1-d material, the mixed-valence complexes and the charge-transfer compounds, have been under intensive experimental investigation. The best-studied example of mixed valence complexes is KCP ($K_2Pt(CN)_4 \cdot Br_{0.3} \cdot 3H_2O$), in which the anisotropically oriented *d* orbitals of Pt represent an easy path for the motion of electrons in the direction of the Pt chains, thus yielding a very large value for the ratio of the conductivities in the parallel and perpendicular directions.

A much richer class is that of the organic charge-transfer compounds. In these materials two different kinds of molecules, donor and acceptor molecules, are stacked separately into donor and acceptor chains. Once the charge transfer has taken place the motion of the electrons is confined almost exclusively to the chains. The richness of this class of material is due to the large number of molecules which can be donors in these compounds. TTF-TCNQ is the most famous member of this group, but there are many other interesting compounds showing widely differing behaviour. Useful reviews of the experimental background can be found in the proceedings of recent conferences (Schuster 1975, Keller 1975, 1977, Pál *et al.* 1977).

The most interesting phenomena which are observed in many of these materials are the high conductivity at high temperatures, the transition to an insulating state at lower temperatures, the formation of charge-density waves with wave-vector

$k=2k_F$ (where k_F is the Fermi momentum) and the appearance of Peierls distortion (Peierls 1955) in the ionic positions. This latter effect and the accompanying phonon softening above the transition temperature are typical 1-d effects in a coupled electron–phonon system. The other phenomena might possibly be understood by neglecting the effect of phonons and studying the electronic processes only. Accordingly, there are essentially two different theoretical approaches to the mathematical description of these systems. In one, the starting Hamiltonian is the Fröhlich Hamiltonian (Fröhlich 1954). The electron–phonon coupling leads to interesting dynamical effects, such as the Kohn anomaly in the phonon dispersion relation and the phonon softening; this problem has a vast literature. In this paper the effect of phonons is not considered; for further references see Rice and Strässler (1973 a, b), Horovitz *et al.* (1974, 1975), Bjeliš *et al.* (1974), Suzumura and Kurihara (1975), Brazovský and Dzyaloshinsky (1976), Barisić (1978) and Lukin (1978).

In the other approach only the electron system is considered, since—as was mentioned—the particular features of the 1-d electron gas themselves explain many properties of 1-d conductors. Even when only the electron system is considered, there are still two different approaches. For a description of systems where the conductivity along the chains is almost metallic, a Fermi gas model can be used. The electron–electron interactions are supposed to be weak, and are taken into account in a consistent but perturbational way. In the other approach, which is more suitable for non-conducting systems, a Hubbard Hamiltonian (Hubbard 1963) with strong intra-atomic correlation is used. These two models can be considered as limiting cases of a general model of interacting electrons written in different representations (momentum or site representation). This paper limits itself to reviewing the results obtained in the past few years for the Fermi gas model; results for the Hubbard model are mentioned only briefly in a comparison of the two models.

The paper is organized as follows. The model for the strictly 1-d case is defined, after which it is shown that this model leads to a logarithmic problem where a perturbational treatment is not sufficient. The subsequent logarithmic corrections can be summed using the renormalization group method. The real merit of the application of the renormalization group is to provide a means of scaling the original problem to other problems which might be simpler to solve. In fact, the Fermi gas model can be solved exactly for particular values of the coupling constants. The exact solution of the Tomonaga model and the Luther–Emery solution of the backward scattering problem are presented. Following this, renormalization and scaling arguments are used to extend these results for arbitrary values of the couplings. Based on this, the possible ground-state configurations are studied and the phase diagram is presented. Further information can be obtained about the behaviour of the system described by this model if its relationship to other models is studied. The 2-d Coulomb plasma, spin models (such as the 1-d $X-Y-Z$ and the 2-d $X-Y$ models) and field theoretical models are among those which are closely related to the Fermi gas model. The results for these models and their relations are also discussed. The choice of cut-off is very important in proving the equivalence of the various models, so the cut-off problem is considered. Finally, the model is generalized to a set of coupled chains to provide a more realistic model for quasi-1-d materials. The effect of inter-chain scattering and hopping in the stabilization of the ordered phase, the type of ordering and the change from 1-d to 3-d behaviour are described. The review concludes by showing the possible application of this model to understand the properties of 1-d conductors.

§ 2. THE MODEL

The Fermi gas model is a model of weakly interacting electrons. Other excitations, such as phonons, and their interactions with the electrons are neglected.

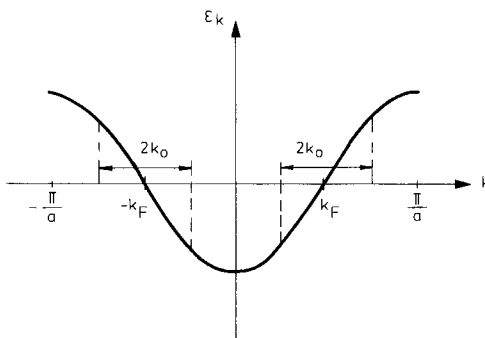
Although it may be thought that the effect of the electron–phonon interaction on the electronic properties can be accounted for by taking an effective electron–electron interaction, this interaction is a retarded one, whereas we will be concerned with a non-retarded interaction.

The unperturbed part of the Hamiltonian is

$$H_0 = \sum_{k, \alpha} \varepsilon_k c_{k\alpha}^+ c_{k\alpha}, \quad (2.1)$$

where $c_{k\alpha}^+(c_{k\alpha})$ is a creation (annihilation) operator of an electron with momentum k and spin α . The kinetic energy of the electrons measured from the Fermi energy is given by ε_k . In the first part of this paper a strictly 1-d model will be considered, in which the electrons can propagate only along the chain. The dispersion relation in a nearly-free-electron or tight-binding approximation is illustrated schematically in fig. 1.

Fig. 1



Dispersion relation of a 1-d electron gas.

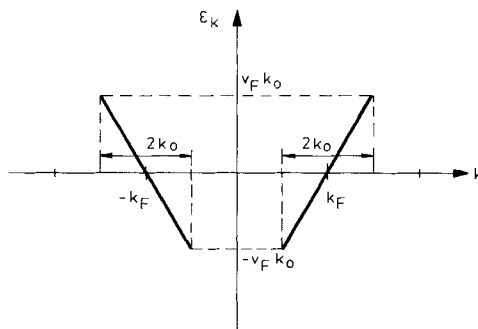
In general, only those electrons lying near the Fermi surface play an important role in physical processes. The Fermi surface of a strictly 1-d metal consists of two points, $+k_F$ and $-k_F$, in the neighbourhood of which the dispersion curve can be approximated by straight lines, giving

$$\varepsilon_k = v_F(|k| - k_F). \quad (2.2)$$

This approximation is a reasonable one in a finite range around the Fermi points. A momentum k_0 is introduced to define the regions $(-k_F - k_0, -k_F + k_0)$ and $(k_F - k_0, k_F + k_0)$. Within these regions the linearized dispersion of eqn. (2.2) will be used, but the states which are further away from the Fermi points will be neglected: therefore k_0 serves as a cut-off for the allowed states, this is called bandwidth cut-off. In this model the bandwidth E_0 is determined by k_0 , according to $E_0 = 2v_F k_0$, and the dispersion relation is as shown in fig. 2.

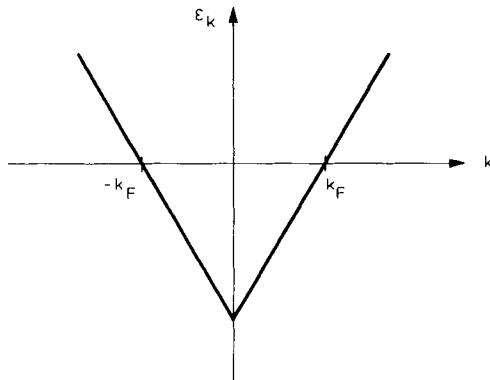
The use of a linear dispersion relation has many calculational advantages. If the states far from the Fermi points do not contribute to the physical properties of the system, a linearized dispersion relation without bandwidth cut-off, such as that

Fig. 2



Dispersion relation of the 1-d Fermi gas model with bandwidth cut-off.

Fig. 3



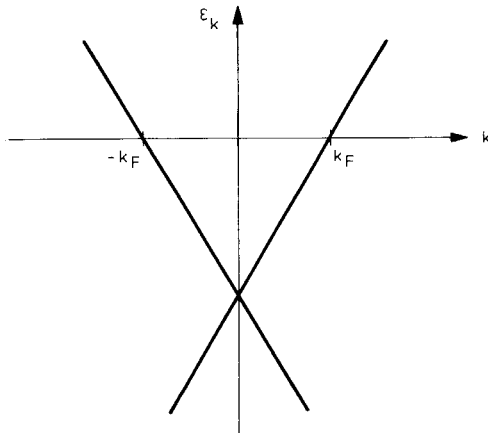
Linearized dispersion relation without bandwidth cut-off.

shown in fig. 3, could be used. However, it is shown later that the introduction of a cut-off is always necessary to avoid unphysical singularities, although it may be different from the bandwidth cut-off. In some cases it is possible to use the whole linearized dispersion curve and to assume a cut-off for the momentum transferred in a scattering process. The difference between the two cut-off procedures will be discussed later in this section and in § 9.

A mathematically more rigorous treatment of the model is possible if the two branches of the dispersion curve do not terminate at $k=0$, and extend instead from $-\infty$ to $+\infty$, as shown in fig. 4. This is the dispersion relation of the Luttinger model (Luttinger 1963). The newly introduced non-physical states do not modify the physical results, at least not if the interaction is not very strong, but they do make the mathematical treatment easier. Most of the considerations in the present paper are limited to the model with bandwidth cut-off, but at some points the other models are also considered.

In any case there are two well-defined branches of the dispersion relation. The operators for the electrons belonging to the branch containing the Fermi point

Fig. 4



Dispersion relation of the Luttinger model.

$+k_F$ ($-k_F$) are denoted by $a_{k\alpha}^+$ and $a_{k\alpha}$ ($b_{k\alpha}^+$ and $b_{k\alpha}$). In terms of these operators, the free Hamiltonian is given by

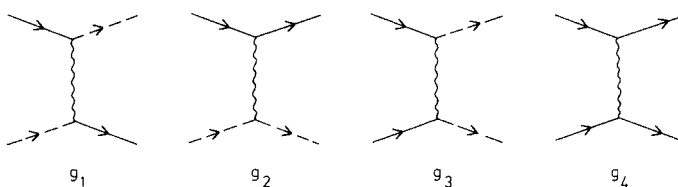
$$H_0 = \sum_{k,\alpha} v_F(k - k_F) a_{k\alpha}^+ a_{k\alpha} + \sum_{k,\alpha} v_F(-k - k_F) b_{k\alpha}^+ b_{k\alpha}. \quad (2.3)$$

The interaction processes can be conveniently classified into the four different types shown in fig. 5. The electrons belonging to the two branches are distinguished by solid and dashed lines. The scattering process with coupling strength g_1 corresponds to backward scattering of electrons, the momentum transfer of which is of the order of $2k_F$. The processes with coupling strengths g_2 and g_4 are forward-scattering terms, and the associated momentum transfer is small. In the g_2 process the two branches are coupled, but in the g_4 process all four participating electrons are from the same branch. The g_3 process is an Umklapp process whose contribution is important only if the band is half-filled, in which case $4k_F$ is equal to a reciprocal lattice vector and all four electrons can be near the Fermi surface.

In all these processes a spin dependence can be introduced. The coupling constant for electrons with parallel spins will be denoted by the subscript \parallel and that for electrons with opposite spins by the subscript \perp .

This classification of the scattering processes is a reasonable one for the model with bandwidth cut-off. For the other models, where the two branches meet at one

Fig. 5



Possible scattering processes. The solid and dashed lines correspond to electrons belonging to the branches containing $+k_F$ and $-k_F$ respectively.

point (see figs. 3 and 4), it can be used only if the momentum dependence of the couplings is properly chosen, as is discussed later. The interaction part of the Hamiltonian can be written in terms of the operators $a_{k\alpha}$ and $b_{k\alpha}$ as

$$\begin{aligned}
 H_{\text{int}} = & \frac{1}{L} \sum_{\substack{k_1, k_2, p \\ \alpha, \beta}} (g_{1\parallel} \delta_{\alpha\beta} + g_{1\perp} \delta_{\alpha, -\beta}) a_{k_1\alpha}^+ b_{k_2\beta}^+ a_{k_2+2k_F+p\beta} b_{k_1-2k_F-p\alpha} \\
 & + \frac{1}{L} \sum_{\substack{k_1, k_2, p \\ \alpha, \beta}} (g_{2\parallel} \delta_{\alpha\beta} + g_{2\perp} \delta_{\alpha, -\beta}) a_{k_1\alpha}^+ b_{k_2\beta}^+ b_{k_2+p\beta} a_{k_1-p\alpha} \\
 & + \frac{1}{2L} \sum_{\substack{k_1, k_2, p \\ \alpha, \beta}} (g_{3\parallel} \delta_{\alpha\beta} + g_{3\perp} \delta_{\alpha, -\beta}) (a_{k_1\alpha}^+ a_{k_2\beta}^+ b_{k_2-2k_F+p\beta} b_{k_1+2k_F-p-G\alpha} \\
 & \quad + b_{k_1\alpha}^+ b_{k_2\beta}^+ a_{k_2+2k_F+p\beta} a_{k_1-2k_F-p+G\alpha}) \\
 & + \frac{1}{2L} \sum_{\substack{k_1, k_2, p \\ \alpha, \beta}} (g_{4\parallel} \delta_{\alpha\beta} + g_{4\perp} \delta_{\alpha, -\beta}) (a_{k_1\alpha}^+ a_{k_2\beta}^+ a_{k_2+p\beta} a_{k_1-p\alpha} \\
 & \quad + b_{k_1\alpha}^+ b_{k_2\beta}^+ b_{k_2+p\beta} b_{k_1-p\alpha}). \tag{2.4}
 \end{aligned}$$

The coupling constants depend, in general, on k_1 , k_2 and p . G in the third term is a reciprocal lattice vector; for a half-filled band $G=4k_F$.

In the model with bandwidth cut-off, where all the momenta are restricted to the regions $(-k_F - k_0, -k_F + k_0)$ or $(k_F - k_0, k_F + k_0)$, depending on whether they correspond to b or a operators, the momentum dependence of the couplings is usually neglected. In this case there should be no distinction between $g_{1\parallel}$ and $g_{2\parallel}$ —they correspond to the same process. Instead of having the four couplings $g_{1\parallel}$, $g_{1\perp}$, $g_{2\parallel}$ and $g_{2\perp}$, only three independent couplings should be used. A common choice is to have $g_{1\parallel}$, $g_{1\perp}$ and $g_2=g_{2\parallel}=g_{2\perp}$ as the three independent couplings. Similarly, the scattering processes determined by $g_{3\parallel}$ and $g_{4\parallel}$ give no contribution, and the remaining couplings between electrons with opposite spins are denoted simply by g_3 and g_4 .

This situation changes somewhat if one uses a momentum transfer cut-off, i.e. a cut-off on p . As will be shown, in this case $g_{4\parallel}$ gives a trivial but non-vanishing contribution and therefore it should be kept; $g_{3\parallel}$, however, gives no contribution and can be neglected in this case as well. The terms with $g_{1\parallel}$ and $g_{2\parallel}$ do not correspond to exactly the same processes if the cut-off is only on the transfer p , while k_1 and k_2 can be anywhere in the respective branch. They become equivalent only if, in addition to the transfer cut-off, a bandwidth cut-off is used as it should be if backward scattering terms are also present.

Finally it should be mentioned that the other convention for the coupling constants often found in the literature can be expressed in terms of g by use of the identification.

$$U_{\parallel} \rightarrow g_{1\parallel}, \quad U_{\perp} \rightarrow g_{1\perp}, \quad V \rightarrow g_2, \quad W_{\perp} \rightarrow g_3 \tag{2.5}$$

and

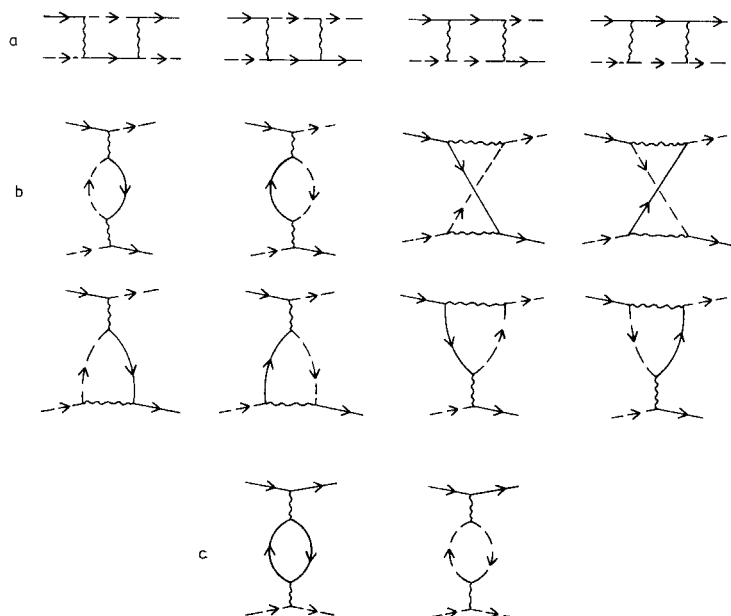
$$W_{\parallel} = 2V - U_{\parallel} \rightarrow 2g_2 - g_{1\parallel} \tag{2.6}$$

since this combination plays a particular role.

§3. PERTURBATIONAL TREATMENT OF THE MODEL

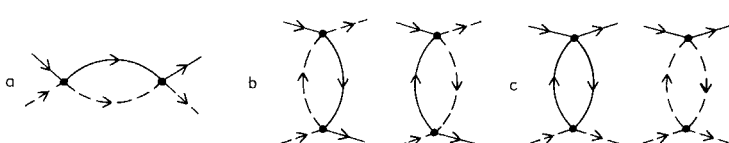
To obtain some sort of idea of what may happen in the model, the model is treated initially in a perturbational way. The behaviour of the Fermi gas can be studied by calculating the vertex function, which describes the scattering of electrons and can reflect the instabilities of the system. The bare vertex functions are the same as the bare interaction processes shown diagrammatically in fig. 5. The first corrections to the scattering of two electrons from different branches, shown in fig. 6, are partly effective g_1 -type (backward scattering) and partly effective g_2 -type (forward scattering) processes. There are three types of diagram. The four diagrams in fig. 6 (a) have the same structure: they contain in the intermediate state two electrons, one from each branch. These are the so-called Cooper pair diagrams. The other diagrams contain an electron-hole pair in the intermediate state. In the zero-sound-type diagrams in fig. 6 (b), the electron and the hole are on different branches; in the diagrams in fig. 6 (c) they are on the same branch. The structure of the diagrams is shown in fig. 7, where the interactions are represented by dots instead of wavy lines.

Fig. 6



First corrections to the vertex in (a) the Cooper pair, (b) zero sound and (c) the third channel.

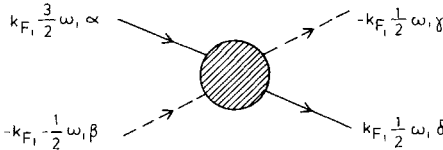
Fig. 7



The structure of the vertex diagrams in (a) the Cooper pair, (b) zero sound and (c) the third channel.

The calculation of the analytic contribution is restricted to a particular choice of the variables of the vertex, since all that is required here is to illustrate the problems that arise. The momenta are fixed at the Fermi momentum ($+k_F$ and $-k_F$ respectively) and the energy variables are chosen in such a way that the usual combinations $\omega_1 + \omega_2$, $\omega_1 - \omega_3$ and $\omega_1 - \omega_4$ are all equal to ω , a single energy variable. This special choice of the momentum and energy variables is shown in fig. 8.

Fig. 8



General vertex diagram showing the special choice of the external variables.

Apart from the factors coming from the coupling constants, the Cooper pair diagrams give

$$-i \int \frac{dk'}{2\pi} \int \frac{d\omega'}{2\pi} G_+(k', \omega') G_-(-k', \omega - \omega') = -\frac{1}{2\pi v_F} \left[\ln \frac{\omega}{E_0} - \frac{i\pi}{2} \right], \quad (3.1)$$

where G_+ and G_- are the Green's functions of electrons for the two branches of the spectrum. The diagram is calculated with a bandwidth cut-off E_0 .

The zero-sound channel gives

$$-i \int \frac{dk'}{2\pi} \int \frac{d\omega'}{2\pi} G_+(k', \omega') G_-(k' - 2k_F, \omega' - \omega) = \frac{1}{2\pi v_F} \left[\ln \frac{\omega}{E_0} - \frac{i\pi}{2} \right]. \quad (3.2)$$

Since the third type of diagram (fig. 6(c)) does not give logarithmic correction, it will be neglected for energies $\omega \ll E_0$. Taking now all the numerical factors into account, the analytic expression of the vertex is

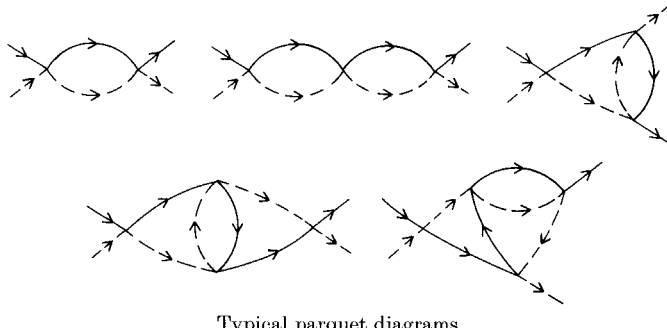
$$\begin{aligned} \Gamma = & g_{1\parallel} \delta_{\alpha\gamma} \delta_{\beta\delta} \delta_{\alpha\beta} + g_{1\perp} \delta_{\alpha\gamma} \delta_{\beta\delta} \delta_{\alpha, -\beta} - g_2 \delta_{\alpha\delta} \delta_{\beta\gamma} \\ & + \left[\frac{1}{\pi v_F} g_{1\perp}^2 \delta_{\alpha\gamma} \delta_{\beta\delta} \delta_{\alpha\beta} + \frac{1}{\pi v_F} g_{1\parallel} g_{1\perp} \delta_{\alpha\gamma} \delta_{\beta\delta} \delta_{\alpha, -\beta} \right. \\ & \left. - \frac{1}{2\pi v_F} (g_{1\perp}^2 - g_3^2) \delta_{\alpha\delta} \delta_{\beta\gamma} \right] \left(\ln \frac{\omega}{E_0} - \frac{i\pi}{2} \right) + \dots \end{aligned} \quad (3.3)$$

The vertex corrections could be calculated for finite incoming momentum k or for finite temperature T . In the logarithmic approximation, where non-singular terms are neglected compared to logarithmically singular contributions, $\ln(\omega/E_0)$ is replaced by $\ln[\max(v_F k, T, \omega)/E_0]$. It is seen from eqn. (3.3) that the perturbational corrections are not small at low energies and low temperatures and that higher-order corrections should also be considered.

The first attempt to take into account the higher-order corrections in a consistent way was made by Bychkov *et al.* (1966), who pointed out that the 1-d Fermi gas is a typical logarithmic problem, i.e. the vertex is logarithmically singular in every order of the perturbational calculation. In the n th order the correction is proportional to

$\ln^{n-1}(\omega/E_0)$. In a consistent calculation all these corrections have to be summed, which can be done by realizing that the leading logarithmic corrections come from a particular set of diagrams, the so-called parquet diagrams. These diagrams are built up from the two basic logarithmic bubbles, the Cooper pair and zero-sound bubbles. The higher-order diagrams can be constructed by inserting these elementary bubbles instead of the bare vertex. A repetition of this procedure generates the so-called parquet diagrams, typical examples of which are shown in fig. 9.

Fig. 9



Typical parquet diagrams.

The contribution of the parquet diagrams can be summed by writing a closed set of integral equations for the vertex (Diatlov *et al.* 1957). This is a common approximation in logarithmic problems and has been used, for example, by Abrikosov (1965) for the Kondo problem, by Roulet *et al.* (1969) and Nozières *et al.* (1969) for the X-ray absorption problem and by Ginzburg (1974) for the critical phenomena in $4-\epsilon$ dimensions. A detailed description of the method can be found in the paper by Roulet *et al.* (1969) and Nozières *et al.* (1969). Bychkov *et al.* (1966) used the parquet summation to calculate the vertex in the particular case when all the interesting couplings are equal: $g_{1\parallel}=g_{1\perp}=g_2=g$. The Umklapp processes have been neglected since they are important only for a half-filled band. They obtained

$$\Gamma = \frac{g}{1 - \frac{g}{\pi v_F} \ln \frac{\omega}{E_0}} \delta_{\alpha\gamma} \delta_{\beta\delta} - \left(\frac{\frac{1}{2}g + \frac{1}{2}}{1 - \frac{g}{\pi v_F} \ln \frac{\omega}{E_0}} \right) \delta_{\alpha\delta} \delta_{\beta\gamma}, \quad (3.4)$$

a result which immediately shows the inadequacy of this approximation. The vertex is singular at a finite frequency or finite temperature given by

$$T_c = E_0 \exp\left(-\frac{\pi v_F}{|g|}\right), \quad (3.5)$$

if $g < 0$. This singularity is an indication of an instability, a phase transition in the system at this temperature, in contradiction with the well-known theorem which states that a 1-d system with short-range forces cannot have a phase transition at any finite temperature. The failure of the parquet approximation follows from neglecting the lower-order logarithmic corrections which, at low temperatures, are not negligible. A method which is capable of taking into account these subsequent corrections is now presented.

The 1-d Fermi gas has many similarities to the Kondo problem. (For a review of the Kondo problem see Grüner and Zawadowski (1974).) Both problems have an infra-red divergence due to the continuum of low-energy excitations. Formally, this gives rise to the logarithmic corrections in the perturbational expansion. The parquet diagram summation in the Kondo problem gives a sharp transition at a temperature T_K , below which a bound polarization cloud is formed around the impurity. The expression for T_K is analogous to that for T_c in eqn. (3.5). The sharp transition is non-physical and the corrections beyond the parquet approximation should also be considered. The renormalization group (Abrikosov and Migdal 1970, Fowler and Zawadowski 1971, Wilson 1975) proved very useful in the Kondo problem in fully understanding the physics of magnetic impurities in normal metals. A similar treatment is now attempted.

An alternative approach is to apply the skeleton graph technique (Ohmi *et al.* 1976). This method allows—in the same way as the renormalization group—to go beyond the parquet approximation. The same results, presented in § 4, can also be obtained in this way.

§ 4. RENORMALIZATION GROUP TREATMENT

In field theory, the multiplicative renormalization group has been used for a long time as a method of improving the results obtained in perturbation theory (see, for example, Bogoliubov and Shirkov 1959, Bjorken and Drell 1965). This method is particularly useful in logarithmic problems where only a few diagrams have to be calculated and the summation of the higher-order contributions is achieved by solving the renormalization group equations. The method has been applied to the logarithmic problems mentioned earlier. Abrikosov and Migdal (1970), as well as Fowler and Zawadowski (1971), studied the Kondo problem, and Di Castro (1972) and Brézin *et al.* (1973) formulated the critical phenomena in $4-\epsilon$ dimensions in this framework. Since the 1-d Fermi gas model is a logarithmic problem, and the parquet approximation, which is equivalent to summing the leading logarithmic corrections is not sufficient, it is hoped that a renormalization group treatment will produce a better approximation.

That aspect of the renormalization group that starting from a perturbational calculation a partial summation is obtained by solving the group equations is almost absent in the modern formulation of the renormalization group (Wilson and Kogut 1974), although it is present in most of the applications in a hidden form. Instead of that the scaling aspect is dominant. The basic idea is that a set of equivalent problems can be found which are described by Hamiltonians of similar form. The coupling constants and other parameters of the Hamiltonians may be different, but the systems should show the same physical behaviour. If there is a model among the equivalent ones which can be solved, the solution of the original problem can also be obtained.

The renormalization group transformations which relate the equivalent problems may differ greatly, depending on the problem at hand. One procedure which is very often used is to eliminate degrees of freedom near the cut-off—if there is a natural cut-off in the problem—and to compensate for their effect by choosing different coupling constants. This idea can be realized in many ways, depending on how the equivalence of the problems is defined. The free energy or partition function is frequently required to be invariant under the renormalization transformation, which is very suitable when thermodynamic properties are studied. Other conditions

may be more convenient when scattering properties and instabilities are considered. First a simple treatment, then a more sophisticated approach, will be presented.

4.1. Poor man's scaling

Anderson (1970) suggested that the equivalent problems can be formulated by requiring that the scattering properties be the same in the systems, i.e. the scattering matrix T be invariant under the renormalization transformation. This poor man's approach to scaling can easily be applied to the 1-d Fermi gas model.

The scattering matrix T obeys the equation

$$T(\omega) = H_{\text{int}} + H_{\text{int}} \frac{1}{\omega - H_0} T(\omega), \quad (4.1)$$

where the free and interaction parts of the Hamiltonian are given by eqns. (2.3) and (2.4). As mentioned previously, there is a natural cut-off in the model with bandwidth cut-off and this will serve as a scaling parameter.

If the cut-off E_0 is changed to a smaller value $E_0 - dE_0$, states which were allowed as intermediate states in scattering processes are no longer available and the Hamiltonian should be modified to compensate for these lost states. A straightforward rearrangement of eqn. (4.1) (Sólyom and Zawadowski 1974) leads, for the new Hamiltonian, to

$$\begin{aligned} H'_{\text{int}}(\omega) = & (1 - P) \left[H_{\text{int}} + H_{\text{int}} P \frac{1}{\omega - H_0} H_{\text{int}} \right. \\ & \left. + H_{\text{int}} P \frac{1}{\omega - H_0} H_{\text{int}} P \frac{1}{\omega - H_0} H_{\text{int}} + \dots \right] (1 - P), \end{aligned} \quad (4.2)$$

where the projection operator P selects those states which contain at least one electron in the energy range $(E_0 - dE_0, E_0)$ or at least one hole in the range $(-E_0, -E_0 + dE_0)$. Strictly speaking, the scattering matrix calculated with this new Hamiltonian and new cut-off is not the same as the original one. The new T matrix has elements only between those states in which the electrons both before and after the scattering belong to the restricted band. These matrix elements are the same in the original and the new systems.

The Hamiltonian of the scaled system, defined by eqn. (4.2), can be very different from that of the original one. It is energy-dependent and may contain—in addition to two-particle scattering—terms which correspond to the scattering of three, four, or more particles. This scaling procedure is useful only if it does not lead to a large number of new types of coupling which are essential and if the dependence of the scaled couplings on the other parameters of the scattering, such as the energy and momentum of the electrons, is not important.

This is the case for the 1-d Fermi gas. The matrix element is taken between initial and final states which both contain two extra electrons from the neighbourhood of the Fermi surface, one from each branch, added to the filled Fermi sea. The initial state $|i\rangle$ and final state, $|f\rangle$ are given by

$$|i\rangle = a_{k_1\alpha}^+ b_{k_2\beta}^+ |0\rangle \quad \text{and} \quad |f\rangle = b_{k_3\gamma}^+ a_{k_4\delta}^+ |0\rangle, \quad (4.3)$$

where $|0\rangle$ is the state vector of the filled Fermi sea. Momentum conservation requires that $k_1 + k_2 = k_3 + k_4$.

The matrix element of H_{int} between these states is

$$\langle i|H_{\text{int}}|f\rangle = \frac{1}{L} [g_{1\parallel}\delta_{\alpha\gamma}\delta_{\beta\delta}\delta_{\alpha\beta} + g_{1\perp}\delta_{\alpha\gamma}\delta_{\beta\delta}\delta_{\alpha,-\beta} - g_2\delta_{\alpha\delta}\delta_{\beta\gamma}]. \quad (4.4)$$

A straightforward calculation of the next term in eqn. (4.2) gives

$$\begin{aligned} \langle i|H'_{\text{int}}|f\rangle &= \frac{1}{L} \left\{ [g_{1\parallel}\delta_{\alpha\gamma}\delta_{\beta\delta}\delta_{\alpha\beta} + g_{1\perp}\delta_{\alpha\gamma}\delta_{\beta\delta}\delta_{\alpha,-\beta} - g_2\delta_{\alpha\delta}\delta_{\beta\gamma}] \right. \\ &\quad + \frac{dE_0}{E_0} \left[\frac{1}{\pi v_F} g_{1\perp}^2 \delta_{\alpha\gamma}\delta_{\beta\delta}\delta_{\alpha\beta} + \frac{1}{\pi v_F} g_{1\parallel} g_{1\perp} \delta_{\alpha\gamma}\delta_{\beta\delta}\delta_{\alpha,-\beta} \right. \\ &\quad \left. \left. - \frac{1}{2\pi v_F} (g_{1\perp}^2 - g_3^2) \delta_{\alpha\delta}\delta_{\beta\gamma} \right] + \dots \right\}, \end{aligned} \quad (4.5)$$

where both ω and the energies of the scattered electrons have been neglected, being much smaller than E_0 .

Equations (4.4) and (4.5) have the same structure. If the new coupling constants of the scaled Hamiltonian are chosen in the form $g_i + dg_i$, the following relations are obtained:

$$dg_{1\parallel} = \frac{dE_0}{E_0} \left[\frac{1}{\pi v_F} g_{1\perp}^2 + \dots \right], \quad (4.6)$$

$$dg_{1\perp} = \frac{dE_0}{E_0} \left[\frac{1}{\pi v_F} g_{1\parallel} g_{1\perp} + \dots \right] \quad (4.7)$$

and

$$dg_2 = \frac{dE_0}{E_0} \left[\frac{1}{2\pi v_F} (g_{1\perp}^2 - g_3^2) + \dots \right]. \quad (4.8)$$

Since we have calculated everywhere only the first correction, this approximation, as can immediately be seen, is equivalent to the parquet approximation. The solution of these equations for spin-independent couplings and for a non-half-filled band, where g_3 can be neglected, gives

$$g'_1 = \frac{g_1}{1 - \frac{g_1}{\pi v_F} \ln \frac{E'_0}{E_0}}, \quad g'_2 = g_2 - \frac{1}{2} g_1 + \frac{1}{2} \frac{g_1}{1 - \frac{g_1}{\pi v_F} \ln \frac{E'_0}{E_0}}, \quad (4.9)$$

where g'_1 and g'_2 are the couplings if the cut-off E_0 is scaled to E'_0 . Similar singular behaviour appears as in the expression of the vertex in the parquet approximation (see eqn. (3.4)). In fact, the use of the first-order scaling equations is equivalent to summing the leading logarithmic corrections. In order to go beyond the parquet approximation, the next corrections in eqns. (4.6)–(4.8) must be calculated.

The couplings in the scaled Hamiltonian are non-physical quantities in the sense that they depend on the invariance property required. When calculated from the T matrix, the couplings are different whether or not the self-energy corrections of the electrons in the initial and final states are considered. Since scaling procedure is to be

used to calculate physical quantities, namely Green's functions, response functions and so on, a new formulation is presented in the next section which allows this in a convenient form.

4.2. Multiplicative renormalization generated by cut-off scaling

The simple physical picture of renormalization by successive elimination of degrees of freedom through cut-off scaling is absent in the usual formulation of multiplicative renormalization. It turns out, however, that in logarithmic problems cut-off scaling generates a multiplicative renormalization of Green's functions, vertices and other related quantities. Thus for these problems a new renormalization procedure can be worked out which combines the physical idea of successive elimination of degrees of freedom with the mathematical framework of multiplicative renormalization. This approach reproduces the known results in X-ray absorption and Kondo problems (Sólyom 1974) and in the critical phenomena (Forgács *et al.* 1978). Here we will present the ideas applied to the 1-d Fermi gas (Menyhárd and Sólyom 1973). The conventional field-theoretical renormalization group has been applied to this system independently by Kimura (1973), but in the lowest approximation only.

Before formulating the multiplicative renormalization transformation in a mathematical way, the dimensionless Green's function and vertices are introduced. In order to simplify the formulae, we will restrict ourselves to the only case in which $g_3=0$ will be considered, i.e. Umklapp processes are not allowed and g_4 -type processes are also neglected. The general case is discussed in §7.

The dimensionless Green's function d is defined by

$$G(k, \omega) = d\left(\frac{k}{k_0}, \frac{\omega}{E_0}\right) G^{(0)}(k, \omega). \quad (4.10)$$

The total vertex describing the scattering of two electrons from different branches is decomposed into three parts corresponding to the three different elementary scattering processes:

$$\begin{aligned} \Gamma_{\alpha\beta\gamma\delta}(k_i, \omega_i) &= g_{1\parallel} \tilde{\Gamma}_{1\parallel} \left(\frac{k_i}{k_0}, \frac{\omega_i}{E_0} \right) \delta_{\alpha\gamma} \delta_{\beta\delta} \delta_{\alpha\beta} \\ &\quad + g_{1\perp} \tilde{\Gamma}_{1\perp} \left(\frac{k_i}{k_0}, \frac{\omega_i}{E_0} \right) \delta_{\alpha\gamma} \delta_{\beta\delta} \delta_{\alpha, -\beta} \\ &\quad - g_2 \tilde{\Gamma}_2 \left(\frac{k_i}{k_0}, \frac{\omega_i}{E_0} \right) \delta_{\alpha\delta} \delta_{\beta\gamma}. \end{aligned} \quad (4.11)$$

The dimensionless vertices $\tilde{\Gamma}_i (i=1\parallel, 1\perp, 2)$ are defined by this relation.

Multiplicative renormalization is usually defined by the transformation

$$G \rightarrow zG \quad \text{or} \quad d \rightarrow zd, \quad (4.12)$$

$$\tilde{\Gamma}_i \rightarrow z_i^{-1} \tilde{\Gamma}_i, \quad i = 1\parallel, 1\perp, 2, \quad (4.13)$$

$$g_i \rightarrow z^{-2} z_i g_i, \quad i = 1\parallel, 1\perp, 2. \quad (4.14)$$

Working with these transformed quantities, all measurable quantities can be made finite in a renormalizable field theory, even if no cut-off is used. The group property of this transformation allows the results obtained in perturbation theory to be improved.

In the present model there is a well-defined cut-off, and, as in the poor man's scaling approach, this cut-off is used to generate the equivalent scaled systems. It turns out that, in the present model, scaling of the physical cut-off generates a multiplicative renormalization analogous to the transformations in field theory, i.e. the model obeys the following scaling relationship.

- (1) Scale the cut-off $E_0 = 2v_F k_0$ to a smaller value $E'_0 = 2v_F k'_0$.
- (2) Change the couplings g_i ($i = 1\parallel, 1\perp, 2$) to g'_i .
- (3) Fix the values of the new couplings from the requirement that the Green's function and vertices of the scaled system preserve the same analytic form as that of the original system, i.e. they should differ only in those multiplicative factor which are independent of the energy and momentum variables.
- (4) The original and new couplings are then related by the same multiplicative factors; the new coupling should be independent of the energy and momentum variables and can depend on the ratio of the new and old cut-offs only.

Formulated mathematically, this means that

$$d\left(\frac{k}{k'_0}, \frac{\omega}{E'_0}, g'_{1\parallel}, g'_{1\perp}, g'_2\right) = z\left(\frac{E'_0}{E_0}, g_{1\parallel}, g_{1\perp}, g_2\right) d\left(\frac{k}{k_0}, \frac{\omega}{E_0}, g_{1\parallel}, g_{1\perp}, g_2\right), \quad (4.15)$$

$$\begin{aligned} \tilde{\Gamma}_i &\left(\frac{k_j}{k'_0}, \frac{\omega_j}{E'_0}, g'_{1\parallel}, g'_{1\perp}, g'_2\right) \\ &= z_i^{-1}\left(\frac{E'_0}{E_0}, g_{1\parallel}, g_{1\perp}, g_2\right) \tilde{\Gamma}_i\left(\frac{k_j}{k_0}, \frac{\omega_j}{E_0}, g_{1\parallel}, g_{1\perp}, g_2\right), \quad i = 1\parallel, 1\perp, 2 \end{aligned} \quad (4.16)$$

and

$$g'_i = g_i z^{-2}\left(\frac{E'_0}{E_0}, g_{1\parallel}, g_{1\perp}, g_2\right) z_i\left(\frac{E'_0}{E_0}, g_{1\parallel}, g_{1\perp}, g_2\right), \quad i = 1\parallel, 1\perp, 2. \quad (4.17)$$

It follows that the quantity $g_i \tilde{\Gamma}_i d^2$ is invariant, i.e. that

$$\begin{aligned} g_i \tilde{\Gamma}_i &\left(\frac{k_j}{k'_0}, \frac{\omega_j}{E'_0}, g'_{1\parallel}, g'_{1\perp}, g'_2\right) d^2\left(\frac{k}{k'_0}, \frac{\omega}{E'_0}, g'_{1\parallel}, g'_{1\perp}, g'_2\right) \\ &= g_i \tilde{\Gamma}_i\left(\frac{k_j}{k_0}, \frac{\omega_j}{E_0}, g_{1\parallel}, g_{1\perp}, g_2\right) d^2\left(\frac{k}{k_0}, \frac{\omega}{E_0}, g_{1\parallel}, g_{1\perp}, g_2\right). \end{aligned} \quad (4.18)$$

This quantity can be considered as an appropriately renormalized vertex, where the self-energy corrections on the incoming and outgoing lines are also taken into account (Sólyom and Zawadowski 1974). The invariance of this quantity is required instead of the invariance of the T matrix, as in the poor man's scaling.

These scaling relations cannot be satisfied for most theories. For the 1-d Fermi gas model and several other logarithmic problems, however, they are satisfied in perturbation theory, at least for the leading and next-to-leading logarithmic terms. It is assumed that they hold for the singular part of the Green's function and vertices in higher orders as well, although they may not be valid for the non-singular part.

Introducing the functions

$$g_i^R\left(\frac{E}{E_0}, g_{1\parallel}, g_{1\perp}, g_2\right) = g_i z^{-2} \left(\frac{E}{E_0}, g_{1\parallel}, g_{1\perp}, g_2\right) z_i \left(\frac{E}{E_0}, g_{1\parallel}, g_{1\perp}, g_2\right),$$

$$i = 1\parallel, 1\perp, 2, \quad (4.19)$$

the new couplings g'_i are obtained when E is identified with the new cut-off E'_0 , i.e.

$$g'_i = g_i^R\left(\frac{E'_0}{E_0}, g_{1\parallel}, g_{1\perp}, g_2\right). \quad (4.20)$$

These quantities are called invariant couplings since they are invariant under the same renormalization transformation

$$\begin{aligned} & g_i^R\left(\frac{E}{E'_0}, g'_{1\parallel}, g'_{1\perp}, g'_2\right) \\ & \equiv g_i^R\left(\frac{E}{E'_0}, g_{1\parallel}^R\left(\frac{E'_0}{E_0}, g_{1\parallel}, g_{1\perp}, g_2\right), g_{1\perp}^R\left(\frac{E'_0}{E_0}, g_{1\parallel}, g_{1\perp}, g_2\right), g_2^R\left(\frac{E'_0}{E_0}, g_{1\parallel}, g_{1\perp}, g_2\right)\right) \\ & = g_i^R\left(\frac{E}{E_0}, g_{1\parallel}, g_{1\perp}, g_2\right). \end{aligned} \quad (4.21)$$

This invariance is a consequence of the group property of the renormalization transformation. Starting from the original couplings and scaling the cut-off directly from E_0 to E leads to the same new couplings that would be obtained by scaling first from E_0 to E'_0 , where the new couplings are given by eqn. (4.20), and then from E'_0 to E .

The scaling equations for d , $\tilde{\Gamma}_i$ and g_i^R can be written in a common form as

$$\begin{aligned} & A\left(\frac{\omega}{E'_0}, g_{1\parallel}^R\left(\frac{E'_0}{E_0}, g_{1\parallel}, g_{1\perp}, g_2\right) g_{1\perp}^R\left(\frac{E'_0}{E_0}, g_{1\parallel}, g_{1\perp}, g_2\right), g_2^R\left(\frac{E'_0}{E_0}, g_{1\parallel}, g_{1\perp}, g_2\right)\right) \\ & = z_A\left(\frac{E'_0}{E_0}, g_{1\parallel}, g_{1\perp}, g_2\right) A\left(\frac{\omega}{E_0}, g_{1\parallel}, g_{1\perp}, g_2\right). \end{aligned} \quad (4.22)$$

A single variable is left in these equations: ω , T or $v_F k$ depending on whether the energy, temperature or momentum dependence is calculated. The further considerations can easily be extended to several variables.

The scaling equations can be written in a differential equation form. Differentiating the logarithm of eqn. (4.22) with respect to ω/E_0 (T/E_0 or $v_F k/E_0$) and setting E'_0 equal to ω (T or $v_F k$) gives

$$\frac{d}{dx} \ln A(x, g_{1\parallel}, g_{1\perp}, g_2) = \frac{1}{x} \frac{d}{d\xi} \ln A(\xi, g_{1\parallel}^R(x, g_{1\parallel}, g_{1\perp}, g_2), g_{1\perp}^R(x, g_{1\parallel}, g_{1\perp}, g_2), g_2^R(x, g_{1\parallel}, g_{1\perp}, g_2))_{\xi=1}, \quad (4.23)$$

where $x = \omega/E_0$ (T/E_0 or $v_F k/E_0$). These are the Lie equations of the renormalization group. The multiplicative factor does not appear in this equation since it is independent of the energy, temperature or momentum variables; it depends only on the ratio of the new and old cut-offs. On the other hand, when, after the differentiation, the new cut-off E'_0 is set equal to ω (T or $v_F k$), the invariant couplings in eqn. (4.23) appear as functions of the energy, temperature or momentum. In this sense it is common to speak about the energy, temperature or momentum dependence of the invariant couplings.

From eqn. (4.23) it can be seen that the quantity A can be calculated as a function of x if the behaviour of the scaled problem is known near the new cut-off. This renormalization transformation, i.e. scaling the cut-off to the energy variable in question, is useful for logarithmic problems since, near the new cut-off, a perturbational treatment of the right-hand side might be sufficient, provided the invariant couplings are small at x . Unfortunately this is not always the case, as will be seen, but even in this case the scaling properties can give some insight into the behaviour of the system.

In the first step of any calculation the perturbational expressions of the Green's function and vertices have to be determined. The renormalization factors and invariant couplings can then be obtained in a perturbational form using the scaling equations (4.15)–(4.17). Using this perturbational result, the solution of the Lie equation (4.23) for the invariant couplings gives a summed expression. Once this expression is known, other quantities can also be determined by solving the respective Lie equations.

According to this programme the invariant couplings are determined in a perturbational form from the self-energy and vertex corrections calculated to second order. A straightforward calculation of the self-energy and vertex diagrams shown in figs. 10 and 11 gives

$$d(\omega) = 1 + \frac{1}{8\pi^2 v_F^2} (g_{1\parallel}^2 + g_{1\perp}^2 - 2g_{1\parallel}g_2 + 2g_2^2) \left(\ln \frac{\omega}{E_0} - \frac{1}{2}i\pi \right) + \dots, \quad (4.24)$$

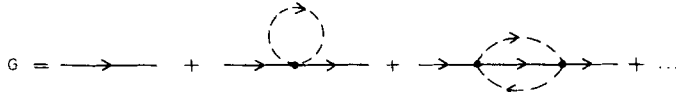
$$\begin{aligned} \tilde{\Gamma}_{1\parallel}(\omega) = 1 &+ \frac{1}{\pi v_F g_{1\parallel}} \left(\ln \frac{\omega}{E_0} - \frac{1}{2}i\pi \right) + \frac{1}{\pi^2 v_F^2 g_{1\perp}^2} \left(\ln^2 \frac{\omega}{E_0} - i\pi \ln \frac{\omega}{E_0} + \dots \right) \\ &+ \frac{1}{4\pi^2 v_F^2} (-g_{1\parallel}^2 + g_{1\perp}^2 + 2g_{1\parallel}g_2 - 2g_2^2) \left(\ln \frac{\omega}{E_0} - \frac{1}{2}i\pi \right) + \dots, \end{aligned} \quad (4.25)$$

$$\begin{aligned} \tilde{\Gamma}_{1\perp}(\omega) = 1 &+ \frac{1}{\pi v_F g_{1\parallel}} \left(\ln \frac{\omega}{E_0} - \frac{1}{2}i\pi \right) + \frac{1}{2\pi^2 v_F^2 (g_{1\parallel}^2 + g_{1\perp}^2)} \left(\ln^2 \frac{\omega}{E_0} - i\pi \ln \frac{\omega}{E_0} + \dots \right) \\ &+ \frac{1}{4\pi^2 v_F^2} (2g_{1\parallel}g_2 - 2g_2^2) \left(\ln \frac{\omega}{E_0} - \frac{1}{2}i\pi \right) + \dots \end{aligned} \quad (4.26)$$

and

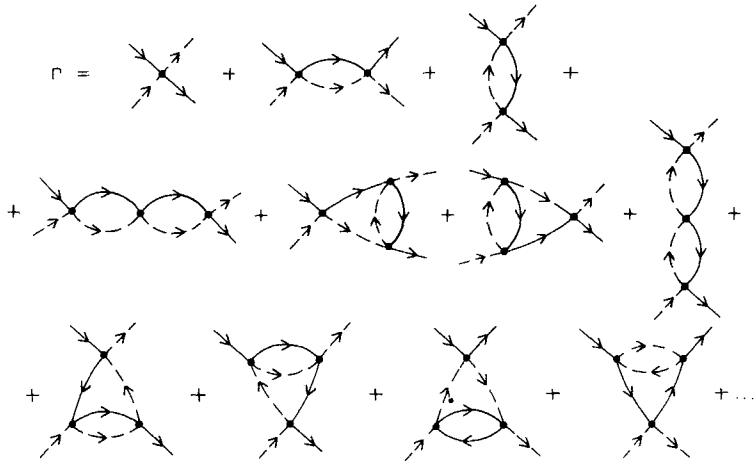
$$\begin{aligned}\Gamma_2(\omega) = & 1 + \frac{1}{2\pi v_F} \frac{g_{1\perp}^2}{g_2} \left(\ln \frac{\omega}{E_0} - \frac{1}{2}i\pi \right) + \frac{1}{2\pi^2 v_F^2} \frac{g_{1\parallel} g_{1\perp}^2}{g_2} \left(\ln^2 \frac{\omega}{E_0} - i\pi \ln \frac{\omega}{E_0} + \dots \right) \\ & + \frac{1}{4\pi^2 v_F^2} \left(\frac{g_{1\parallel} g_{1\perp}^2}{g_2} - g_{1\parallel}^2 - g_{1\perp}^2 + 2g_{1\parallel} g_2 - 2g_2^2 \right) \left(\ln \frac{\omega}{E_0} - \frac{1}{2}i\pi \right) + \dots \quad (4.27)\end{aligned}$$

Fig. 10



Low-order diagrams for the Green's function. The dots stand for $g_{1\parallel}^-$, $g_{1\perp}^-$ and g_2^- -type couplings.

Fig. 11



Low-order diagrams for the vertex.

The scaling equations are satisfied if the renormalized couplings have the form

$$\begin{aligned}g_{1\parallel}^R \left(\frac{E'_0}{E_0}, g_{1\parallel}, g_{1\perp}, g_2 \right) = & g_{1\parallel} + \frac{g_{1\perp}^2}{\pi v_F} \ln \frac{E'_0}{E_0} \\ & + \frac{1}{\pi^2 v_F^2} g_{1\parallel} g_{1\perp}^2 \left(\ln^2 \frac{E'_0}{E_0} + \frac{1}{2} \ln \frac{E'_0}{E_0} \right) + \dots, \quad (4.28)\end{aligned}$$

$$\begin{aligned}g_{1\perp}^R \left(\frac{E'_0}{E_0}, g_{1\parallel}, g_{1\perp}, g_2 \right) = & g_{1\perp} + \frac{1}{\pi v_F} g_{1\parallel} g_{1\perp} \ln \frac{E'_0}{E_0} \\ & + \frac{1}{2\pi^2 v_F^2} \left(g_{1\parallel}^2 g_{1\perp} + g_{1\perp}^3 \right) \left(\ln^2 \frac{E'_0}{E_0} + \frac{1}{2} \ln \frac{E'_0}{E_0} \right) + \dots, \quad (4.29)\end{aligned}$$

and

$$\begin{aligned} g_2^R\left(\frac{E'_0}{E_0}, g_{1\parallel}, g_{1\perp}, g_2\right) = & g_2 + \frac{1}{2\pi v_F} g_{1\perp}^2 \ln \frac{E'_0}{E_0} \\ & + \frac{1}{2\pi^2 v_F^2} g_{1\parallel} g_{1\perp}^2 \left(\ln^2 \frac{E'_0}{E_0} + \frac{1}{2} \ln \frac{E'_0}{E_0} \right) + \dots \end{aligned} \quad (4.30)$$

The invariant couplings are real, as they should be, and independent of the variables of the Green's function and vertex (Menyhárd and Sólyom 1975).

The Lie equations for the invariant couplings are obtained from the perturbational expression in the form

$$\frac{dg_{1\parallel}^R(x)}{dx} = \frac{1}{x} \left\{ \frac{1}{\pi v_F} g_{1\perp}^{R2}(x) + \frac{1}{2\pi^2 v_F^2} g_{1\parallel}^R(x) g_{1\perp}^{R2}(x) + \dots \right\}, \quad (4.31)$$

$$\frac{dg_{1\perp}^R}{dx} = \frac{1}{x} \left\{ \frac{1}{\pi v_F} g_{1\parallel}^R(x) g_{1\perp}^R(x) + \frac{1}{4\pi^2 v_F^2} [g_{1\parallel}^{R2}(x) g_{1\perp}^{R2}(x) + g_{1\perp}^{R3}(x)] + \dots \right\} \quad (4.32)$$

and

$$\frac{dg_2^R(x)}{dx} = \frac{1}{x} \left\{ \frac{1}{2\pi v_F} g_{1\perp}^{R2}(x) + \frac{1}{4\pi^2 v_F^2} g_{1\parallel}^R(x) g_{1\perp}^{R2}(x) + \dots \right\}, \quad (4.33)$$

where $x = E'_0/E_0$.

In the next order (third-order renormalization), 58 fourth-order vertex diagrams and two third-order self-energy diagrams should be considered. Ting (1976) performed the calculation in this order for spin-independent couplings and obtained for the invariant couplings

$$\begin{aligned} g_1^R\left(\frac{E'_0}{E_0}, g_1, g_2\right) = & g_1 + \frac{1}{\pi v_F} g_1^2 \ln \frac{E'_0}{E_0} + \frac{1}{\pi^2 v_F^2} g_1^3 \left(\ln^2 \frac{E'_0}{E_0} + \frac{1}{2} \ln \frac{E'_0}{E_0} \right) \\ & + \frac{1}{\pi^3 v_F^3} g_1^4 \left(\ln^3 \frac{E'_0}{E_0} + \frac{5}{4} \ln^2 \frac{E'_0}{E_0} - \frac{7}{8} \ln \frac{E'_0}{E_0} \right) \\ & + \frac{1}{2\pi^3 v_F^3} (g_1^3 g_2 - g_1^2 g_2^2) \ln \frac{E'_0}{E_0} + \dots \end{aligned} \quad (4.34)$$

and

$$\begin{aligned} g_2^R\left(\frac{E'_0}{E_0}, g_1, g_2\right) = & g_2 + \frac{1}{2\pi v_F} g_1^2 \ln \frac{E'_0}{E_0} + \frac{1}{2\pi^2 v_F^2} g_1^3 \left(\ln^2 \frac{E'_0}{E_0} + \frac{1}{2} \ln \frac{E'_0}{E_0} \right) \\ & + \frac{1}{2\pi^3 v_F^3} g_1^4 \left(\ln^3 \frac{E'_0}{E_0} + \frac{5}{4} \ln^2 \frac{E'_0}{E_0} - \frac{7}{8} \ln \frac{E'_0}{E_0} \right) \\ & + \frac{1}{4\pi^3 v_F^3} (g_1^3 g_2 - g_1^2 g_2^2) \ln \frac{E'_0}{E_0} + \dots \end{aligned} \quad (4.35)$$

The Lie equations in this order are

$$\begin{aligned} \frac{dg_1^R(x)}{dx} = & \frac{1}{x} \left\{ \frac{1}{\pi v_F} g_1^{R2}(x) + \frac{1}{2\pi^2 v_F^2} g_1^{R3}(x) - \frac{7}{8\pi^3 v_F^3} g_1^{R4}(x) \right. \\ & \left. + \frac{1}{2\pi^3 v_F^3} [g_1^{R3}(x) g_2^R(x) - g_1^{R2}(x) g_2^{R2}(x)] + \dots \right\} \end{aligned} \quad (4.36)$$

and

$$\begin{aligned} \frac{dg_2^R(x)}{dx} = & \frac{1}{x} \left\{ \frac{1}{2\pi v_F} g_1^{R2}(x) + \frac{1}{4\pi^2 v_F^2} g_1^{R3}(x) - \frac{7}{16\pi^3 v_F^3} g_1^{R4}(x) \right. \\ & \left. + \frac{1}{4\pi^3 v_F^3} [g_1^{R3}(x) g_2^R(x) - g_1^{R2}(x) g_2^{R2}(x)] + \dots \right\} \end{aligned} \quad (4.37)$$

The result obtained by Ting is actually more complicated. Fowler (1976) has shown that $g_1^R - 2g_2^R$ is an exact invariant, at least for $g_1 - 2g_2 = 0$, and conjectured that it holds for $g_1 - 2g_2 \neq 0$ as well. The approximation leading to eqns. (4.34)–(4.37) ensures this invariance. See also note added in proof.

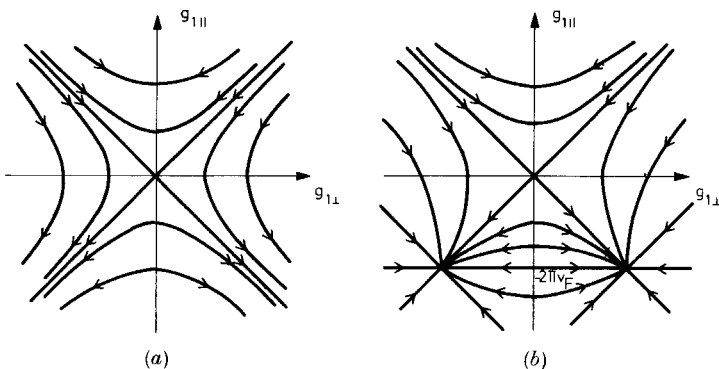
By keeping the first term on the right-hand side of each of eqns. (4.31)–(4.33), the scaling equations (4.6)–(4.8) are recovered. The first-order scaling equations led to non-physical singularities for $g_{1\parallel} = g_{1\perp} = g_1 < 0$. The effect of higher order corrections is now considered.

The best way to analyse these equations is to plot the scaling trajectories, i.e. the lines connecting the equivalent problems in the space of couplings. Using the invariance

$$g_{1\parallel}^R(x) - 2g_2^R(x) = g_{1\parallel} - 2g_2, \quad (4.38)$$

$g_2^R(x)$ is easily obtained from $g_{1\parallel}^R(x)$ and therefore the scaling trajectories are plotted on the $(g_{1\parallel}, g_{1\perp})$ plane. Figures 12 (a) and 12 (b) show the scaling curves in two different approximations, taking into account the second-order terms only or the third-order terms as well. The arrows on the flow lines represent the directions of scaling when the cut-off is decreased.

Fig. 12



Scaling trajectories in the $(g_{1\parallel}, g_{1\perp})$ plane in (a) the leading and (b) the next-to-leading logarithmic approximation.

There are two well separated regions in the $(g_{1\parallel}, g_{1\perp})$ plane where the behaviour of the system is expected to be different. For $g_{1\parallel} \geq |g_{1\perp}|$ the scaling trajectories go to the line $g_{1\perp} = 0$, i.e. the problems for which the coupling constants are situated in this region are equivalent to a problem where the backward scattering is unimportant. (The $g_{1\parallel}$ processes cannot be distinguished from the forward scattering processes if bandwidth cut-off is used.) If $g_{1\perp}$ is zero in the original problem, it remains zero in the scaled problems, and therefore the line $g_{1\perp} = 0$ is a line of fixed points of the renormalization transformation. Starting from weak couplings, the renormalized couplings remain weak and a perturbational treatment of the right-hand sides of the Lie equations is a reasonable approximation.

In the other part of the $(g_{1\parallel}, g_{1\perp})$ plane, scaling goes to a strong coupling regime. In the lowest approximation the scaling curves extend to infinity, but in the next order they converge to the points $g_{1\parallel}^* = g_{1\perp}^* = -2\pi v_F$ or $g_{1\parallel}^* = -g_{1\perp}^* = -2\pi v_F$. These are the two fixed points which are obtained from the zeros of the right-hand sides of the Lie equations. In the next order (Ting 1976) the value of the fixed point is further decreased, and instead of $-2\pi v_F$ the value $-0.87\pi v_F$ appears. Since these points are outside the region of applicability of a series expansion in eqns. (4.31)–(4.32), only the tendency that the problems are equivalent to a strong coupling problem should be taken seriously.

4.3. Determination of the response functions

As already mentioned, one of the aims of studying this model is to understand what kind of instabilities are likely to occur in the system. The best way to do this is to calculate response functions or generalized susceptibilities. The response of the system to various external perturbations can be considered and a singularity in the response is an indication that a spontaneous distortion or ordering can occur in the system. Following Dzyaloshinsky and Larkin (1971), Sólyom (1973) and Fukuyama *et al.* (1974 a), the response functions which are expected to be singular for a given range of the couplings are studied here, since they contain logarithmically singular terms in every order of perturbation theory. These quantities are the charge-density wave (CDW), spin-density wave (SDW), and the singlet-superconductor (SS) and triplet-superconductor (TS) response functions. An instability in the CDW or SDW response function shows that a CDW or SDW state is formed in the system with that value of the wave-vector, where the instability occurs first. This instability is expected to occur at $k = 2k_F$, reflecting the logarithmic singularity in the electron-hole bubble with this wave-vector. Singlet or triplet superconductivity is obtained if the response function of the singlet or triplet Cooper pairs is singular.

These functions, whose general formula is

$$R(k, \omega) = -i \int dt \exp(i\omega t) \langle T[\theta(k, t)\theta^+(k, 0)] \rangle, \quad (4.39)$$

are defined individually as follows.

(1) For the charge-density response function $N(k, \omega)$,

$$\mathcal{O}(k, t) = \frac{1}{L^{1/2}} \sum_{k_1} [b_{k_1\uparrow}^+(t)a_{k_1+k\uparrow}(t) + b_{k_1\uparrow}^+(t)a_{k_1+k\downarrow}(t)] \quad (4.40)$$

is the Fourier component of the charge-density for large momentum.

(2) For the spin-density response function $\chi(k, \omega)$,

$$\mathcal{O}(k, t) = \frac{1}{L^{1/2}} \sum_{k_1} [b_{k_1\uparrow}^+(t) a_{k_1+k\uparrow}(t) - b_{k_1\downarrow}^+(t) a_{k_1+k\downarrow}(t)] \quad (4.41)$$

or

$$\mathcal{O}(k, t) = \frac{1}{L^{1/2}} \sum_{k_1} [b_{k_1\uparrow}^+(t) a_{k_1+k\downarrow}(t) \pm b_{k_1\downarrow}^+(t) a_{k_1+k\uparrow}(t)] \quad (4.42)$$

are the Fourier components of the longitudinal and transverse spin densities for large momentum, which should be equal in the disordered phase.

(3) for the singlet-superconductor response $\Delta_s(k, \omega)$,

$$\mathcal{O}(k, t) = \frac{1}{L^{1/2}} \sum_{k_1} [b_{k_1\uparrow}(t) a_{-k_1+k\downarrow}(t) + a_{k_1\uparrow}(t) b_{-k_1+k\downarrow}(t)] \quad (4.43)$$

corresponds to singlet Cooper pairs.

(4) for the triplet-superconductor response $\Delta_t(k, \omega)$,

$$\mathcal{O}(k, t) = \frac{1}{L^{1/2}} \sum_{k_1} [b_{k_1\uparrow}(t) a_{-k_1+k\downarrow}(t) - a_{k_1\uparrow}(t) b_{-k_1+k\downarrow}(t)] \quad (4.44)$$

or

$$\mathcal{O}(k, t) = \frac{2}{L^{1/2}} \sum_{k_1} b_{k_1\alpha}(t) a_{-k_1+k\alpha}(t), \quad \alpha = \uparrow \text{ or } \downarrow \quad (4.45)$$

correspond to triplet Cooper pairs. The different forms correspond to different values of the spin projection ($S^z=0$ and $S^z=\pm 1$). The wave-vectors will be fixed at $k=2k_F$ in the density responses and to $k=0$ in the pairing functions.

Throughout the calculation the ω dependence was studied at $T=0$. The temperature dependence is easily obtained from this result, since in the logarithmic approximation $\ln(\omega/E_0)$ should be replaced by $\ln[\max(\omega, T)/E_0]$.

The perturbational expressions of these quantities are straightforwardly obtained as

$$\begin{aligned} N(\omega) = & \frac{1}{\pi v_F} \ln \frac{\omega}{E_0} \left[1 + \frac{1}{2\pi v_F} (g_{1\parallel} + g_{1\perp} - g_2) \ln \frac{\omega}{E_0} \right. \\ & + \frac{1}{12\pi^2 v_F^2} (2g_{1\parallel}^2 + 6g_{1\parallel}g_{1\perp} + 3g_{1\perp}^2 - 2g_{1\parallel}g_2 - 2g_{1\perp}g_2 + 2g_2^2) \ln^2 \frac{\omega}{E_0} \\ & \left. + \frac{1}{8\pi^2 v_F^2} (g_{1\parallel}^2 + g_{1\perp}^2 - 2g_{1\parallel}g_2 + 2g_2^2) \ln \frac{\omega}{E_0} + \dots \right], \end{aligned} \quad (4.46)$$

$$\begin{aligned} \chi(\omega) = & \frac{1}{\pi v_F} \ln \frac{\omega}{E_0} \left[1 - \frac{1}{2\pi v_F} g_2 \ln \frac{\omega}{E_0} + \frac{1}{12\pi^2 v_F^2} (2g_2^2 - g_{1\perp}^2) \ln^2 \frac{\omega}{E_0} \right. \\ & \left. + \frac{1}{8\pi^2 v_F^2} (g_{1\parallel}^2 + g_{1\perp}^2 - 2g_{1\parallel}g_2 + 2g_2^2) \ln \frac{\omega}{E_0} + \dots \right], \end{aligned} \quad (4.47)$$

$$\begin{aligned}\Delta_s(\omega) = & \frac{1}{\pi v_F} \ln \frac{\omega}{E_0} \left[1 + \frac{1}{2\pi v_F} (g_{1\perp} + g_2) \ln \frac{\omega}{E_0} \right. \\ & + \frac{1}{12\pi^2 v_F^2} (2g_{1\parallel} g_{1\perp} + 3g_{1\perp}^2 + 4g_{1\perp} g_2 + 2g_2^2) \ln^2 \frac{\omega}{E_0} \\ & \left. + \frac{1}{8\pi^2 v_F^2} (g_{1\parallel}^2 + g_{1\perp}^2 - 2g_{1\parallel} g_2 + 2g_2^2) \ln \frac{\omega}{E_0} + \dots \right] \quad (4.48)\end{aligned}$$

and

$$\begin{aligned}\Delta_t(\omega) = & \frac{1}{\pi v_F} \ln \frac{\omega}{E_0} \left[1 + \frac{1}{2\pi v_F} (-g_{1\parallel} + g_2) \ln \frac{\omega}{E_0} \right. \\ & + \frac{1}{12\pi^2 v_F^2} (2g_{1\parallel}^2 - 4g_{1\parallel} g_2 - g_{1\perp}^2 + 2g_2^2) \ln^2 \frac{\omega}{E_0} \\ & \left. + \frac{1}{8\pi^2 v_F^2} (g_{1\parallel}^2 + g_{1\perp}^2 - 2g_{1\parallel} g_2 + 2g_2^2) \ln \frac{\omega}{E_0} + \dots \right]. \quad (4.49)\end{aligned}$$

Everywhere, only the real part has been calculated.

These susceptibilities do not obey the scaling hypothesis of eqn. (4.22), but do obey the relation

$$R\left(\frac{\omega}{E'_0}, g'_{1\parallel}, g'_{1\perp}, g'_2\right) = z_R R\left(\frac{\omega}{E_0}, g_{1\parallel}, g_{1\perp}, g_2\right) + C\left(\frac{E'_0}{E_0}, g_{1\parallel}, g_{1\perp}, g_2\right). \quad (4.50)$$

The functions are not simply multiplicatively renormalized when the cut-off is scaled, as an addition constant appears. This constant disappears when eqn. (4.50) is differentiated with respect to ω , and the scaling equations can be used. It is more convenient to define the auxiliary functions \bar{R} , following a suggestion by Zawadowski, as

$$\bar{R}(\omega) = \pi v_F \frac{\partial R(\omega)}{\partial \ln \omega} \quad (4.51)$$

and to use the scaling equations for these functions. The Lie equations have the form

$$\frac{d \ln \bar{N}(x)}{dx} = \frac{1}{x} \left\{ \frac{1}{\pi v_F} [g_{1\parallel}^R(x) + g_{1\perp}^R(x) - g_2^R(x)] + F(x) + \dots \right\}, \quad (4.52)$$

$$\frac{d \ln \bar{\chi}(x)}{dx} = \frac{1}{x} \left\{ -\frac{1}{\pi v_F} g_2^R(x) + F(x) + \dots \right\}, \quad (4.53)$$

$$\frac{d \ln \bar{\Delta}_s(x)}{dx} = \frac{1}{x} \left\{ \frac{1}{\pi v_F} [g_{1\perp}^R(x) + g_2^R(x)] + F(x) + \dots \right\} \quad (4.54)$$

and

$$\frac{d \ln \bar{\Delta}_t(x)}{dx} = \frac{1}{x} \left\{ \frac{1}{\pi v_F} [-g_{1\parallel}^R(x) + g_2^R(x)] + F(x) + \dots \right\}, \quad (4.55)$$

where

$$F(x) = \frac{1}{4\pi^2 v_F^2} \left[g_{1\parallel}^{R2}(x) + g_{1\perp}^{R2}(x) - 2g_{1\parallel}^R(x)g_2^R(x) + 2g_2^{R2}(x) \right], \quad (4.56)$$

and $x = \omega/E_0$, or $x = T/E_0$ if the temperature dependence is studied.

Inserting the invariant couplings into these equations, the energy or temperature dependence of the response functions can be obtained. The invariant couplings are non-singular functions of x beyond the first approximation, and so any singularity in the response functions can appear at $x=0$ only, i.e. at $\omega=0$ and $T=0$. The leading behaviour at small x is obtained by inserting the invariant couplings at $x=0$, i.e. the fixed-point values.

According to the discussion in § 4.2, the scaling curves go to the fixed line $g_{1\perp}^*=0$ if $|g_{1\parallel}| \geq |g_{1\perp}|$ is satisfied for the original couplings. The fixed-point value of $g_{1\parallel}$ is not universal; in a first approximation

$$g_1^* \approx \sqrt{(g_{1\parallel}^2 - g_{1\perp}^2)} \quad \text{and} \quad g_2^* \approx g_2 - \frac{1}{2}g_{1\parallel} + \frac{1}{2}\sqrt{(g_{1\parallel}^2 - g_{1\perp}^2)}. \quad (4.57)$$

Since the fixed-point value is small, the higher-order corrections in eqns. (4.52)–(4.55) can be neglected and the solution of the equations gives, for the leading terms,

$$N(x) \sim x^\alpha, \quad \alpha = \frac{1}{2}g_{1\parallel} - g_2 + \frac{1}{2}g_1^* + \dots, \quad (4.58)$$

$$\chi(x) \sim x^\beta, \quad \beta = \frac{1}{2}g_{1\parallel} - g_2 - \frac{1}{2}g_1^* + \dots, \quad (4.59)$$

$$\Delta_s(x) \sim x^\gamma, \quad \gamma = -\frac{1}{2}g_{1\parallel} + g_2 + \frac{1}{2}g_1^* + \dots \quad (4.60)$$

$$\Delta_t(x) \sim x^\delta, \quad \delta = -\frac{1}{2}g_{1\parallel} + g_2 - \frac{1}{2}g_1^* + \dots. \quad (4.61)$$

The result is very simple for spin-independent couplings. In this case $g_{1\parallel}^* = 0$ and, depending on the sign of $\frac{1}{2}g_1 - g_2$, either the density response functions or the pairing responses are singular at $\omega=0$.

The domain of attraction of the fixed point $g_{1\parallel}^* = g_{1\perp}^* = -2\pi v_F$, $g_2^* = g_2 - \frac{1}{2}g_{1\parallel} - \pi v_F$ is $g_{1\parallel} < |g_{1\perp}|$ and $g_{1\perp} < 0$, whereas for the fixed point $g_{1\parallel}^* = -g_{1\perp}^* = -2\pi v_F$, $g_2^* = g_2 - \frac{1}{2}g_{1\parallel} - \pi v_F$ it is $g_{1\perp} > 0$ and $g_{1\parallel} < g_{1\perp}$. Since the fixed-point value is not well determined in the approximation considered in § 4.2, and since the higher-order corrections in eqns. (4.52)–(4.55) cannot be neglected, only a rough estimate of the exponents can be obtained. In second-order scaling,

$$N(x) \sim x^\alpha, \quad \alpha = \begin{cases} \frac{5}{2} + \frac{1}{\pi v_F}(\frac{1}{2}g_{1\parallel} - g_2) & \text{if } g_{1\perp} > 0 \\ -\frac{3}{2} + \frac{1}{\pi v_F}(\frac{1}{2}g_{1\parallel} - g_2) & \text{if } g_{1\perp} < 0, \end{cases} \quad (4.62)$$

$$\chi(x) \sim x^\beta, \quad \beta = \frac{5}{2} + \frac{1}{\pi v_F}(\frac{1}{2}g_{1\parallel} - g_2), \quad (4.63)$$

$$\Delta_s(x) \sim x^\gamma, \quad \gamma = \begin{cases} \frac{5}{2} - \frac{1}{\pi v_F}(\frac{1}{2}g_{1\parallel} - g_2) & \text{if } g_{1\perp} > 0 \\ -\frac{3}{2} - \frac{1}{\pi v_F}(\frac{1}{2}g_{1\parallel} - g_2) & \text{if } g_{1\perp} < 0 \end{cases} \quad (4.64)$$

and

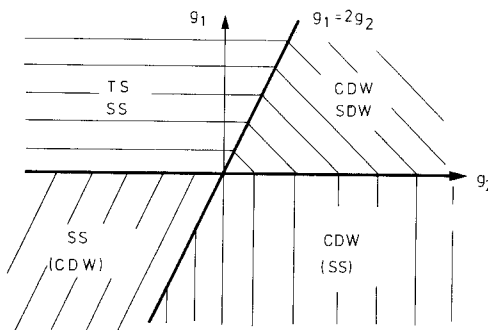
$$\Delta_t(x) \sim x^\delta, \quad \delta = \frac{5}{2} - \frac{1}{\pi v_F}(\frac{1}{2}g_{1\parallel} - g_2). \quad (4.65)$$

Singularity can appear in the charge-density response function and in the singlet-superconductor response if $g_{1\perp} < 0$. The exponents are certainly modified by higher-

order corrections; in the next approximation (Ting 1976) the exponent $-\frac{3}{2}$ is changed to -1.02 . It can be assumed, however, that the tendency is correctly obtained, only the charge-density and singlet-superconductor responses are divergent for $g_{1\perp} < 0$. The singularity in the singlet-superconductor response is stronger if $\frac{1}{2}g_{1\parallel} - g_2 > 0$; on the other hand, for $\frac{1}{2}g_{1\parallel} - g_2 < 0$ the charge-density response is more strongly divergent.

The results are summarized in fig. 13, where the phase diagram is shown, i.e. the possible ground states of the system inferred from the singularity of the response function are indicated for spin-independent couplings in the (g_1, g_2) plane. The solution is probably quite good in the upper half-plane ($g_1 > 0$); however, there may be doubts concerning the results obtained for $g_1 < 0$. In the following paragraphs other approaches will be considered which—combined with the scaling argument—can provide a better treatment of the model.

Fig. 13



Phase diagram of the 1-d Fermi gas obtained in the second-order scaling approximation. The response functions corresponding to the phases indicated in parentheses have a lower degree of divergence than the others.

There is yet another response function which is of interest when a comparison is made with the behaviour of quasi-1-d materials. This is the $4k_F$ response function $\Pi(4k_F, \omega)$ calculated by Lee *et al.* (1977), using the renormalization group approach. Without considering the mechanism by which the $4k_F$ fluctuations are excited by two-particle interactions, the response function $\Pi(4k_F, \omega)$ is defined through eqn. (4.39) with

$$\mathcal{O}(4k_F, t) = \frac{1}{L^{3/2}} \sum_{k_1, k_2, k_3} b_{k_1\uparrow}^+(t) b_{k_2\downarrow}^+(t) a_{k_3\downarrow}(t) a_{k_1+k_2-k_3+4k_F\uparrow}(t) \quad (4.66)$$

A straightforward perturbational calculation gives

$$\Pi(\omega) = \text{const.} + \frac{1}{32\pi^3 v_F^3} \omega^2 \ln \frac{\omega}{E_0} \left[1 + \frac{1}{\pi v_F} (g_{1\parallel} - 2g_2) \ln \frac{\omega}{E_0} + \dots \right]. \quad (4.67)$$

Since the factor ω^2 appears in the contribution of all diagrams, and the remaining logarithms can give an extra power, the function

$$\Pi'(\omega) = \frac{1}{\pi v_F} \ln \frac{\omega}{E_0} \left[1 + \frac{1}{\pi v_F} (g_{1\parallel} - 2g_2) \ln \frac{\omega}{E_0} + \dots \right] \quad (4.68)$$

can be studied. Assuming that the function Π' defined by eqn. (4.51) from the truncated function satisfies the scaling equation,

$$\frac{d \ln \Pi'(x)}{dx} = \frac{1}{x} \left\{ \frac{2}{\pi v_F} [g_{1\parallel}^R(x) - 2g_2^R(x)] + \dots \right\}. \quad (4.69)$$

Since the combination $g_{1\parallel} - 2g_2$ is invariant under scaling, for the $4k_F$ response function when the factor ω^2 is taken into account becomes

$$\Pi(\omega) \sim \omega^{2+(2/\pi v_F)(g_{1\parallel} - 2g_2) + \dots} \quad (4.70)$$

A singularity can appear, provided $g_{1\parallel} - 2g_2$ has a large negative value at which the higher-order corrections are not negligible. As is shown later, an exact solution of this problem can be obtained. It will still be true that $\Pi(\omega)$ is singular for large negative $g_{1\parallel} - 2g_2$.

§5. EXACT SOLUTION OF THE TOMONAGA-LUTTINGER MODEL

The Tomonaga model (Tomonaga 1950) is that particular case of the Fermi gas model in which the large momentum transfer interactions are neglected. These are the $g_{1\perp}$ and g_3 terms in the Hamiltonian. In the model with bandwidth cut-off, $g_{4\parallel}$ gives no contribution and the effect of $g_{1\parallel}$ is indistinguishable from that of $g_{2\parallel}$; therefore three couplings, $g_{2\parallel}$, $g_{2\perp}$ and $g_{4\perp}$ remain. It follows from the scaling equations (4.31)–(4.33) and the more detailed treatment presented in §7, where all the couplings are considered, that the couplings do not become renormalized when $g_{1\perp} = g_3 = 0$, i.e. the invariant couplings are the same as the bare couplings. Consequently, $g_{1\perp}$ itself remains zero in the equivalent models. This model is of particular interest since—as will be seen—models with $g_{1\perp} \neq 0$ and $g_3 \neq 0$ can be scaled onto it if $|g_{1\parallel}| \geq |g_{1\perp}|$ and $|g_{1\parallel} - 2g_2| \geq |g_3|$. It turns out that the Tomonaga model can be solved exactly, so the solution of the Fermi gas model is known for the models which belong to the domain of attraction of the Tomonaga fixed points.

In the usual treatments of the Tomonaga model the dispersion relation is that shown in fig. 3, and a momentum transfer cut-off is used instead of the bandwidth cut-off. In this case $g_{4\parallel}$ gives a finite contribution coming from the first-order self-energy corrections shown in fig. 14. The contributions of the two processes cancel each other out in the model with bandwidth cut-off; with momentum transfer cut-off, however, the cancellation is not complete and a contribution proportional to the incoming momentum is obtained, which leads to a Fermi velocity renormalization. In the higher-order diagrams the difference between the two kinds of cut-off is not important and either can be used. Another complication can arise from the $g_{1\parallel}$ and $g_{2\parallel}$ processes which become inequivalent in the model with momentum transfer cut-off; the problem of cut-offs will be considered in §9. In this section momentum transfer cut-off is used and the coupling $g_{2\parallel}$ will be considered together with $g_{2\perp}$, $g_{4\parallel}$ and $g_{4\perp}$.

Fig. 14



First-order self-energy diagrams.

A similar model was proposed by Luttinger (1963). (The free-particle spectrum is linear, as shown in fig. 4.) Compared to the Tomonaga model new states are introduced, far from the Fermi points, which are all filled in the ground state. Since it is usually assumed that only electrons and holes lying in the neighbourhood of the Fermi surface are important in physical processes, the Luttinger and Tomonaga models are equivalent. Mathematically, it is more convenient to work with the Luttinger model. The results—at least in the weak coupling case, when the states with electrons and holes far from the Fermi surface can be neglected—can also be applied to the Tomonaga model.

5.1. Green's function in the Tomonaga–Luttinger model

Dzyaloshinsky and Larkin (1973) have shown that the Green's function of the Tomonaga model can be calculated exactly in a simple form in real space and time representation. This is the consequence of two essential features of the model, namely that the dispersion relation is linear and that the number of particles in each branch and for each spin direction is conserved in every scattering process. They lead to the cancellation of many contributions and to a simple Ward identity and allow an exact summation of the contributions.

The Green's functions of the unperturbed system, denoted by $G_+^{(0)}(k, \omega)$ and $G_-^{(0)}(k, \omega)$ corresponding to electrons on the two different branches, are

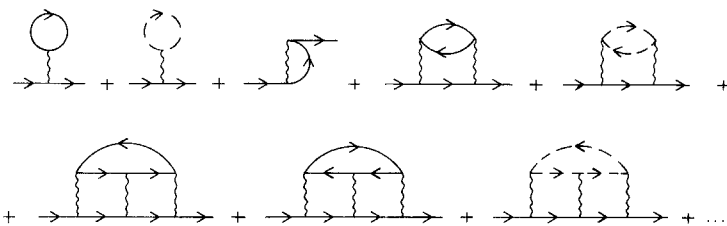
$$G_+^{(0)}(k, \omega) = \frac{1}{\omega - v_F(k - k_F) + i\delta \operatorname{sign}(k - k_F)} \quad (5.1)$$

and

$$G_-^{(0)}(k, \omega) = \frac{1}{\omega - v_F(-k - k_F) + i\delta \operatorname{sign}(-k - k_F)}.$$

The low-order self-energy diagrams are shown in fig. 15. The diagrams contain one solid line connecting the incoming and outgoing lines and may contain several

Fig. 15



Low-order self-energy diagrams in the Tomonaga model for electrons on the right going branch.

loops, but solid and dashed lines never mix in the loops. This is due to the neglect of backward scattering processes. In the calculation of the contributions, the relations

$$G_+^{(0)}(k+p, \omega + \varepsilon) G_+^{(0)}(k, \omega) = \frac{1}{\varepsilon - v_F p} [G_+^{(0)}(k, \omega) - G_+^{(0)}(k+p, \omega + \varepsilon)] \quad (5.2)$$

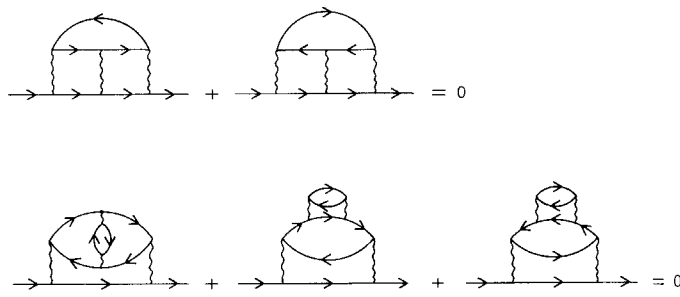
and

$$G_-^{(0)}(k+p, \omega + \varepsilon) G_-^{(0)}(k, \omega) = \frac{1}{\varepsilon + v_F p} [G_-^{(0)}(k, \omega) - G_-^{(0)}(k+p, \omega + \varepsilon)] \quad (5.3)$$

can be used, which represent the consequences of linear dispersion. It turns out that all the diagrams which contain loops with more than two interaction vertices are cancelled; such mutually cancelling diagrams are shown in fig. 16.

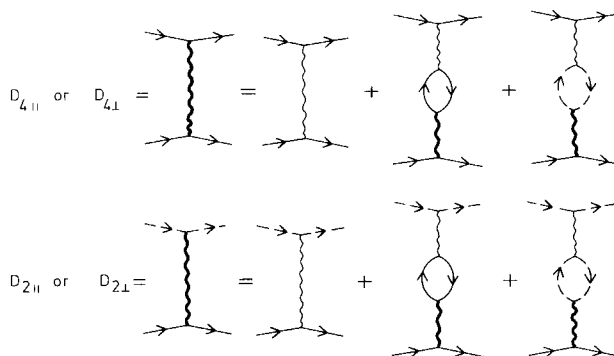
As a consequence of this cancellation the remaining self-energy diagrams may contain bubbles and series of bubbles only. The series of bubbles can easily be summed, leading to effective interactions. The diagrammatic equations for the effective g_2 - and g_4 -type interactions are shown in fig. 17.

Fig. 16



Self-energy diagrams with cancelling contributions.

Fig. 17



Diagrammatic equations for the effective interactions. The diagrammatic equations are the same for parallel and antiparallel spin orientations.

Denoting the effective couplings by $D_{2\parallel}$, $D_{2\perp}$, $D_{4\parallel}$ and $D_{4\perp}$, these equations have simple algebraic forms:

$$\begin{aligned} D_{4\parallel} = & g_{4\parallel} \Pi_+ D_{4\parallel} + g_{4\perp} \Pi_+ D_{4\perp} \\ & + g_{2\parallel} \Pi_- D_{2\parallel} + g_{2\perp} \Pi_- D_{2\perp}, \end{aligned} \quad (5.4)$$

$$\begin{aligned} D_{4\perp} = & g_{4\perp} \Pi_+ D_{4\perp} + g_{4\parallel} \Pi_+ D_{4\parallel} \\ & + g_{2\parallel} \Pi_- D_{2\perp} + g_{2\perp} \Pi_- D_{2\parallel}, \end{aligned} \quad (5.5)$$

$$\begin{aligned} D_{2\parallel} = & g_{2\parallel} \Pi_+ D_{4\parallel} + g_{2\perp} \Pi_+ D_{4\perp} \\ & + g_{4\parallel} \Pi_- D_{2\parallel} + g_{4\perp} \Pi_- D_{2\perp} \end{aligned} \quad (5.6)$$

and

$$\begin{aligned} D_{2\perp} = & g_{2\perp} \Pi_+ D_{4\perp} + g_{2\parallel} \Pi_+ D_{4\parallel} \\ & + g_{4\parallel} \Pi_- D_{2\perp} + g_{4\perp} \Pi_- D_{2\parallel}, \end{aligned} \quad (5.7)$$

where Π_+ and Π_- are the polarization bubbles for electrons on the positive and negative branches, respectively, for one spin orientation.

Equations (5.4)–(5.7) are solved by using the expressions

$$\Pi_+(k, \omega) = \frac{k}{2\pi(\omega - v_F k)} \quad \text{and} \quad \Pi_-(k, \omega) = -\frac{k}{2\pi(\omega + v_F k)}. \quad (5.8)$$

For example the solution of eqn. (5.4) for $D_{4\parallel}$, which couples two electrons on the positive branch, is

$$\begin{aligned} D_{4\parallel}(k, \omega) = & (\omega - v_F k) \left[\frac{A}{\omega - u_\sigma k + i\delta \operatorname{sign} k} + \frac{B}{\omega + u_\sigma k - i\delta \operatorname{sign} k} \right. \\ & \left. + \frac{C}{\omega - u_p k + i\delta \operatorname{sign} k} + \frac{D}{\omega + u_p k - i\delta \operatorname{sign} k} \right], \end{aligned} \quad (5.9)$$

where

$$u_\sigma^2 = \left[v_F + \frac{1}{2\pi} (g_{4\parallel} - g_{4\perp}) \right]^2 - \left[\frac{1}{2\pi} (g_{2\parallel} - g_{2\perp}) \right]^2, \quad (5.10)$$

$$u_p^2 = \left[v_F + \frac{1}{2\pi} (g_{4\parallel} + g_{4\perp}) \right]^2 - \left[\frac{1}{2\pi} (g_{2\parallel} + g_{2\perp}) \right]^2, \quad (5.11)$$

$$A = \frac{1}{4} (g_{4\parallel} - g_{4\perp}) + \frac{1}{4u_\sigma} \left[v_F (g_{4\parallel} - g_{4\perp}) + \frac{1}{2\pi} (g_{4\parallel} - g_{4\perp})^2 - \frac{1}{2\pi} (g_{2\parallel} - g_{2\perp})^2 \right], \quad (5.12)$$

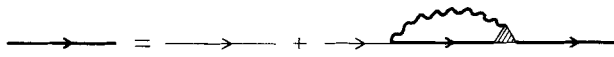
$$B = \frac{1}{4} (g_{4\parallel} - g_{4\perp}) - \frac{1}{4u_\sigma} \left[v_F (g_{4\parallel} - g_{4\perp}) + \frac{1}{2\pi} (g_{4\parallel} - g_{4\perp})^2 - \frac{1}{2\pi} (g_{2\parallel} - g_{2\perp})^2 \right], \quad (5.13)$$

$$C = \frac{1}{4} (g_{4\parallel} + g_{4\perp}) + \frac{1}{4u_p} \left[v_F (g_{4\parallel} + g_{4\perp}) + \frac{1}{2\pi} (g_{4\parallel} + g_{4\perp})^2 - \frac{1}{2\pi} (g_{2\parallel} + g_{2\perp})^2 \right] \quad (5.14)$$

and

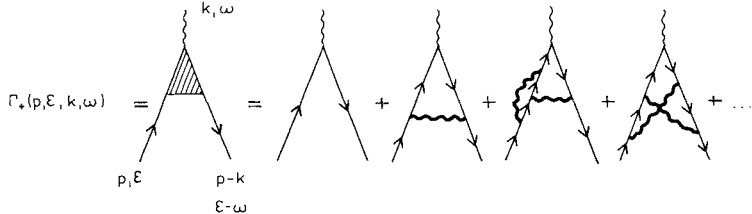
$$D = \frac{1}{4} (g_{4\parallel} + g_{4\perp}) - \frac{1}{4u_p} \left[v_F (g_{4\parallel} + g_{4\perp}) + \frac{1}{2\pi} (g_{4\parallel} + g_{4\perp})^2 - \frac{1}{2\pi} (g_{2\parallel} + g_{2\perp})^2 \right]. \quad (5.15)$$

Fig. 18



Dyson equation for the Green's function.

Fig. 19



Three-legged vertex appearing in the Dyson equation.

It should be noted that the effective coupling between two electrons on the negative branch is somewhat different.

The Dyson equation for the Green's function is given in fig. 18. The three-legged vertex appearing in it again contains only effective interactions, as shown in fig. 19. It is denoted by $\Gamma_+(p, \varepsilon, k, \omega)$. A similar vertex, $\Gamma_-(p, \varepsilon, k, \omega)$, can be introduced for electrons on the negative branch.

From eqns. (5.2) and (5.3), the Ward identity

$$\Gamma_+(p, \varepsilon, k, \omega) = \frac{G_+^{-1}(p, \varepsilon) - G_+^{-1}(p - k, \varepsilon - \omega)}{\omega - v_F k} \quad (5.16)$$

can be derived and, analogously,

$$\Gamma_-(p, \varepsilon, k, \omega) = \frac{G_-^{-1}(p, \varepsilon) - G_-^{-1}(p - k, \varepsilon - \omega)}{\omega + v_F k}. \quad (5.17)$$

It should be emphasized that the Ward identities are direct consequence of the conservation of the number of particles in each branch for each spin orientation and of the linear dispersion relation. They can also be obtained by writing the equation of motion for the vertex Γ_{\pm} (Everts and Schulz 1974). The Ward identity allows the Dyson equation to be expressed as the closed integral equation

$$[\varepsilon - v_F(p - k_F)]G_+(p, \varepsilon) = 1 + \frac{i}{4\pi^2} \int dk d\omega \frac{D_{4||}(k, \omega)}{\omega - v_F k} G_+(p - k, \varepsilon - \omega), \quad (5.18)$$

where the term leading to Fermi energy renormalization has been neglected.

A simple solution of this equation, obtained by transforming it to real space and time, is

$$\begin{aligned} G_+(x, t) &= \frac{1}{2\pi} \frac{1}{x - v_F t + i\delta(t)} \frac{x - v_F t + i/\Lambda(t)}{[x - u_\sigma t + i/\Lambda(t)]^{1/2} [x - u_p t + i/\Lambda(t)]^{1/2}} \\ &\times [\Lambda^2(x - u_\sigma t + i/\Lambda(t)) (x + u_\sigma t - i/\Lambda(t))]^{-\alpha_\sigma} \\ &\times [\Lambda^2(x - u_p t + i/\Lambda(t)) (x + u_p t - i/\Lambda(t))]^{-\alpha_p}, \end{aligned} \quad (5.19)$$

where

$$\alpha_\sigma = \frac{1}{4u_\sigma} \left[v_F + \frac{1}{2\pi} (g_{4\parallel} - g_{4\perp}) - u_\sigma \right] \quad (5.20)$$

and

$$\alpha_\rho = \frac{1}{4u_\rho} \left[v_F + \frac{1}{2\pi} (g_{4\parallel} + g_{4\perp}) - u_\rho \right] \quad (5.21)$$

In the calculation a smooth cut-off is used for the momentum transfer, i.e. a factor $\exp(-|k|/\Lambda)$ is introduced in the effective interaction and $\Lambda(t) = \Lambda \operatorname{sign} t$. A band-width cut-off $\delta \sim 1/k_F$ ($\delta(t) = \delta \operatorname{sign} t$) should also appear in the free Green's function.

The analytic expression of the Green's function is complicated in momentum space. The interesting feature of the solution is that the Green's function has a branch cut instead of the usual pole structure. The cut is between $\varepsilon = u_\sigma(p - k_F)$ and $\varepsilon = u_\rho(p - k_F)$. The influence of the branch cut is negligible for electrons far from the Fermi surface. Near the Fermi surface, however, a drastic change occurs compared to normal Fermi systems. As a consequence of the branch cut, the momentum distribution $n(p)$ (Luttinger 1963, Gutfreund and Schick 1968) has a power-law-type behaviour at the Fermi points

$$n(p) = \frac{1}{2} - \text{const.} |p \mp k_F|^{2\alpha_\sigma + 2\alpha_\rho} \operatorname{sign}(\pm p - k_F), \quad (5.22)$$

with infinite slope at $p = \pm k_F$, since both α_σ and α_ρ are small positive numbers in the weak coupling case. This has to be contrasted with the jump discontinuity in normal Fermi systems. The difference in the distribution function is an indication that the usual quasi-particle picture breaks down in the Tomonaga model—that the excitations of the system are collective excitations. On the other hand, the effective interactions are very similar to boson propagators. Equation (5.9) can be interpreted as describing the propagation of two bosons, one with velocity u_σ the other with velocity u_ρ . These bosons are the density fluctuations of the fermion system. It will be shown in § 5.3 that the Tomonaga model can in fact be solved in terms of boson fields related to the densities.

5.2. Response functions of the Tomonaga–Luttinger model

Arguments similar to those applied in the calculation of the Green's function can be used for the response functions. The same response functions will be studied as in § 4.3. It will be seen that, as before, they have a simple form in real space and time representation. These charge-density and spin-density response functions correspond to large momentum transfer. The same response functions can also be calculated for small k and ω in momentum representation. In this case

$$\begin{aligned} \mathcal{O}(k, t) = & \frac{1}{L^{1/2}} \sum_{k_1} [a_{k_1\uparrow}^+(t) a_{k_1+k\uparrow}(t) \\ & + b_{k_1\uparrow}^+(t) b_{k_1+k\uparrow}(t) + a_{k_1\downarrow}^+(t) a_{k_1+k\downarrow}(t) + b_{k_1\downarrow}^+(t) b_{k_1+k\downarrow}(t)] \end{aligned} \quad (5.23)$$

for the charge-density response, and

$$\begin{aligned} \mathcal{O}(k, t) = & \frac{1}{L^{1/2}} \sum_{k_1} [a_{k_1\uparrow}^+(t) a_{k_1+k\uparrow}(t) \\ & + b_{k_1\uparrow}^+(t) b_{k_1+k\uparrow}(t) - a_{k_1\downarrow}^+(t) a_{k_1+k\downarrow}(t) - b_{k_1\downarrow}^+(t) b_{k_1+k\downarrow}(t)] \end{aligned} \quad (5.24)$$

for the spin-density response. The diagrams which contribute to these response functions are the bubble series diagrams, as in the effective couplings, i.e. the external vertices are connected with a bubble series. It is found that

$$N(k, \omega) = \frac{2}{\pi} \gamma_{\rho} \frac{u_{\rho} k^2}{\omega^2 - u_{\rho}^2 k^2}, \quad \chi(k, \omega) = \frac{2}{\pi} \gamma_{\sigma} \frac{u_{\sigma} k^2}{\omega^2 - u_{\sigma}^2 k^2}, \quad (5.25)$$

where

$$\gamma_{\sigma} = \left[\frac{1 + \frac{1}{2\pi v_F} (g_{4||} - g_{4\perp}) - \frac{1}{2\pi v_F} (g_{2||} - g_{2\perp})}{1 + \frac{1}{2\pi v_F} (g_{4||} - g_{4\perp}) + \frac{1}{2\pi v_F} (g_{2||} - g_{2\perp})} \right]^{1/2} \quad (5.26)$$

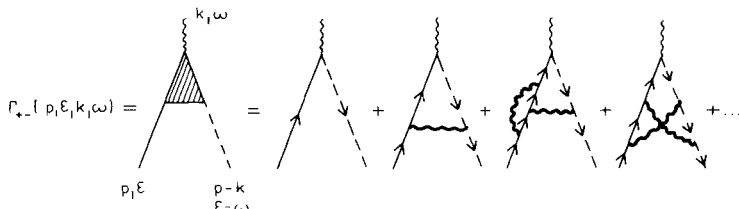
and

$$\gamma_{\rho} = \left[\frac{1 + \frac{1}{2\pi v_F} (g_{4||} + g_{4\perp}) - \frac{1}{2\pi v_F} (g_{2||} + g_{2\perp})}{1 + \frac{1}{2\pi v_F} (g_{4||} + g_{4\perp}) + \frac{1}{2\pi v_F} (g_{2||} + g_{2\perp})} \right]^{1/2} \quad (5.27)$$

This result shows that the density fluctuations with velocity u_{σ} are in fact spin-density fluctuations, whereas those with velocity u_{ρ} are charge-density fluctuations.

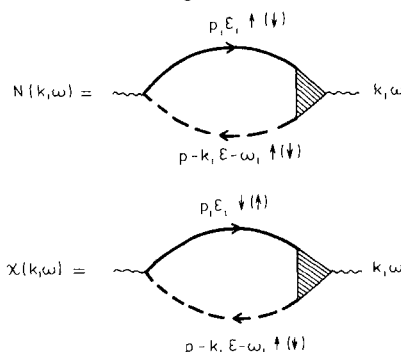
Turning now to the density responses at $2k_F$ and to the pairing functions, it is still the case that apart from the two lines connecting the external vertices of the response functions, only simple bubbles should appear. A new vertex Γ_{+-} can be introduced which corresponds to large momentum transfer, the incoming and outgoing electrons being on different branches; it is shown in fig. 20. The charge-density and spin-density response functions can be written in terms of this vertex, as shown diagrammatically in fig. 21.

Fig. 20



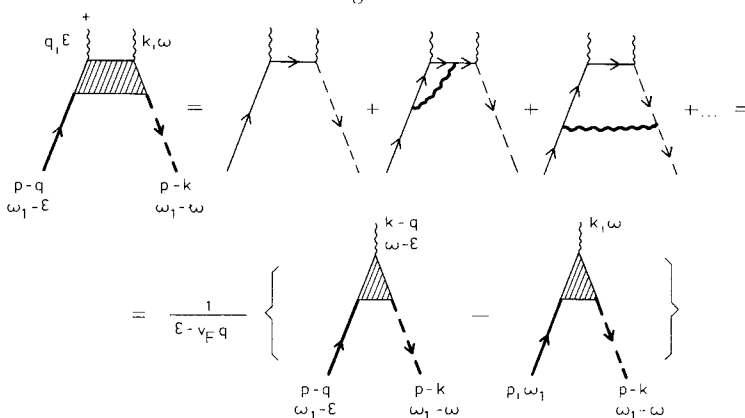
Vertex with a large momentum transfer.

Fig. 21



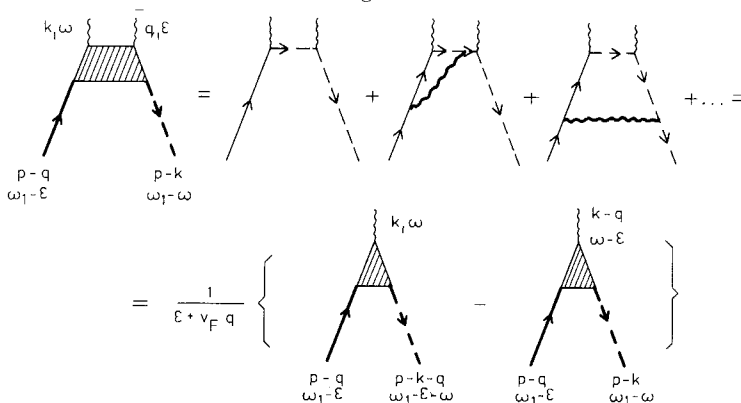
Diagrammatic representation of the charge-density and transverse spin-density response functions.

Fig. 22



Four-legged vertex with a large momentum transfer interaction, and with a small momentum transfer interaction, coupling two electrons on the positive branch.

Fig. 23



Four-legged vertex with a large momentum transfer interaction, and with a small momentum transfer interaction, coupling two electrons on the negative branch.

The vertex Γ_{+-} is not related to the Green's functions by a simple Ward identity. A generalized Ward identity can, however, be derived which relates Γ_{+-} to vertices with two electron lines and two interaction lines. Consider a vertex in which the incoming and outgoing electrons belong to different branches, one interaction line corresponds to the coupling to the external field with large momentum transfer, the other interaction line couples to electrons on the positive branch; this vertex is shown in fig. 22. Using eqn. (5.2) or the Ward identity in eqn. (5.16), this vertex can be expressed in terms of Γ_{+-} , as also shown in fig. 22. A similar four-legged vertex can be introduced in which the interaction line couples to electrons on the negative branch. A generalized Ward identity can be derived for this vertex too, as shown in fig. 23. These relations are valid only if the self-energy corrections on the external Green's function legs are also taken into account.

The response functions can be expressed with the help of the four-legged vertices as shown, for example, for $N(k, \omega)$ in fig. 24. The spin-density response $\chi(k, \omega)$ can be written similarly, with $D_{2\perp}$ instead of $D_{2\parallel}$. By comparing the two representations of

Fig. 24



Diagrammatic representation of the charge-density response in terms of the four-legged vertices shown in figures 22 and 23.

the response functions in figs. 21 and 24 and using the relations given in figs. 22 and 23, the vertex Γ_{+-} and the response functions can be calculated. Solving the integral equation in real space and time gives

$$\begin{aligned} N(x, t) = & -2iG_+(x, t)G_-(-x, -t) \\ & \times [\Lambda^2(x - u_\sigma t + i/\Lambda(t))(x + u_\sigma t - i/\Lambda(t))]^{\beta_\sigma} \\ & \times [\Lambda^2(x - u_\rho t + i/\Lambda(t))(x + u_\rho t - i/\Lambda(t))]^{\beta_\rho}, \end{aligned} \quad (5.28)$$

where

$$\beta_\sigma = \frac{1}{4\pi u_\sigma}(g_{2\parallel} - g_{2\perp}) \quad \text{and} \quad \beta_\rho = \frac{1}{4\pi u_\rho}(g_{2\parallel} + g_{2\perp}). \quad (5.29)$$

$\chi(x, t)$ has the same structure as $N(x, t)$ except that the exponent β_σ is replaced by $-\beta_\sigma$.

A similar calculation performed for the pairing functions gives

$$\begin{aligned} \Delta_s(x, t) = & 2iG_+(x, t)G_-(x, t) \\ & \times [\Lambda^2(x - u_\sigma t + i/\Lambda(t))(x + u_\sigma t - i/\Lambda(t))]^{\beta_\sigma} \\ & \times [\Lambda^2(x - u_\rho t + i/\Lambda(t))(x + u_\rho t - i/\Lambda(t))]^{-\beta_\rho}. \end{aligned} \quad (5.30)$$

The triplet-superconductor response is obtained by replacing β_σ by $-\beta_\sigma$. In the case of spin-independent couplings these expressions reduce to those obtained by Fogedby (1976) by a different method.

The analytic expressions of the response functions in (k, ω) representation are quite involved. Their asymptotic form can, however, be obtained from dimensionality arguments when ω and $v_F(k - 2k_F)$ or $v_F k$ are small and of the same order of magnitude:

$$N(\omega \sim v_F(k - 2k_F)) \sim \omega^{\gamma_\sigma + \gamma_\rho - 2}, \quad (5.31)$$

$$\chi(\omega \sim v_F(k - 2k_F)) \sim \omega^{1/\gamma_\sigma + \gamma_\rho - 2}, \quad (5.32)$$

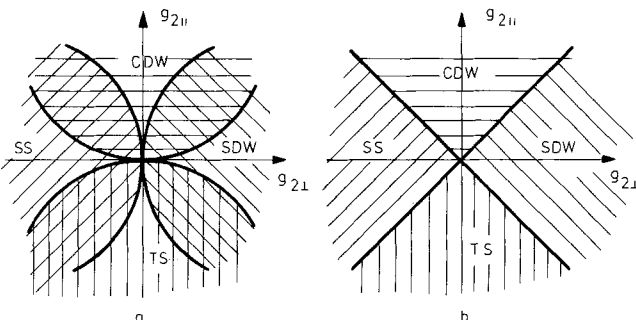
$$\Delta_s(\omega \sim v_F k) \sim \omega^{\gamma_\sigma + 1/\gamma_\rho - 2} \quad (5.33)$$

and

$$\Delta_t(\omega \sim v_F k) \sim \omega^{1/\gamma_\sigma + 1/\gamma_\rho - 2}, \quad (5.34)$$

where γ_σ and γ_ρ are given by eqns. (5.26) and (5.27). Expanding the exponents in powers of the couplings, neglecting g_4 and taking into account that the choice of the couplings in § 4.3 corresponds to $g_{2\parallel} \rightarrow g_2 - g_{1\parallel}$ and $g_{2\perp} \rightarrow g_2$, it is seen from eqns. (4.58)–(4.61) that the renormalization group treatment in its first approximation gives the first terms in the exponents. Higher-order terms in the Lie equations could

Fig. 25



Phase diagram of the spin-dependent Tomonaga model. (a) The regions where the various response functions are singular; (b) the phase diagram obtained from the dominant singularity.

produce the higher-order terms in the exponents. The branch cut in the Green's function is not obtained by this simple scaling procedure, since it comes from non-logarithmic terms which have been neglected in the scaling.

The phase diagram analogous to the one shown in fig. 13 is shown in fig. 25 in the $(g_{2\parallel}, g_{2\perp})$ plane. There are such regions in the plane of couplings where two response functions diverge. Assuming that the leading singularity will determine the structure of the system, the phase diagram is a very simple one: the different phases are separated by the diagonals $g_{2\parallel} = g_{2\perp}$ and $g_{2\parallel} = -g_{2\perp}$.

Generalized Ward identities can also be used in the calculation of the $4k_F$ response function. A straightforward but tedious calculation of the Fourier transform of $\Pi(k \sim 4k_F, \omega)$ defined by eqns. (4.39) and (4.66) leads to the result

$$\begin{aligned} \Pi(x, t) = & G_+(x, t)G_+(x, t)G_-(-x, -t)G_-(-x, -t) \\ & \times \frac{(x - u_\sigma t + i/\Lambda(t))(x + u_\sigma t - i/\Lambda(t))}{(x - u_\rho t + i/\Lambda(t))(x + u_\rho t - i/\Lambda(t))} \\ & \times [\Lambda^2(x - u_\sigma t + i/\Lambda(t))(x + u_\sigma t - i/\Lambda(t))]^{4\alpha_\sigma} \\ & \times [\Lambda^2(x - u_\rho t + i/\Lambda(t))(x + u_\rho t - i/\Lambda(t))]^{-4\alpha_\rho + 4\beta_\rho}, \end{aligned} \quad (5.35)$$

where α and β are given by eqns. (5.20), (5.21) and (5.29). Inserting the expressions for the Green's functions

$$\begin{aligned} \Pi(x, t) = & \left[\frac{(x - v_F t + i/\Lambda(t))(x + v_F t - i/\Lambda(t))}{(x - v_F t + i\delta(t))(x + v_F t - i\delta(t))} \right]^2 \\ & \times [\Lambda^2(x - u_\rho t + i/\Lambda(t))(x + u_\rho t - i/\Lambda(t))]^{-2\gamma_\rho}, \end{aligned} \quad (5.36)$$

where γ_ρ is given by eqn. (5.27). It is interesting to note that this response function depends only on the charge-density modes, as noticed by Emery (1976 a). In the spin-independent case this result agrees with his result and with the result obtained by Klemm and Larkin (1978).

5.3. Boson representation of the Tomonaga–Luttinger Hamiltonian

In § 5.2 it has been shown that two kinds of boson-like collective excitation appear in the Tomonaga–Luttinger model, one of which corresponds to long-wavelength charge-density oscillations and the other to spin-density oscillations. Mattis and Lieb (1965) showed that the Luttinger model Hamiltonian can be written in terms of boson operators in a diagonal form and the exact spectrum is easily obtained.

The density operators for the two branches are defined as

$$\begin{aligned}\rho_{1\alpha}(p) &= \sum_k a_{k+p\alpha}^+ a_{k\alpha}, & \rho_{1\alpha}(-p) &= \sum_k a_{k\alpha}^+ a_{k+p\alpha}, \\ \rho_{2\alpha}(p) &= \sum_k b_{k+p\alpha}^+ b_{k\alpha}, & \rho_{2\alpha}(-p) &= \sum_k b_{k\alpha}^+ b_{k+p\alpha},\end{aligned}\tag{5.37}$$

where $p > 0$. The summation over k goes for the whole branch in the Luttinger model; in the Tomonaga model, however, the momenta k and $k+p$ should belong to the same branch: for example, in $\rho_{2\alpha}(p)$ the summation goes for $k < -p$. These operators obey the boson-like commutation relations

$$[\rho_{1\alpha}(-p), \rho_{1\beta}(p')] = [\rho_{2\alpha}(p), \rho_{2\beta}(-p')] = \frac{pL}{2\pi} \delta_{\alpha\beta} \delta_{pp'} \quad \text{and} \quad [\rho_{1\alpha}(p), \rho_{2\beta}(p')] = 0.\tag{5.38}$$

These relations are exact in the Luttinger model. The same commutation relations are obtained in the Tomonaga model, but here they are obeyed approximately only. The non-vanishing contribution in the commutators comes from particles near $k=0$, i.e. from a region far from the Fermi points $\pm k_F$. Equations (5.38) are valid for states in which no holes are excited in that region, which is so in the weak coupling case. In the strong coupling limit, when states far from the Fermi points are also excited, the use of a linearized dispersion relation cannot be justified and a different treatment of the electron gas model is required (see § 11.4).

The charge and spin densities are defined by

$$\rho_i(p) = \frac{1}{\sqrt{2}} [\rho_{i\uparrow}(p) + \rho_{i\downarrow}(p)], \quad i = 1, 2\tag{5.39}$$

and

$$\sigma_i(p) = \frac{1}{\sqrt{2}} [\rho_{i\uparrow}(p) - \rho_{i\downarrow}(p)], \quad i = 1, 2.\tag{5.40}$$

They obey the same commutation relations

$$[\rho_1(-p), \rho_1(p')] = [\rho_2(p), \rho_2(-p')] = \frac{pL}{2\pi} \delta_{pp'}, \quad \text{and} \quad [\rho_1(p), \rho_2(p')] = 0,\tag{5.41}$$

and similar relations hold for the spin-density operators. The charge and spin-density operators commute.

The interaction part of the Hamiltonian in the Tomonaga–Luttinger model can be expressed straightforwardly in terms of the charge and spin-density operators as

$$\begin{aligned}
 H_{\text{int}} = & \frac{1}{L} \sum_{p>0} (g_{2\parallel} + g_{2\perp}) [\rho_1(p)\rho_2(-p) + \rho_1(-p)\rho_2(p)] \\
 & + \frac{1}{L} \sum_{p>0} (g_{2\parallel} - g_{2\perp}) [\sigma_1(p)\sigma_2(-p) + \sigma_1(-p)\sigma_2(p)] \\
 & + \frac{1}{L} \sum_{p>0} (g_{4\parallel} + g_{4\perp}) [\rho_1(p)\rho_1(-p) + \rho_2(-p)\rho_2(p)] \\
 & + \frac{1}{L} \sum_{p>0} (g_{4\parallel} - g_{4\perp}) [\sigma_1(p)\sigma_1(-p) + \sigma_2(-p)\sigma_2(p)]. \quad (5.42)
 \end{aligned}$$

The interaction Hamiltonian is bilinear in the charge- and spin-density operators, which is a consequence of the neglect of the backward scattering terms.

As a consequence of the linear dispersion relation, the free Hamiltonian of eqn. (2.3) can also be written in terms of the density operators in a bilinear form:

$$\begin{aligned}
 H_0 = & \frac{2\pi v_F}{L} \sum_{p>0} [\rho_1(p)\rho_1(-p) + \rho_2(-p)\rho_2(p)] \\
 & + \frac{2\pi v_F}{L} \sum_{p>0} [\sigma_1(p)\sigma_1(-p) + \sigma_2(-p)\sigma_2(p)]. \quad (5.43)
 \end{aligned}$$

This form of the Hamiltonian follows from

$$\begin{aligned}
 H_1 = & \sum_{k,\alpha} v_F(k - k_F) a_{k\alpha}^+ a_{k\alpha} + \sum_{k,\alpha} v_F(-k - k_F) b_{k\alpha}^+ b_{k\alpha} \\
 & - \frac{2\pi v_F}{L} \sum_{p>0} [\rho_1(p)\rho_1(-p) + \rho_2(-p)\rho_2(p)] \\
 & - \frac{2\pi v_F}{L} \sum_{p>0} [\sigma_1(p)\sigma_1(-p) + \sigma_2(-p)\sigma_2(p)] \quad (5.44)
 \end{aligned}$$

commuting with

$$\begin{aligned}
 H_2 = & \frac{2\pi v_F}{L} \sum_{p>0} [\rho_1(p)\rho_1(-p) + \rho_2(-p)\rho_2(p)] \\
 & + \frac{2\pi v_F}{L} \sum_{p>0} [\sigma_1(p)\sigma_1(-p) + \sigma_2(-p)\sigma_2(p)] + H_{\text{int}}, \quad (5.45)
 \end{aligned}$$

and the commutators of H_0 with the density operators being the same, irrespective of whether eqn. (2.3) or (5.43) is used. As it will be seen, H_2 can be exactly diagonalized. The eigenstates of H_2 which are constructed with the help of ρ_i and σ_i are at the same time eigenstates of H_1 , with eigenvalues depending only on the filling of the Fermi sea. For a fixed number of particles in the Fermi system H_1 gives only a ground-state energy renormalization and will be neglected. H_2 can be considered as the Hamiltonian of the system, and is therefore denoted simply by H .

The total Hamiltonian given by eqns. (5.45) and (5.42) is conveniently split into a charge-density part H_ρ and a spin-density part H_σ . Both parts can be diagonalized by a canonical transformation

$$\tilde{H} = \exp(iS) H \exp(-iS), \quad (5.46)$$

where

$$S = \frac{2\pi i}{L} \sum_{p>0} \frac{\phi(p)}{p} [\rho_1(p)\rho_2(-p) - \rho_1(-p)\rho_2(p)] \quad (5.47)$$

for the charge-density part and

$$S = \frac{2\pi i}{L} \sum_{p>0} \frac{\psi(p)}{p} [\sigma_1(p)\sigma_2(-p) - \sigma_1(-p)\sigma_2(p)] \quad (5.48)$$

for the spin-density part. Using the relations

$$\exp(iS)\rho_1(p)\exp(-iS) = \rho_1(p)\cosh\phi(p) + \rho_2(p)\sinh\phi(p) \quad (5.49)$$

and

$$\exp(iS)\rho_2(p)\exp(-iS) = \rho_2(p)\cosh\phi(p) + \rho_1(p)\sinh\phi(p), \quad (5.50)$$

and similar relations for the spin-density operators, which are valid for all p , diagonalization is achieved if

$$\tanh 2\phi(p) = -\frac{g_{2\parallel} + g_{2\perp}}{2\pi v_F + g_{4\parallel} + g_{4\perp}} \text{ and } \tanh 2\psi(p) = -\frac{g_{2\parallel} - g_{2\perp}}{2\pi v_F + g_{4\parallel} - g_{4\perp}}. \quad (5.51)$$

The dependence of ϕ and ψ on p arises from the dependence of the couplings on the momentum transfer. Finally it is found that

$$\tilde{H} = \tilde{H}_\sigma + \tilde{H}_\rho \quad (5.52)$$

$$\tilde{H}_\sigma = \frac{2\pi u_\sigma}{L} \sum_{p>0} [\sigma_1(p)\sigma_1(-p) + \sigma_2(-p)\sigma_2(p)] \quad (5.53)$$

and

$$\tilde{H}_\rho = \frac{2\pi u_\rho}{L} \sum_{p>0} [\rho_1(p)\rho_1(-p) + \rho_2(-p)\rho_2(p)], \quad (5.54)$$

where u_σ and u_ρ are given by eqns. (5.10) and (5.11).

After a suitable normalization, boson operators can be defined as

$$\begin{aligned} \alpha^+(p) &= \left(\frac{2\pi}{pL}\right)^{1/2} \rho_1(p), & \alpha(p) &= \left(\frac{2\pi}{pL}\right)^{1/2} \rho_1(-p), \\ \beta^+(p) &= \left(\frac{2\pi}{pL}\right)^{1/2} \rho_2(-p), & \beta(p) &= \left(\frac{2\pi}{pL}\right)^{1/2} \rho_2(p), \end{aligned} \quad (5.55)$$

and similar operators for the spin-density part, which satisfy the canonical commutation relations. Written in terms of these boson operators, the Hamiltonian is the sum of free boson field Hamiltonians, the dispersion relation is $\epsilon_k = u_\sigma k$ for the spin-density part and $\epsilon_k = u_\rho k$ for the charge-density part, in agreement with the conclusions of §5.2.

Using the bosonized Hamiltonian, all quantities which are expressed in terms of the density operators can be easily calculated. This is the case for the long-wavelength susceptibilities. The single-particle Green's function, the CDW and SDW response functions at $k=2k_F$ and the superconductor responses are not trivially expressed in terms of the density operators. Theumann (1967) succeeded in calculating the Green's function after very lengthy algebra. The advantage of the bosonized Hamiltonian became evident later, when Luther and Peschel (1974 a) and Mattis (1974 a) showed independently that an operator identity can be used to calculate matrix elements of fermion operators in boson representation. The identities

$$\begin{aligned}\psi_{1s}(x) &= \frac{1}{L^{1/2}} \sum_k a_{ks} \exp(ikx) \leftrightarrow \frac{\exp(ik_F x)}{L^{1/2}} \\ &\times \exp(i\phi_{1s}) \exp \left[\frac{2\pi}{L} \sum_{p>0} \frac{\exp(-\frac{\alpha}{2}p - ipx)}{p} \rho_{1s}(p) \right] \\ &\times \exp \left[-\frac{2\pi}{L} \sum_{p>0} \frac{\exp(-\frac{\alpha}{2}p + ipx)}{p} \rho_{1s}(-p) \right] \\ &= \frac{\exp(ik_F x)}{(2\pi\alpha)^{1/2}} \exp(i\phi_{1s}) \exp \left[\frac{2\pi}{L} \sum_p \frac{\exp(-\frac{\alpha}{2}|p| - ipx)}{|p|} \rho_{1s}(p) \right] \quad (5.56)\end{aligned}$$

and

$$\begin{aligned}\psi_{2s}(x) &= \frac{1}{L^{1/2}} \sum_k b_{ks} \exp(ikx) \leftrightarrow \frac{\exp(-ik_F x)}{L^{1/2}} \exp(i\phi_{2s}) \\ &\times \exp \left[-\frac{2\pi}{L} \sum_{p>0} \frac{\exp(-\frac{\alpha}{2}p - ipx)}{p} \rho_{2s}(p) \right] \\ &\times \exp \left[\frac{2\pi}{L} \sum_{p>0} \frac{\exp(-\frac{\alpha}{2}p + ipx)}{p} \rho_{2s}(-p) \right] \\ &= \frac{\exp(-ik_F x)}{(2\pi\alpha)^{1/2}} \exp(i\phi_{2s}) \exp \left[-\frac{2\pi}{L} \sum_p \frac{\exp(-\frac{\alpha}{2}|p| - ipx)}{|p|} \rho_{2s}(p) \right] \quad (5.57)\end{aligned}$$

are operator identities in the sense that the matrix elements are the same for properly chosen states, i.e. since $\psi_{1s}(x)$ decreases the number of particles by one,

$$\begin{aligned}\psi_{1s}(x) \Omega_1 |F, N+1\rangle &= \frac{\exp(ik_F x)}{(2\pi\alpha)^{1/2}} \exp(i\phi_{1s}) \exp \left[\frac{2\pi}{L} \sum_p \frac{\exp(-\frac{\alpha}{2}|p| - ipx)}{|p|} \rho_{1s}(p) \right] \Omega_1 |F, N\rangle, \quad (5.58)\end{aligned}$$

where $|F, N\rangle$ is the ground state having N particles on the positive branch and Ω_1 is an arbitrary function of ρ_{1s} . The parameter α is introduced to make the summation over p convergent, but the identity is in fact correct, the anticommutation relation of ψ_{1s} and ψ_{1s}^+ is satisfied only if the limit $\alpha \rightarrow 0$ is taken at the end of the calculation. The

anticommutation relations of ψ_{js} with different j and s are ensured by the phase factors

$$\begin{aligned}\phi_{1\uparrow} &= 0, \\ \phi_{1\downarrow} &= \pi \int dx \psi_{1\uparrow}^+(x) \psi_{1\uparrow}(x), \\ \phi_{2\uparrow} &= \pi \sum_s \int dx \psi_{1s}^+(x) \psi_{1s}(x)\end{aligned}\tag{5.59}$$

and

$$\phi_{2\downarrow} = \phi_{2\uparrow} + \pi \int dx \psi_{2\uparrow}^+(x) \psi_{2\uparrow}(x).$$

With this transformation from fermion to boson operators the Green's function and the response functions can be calculated (Luther and Peschel 1974 a). The results are the same as obtained in the preceding paragraphs. In fact Luther and Peschel did the calculation for the spinless Tomonaga model, which can be obtained from our earlier treatment by setting $g_{2\perp} = g_{4\perp} = 0$. As was shown earlier, in a consequent treatment of the Tomonaga model a cut-off is necessary to avoid the non-physical divergences. This cut-off is usually taken in the momentum transfer. A consistent treatment of the Tomonaga model in the bosonized representation would be to introduce a momentum transfer cut-off Λ and the parameter α , and take the limit $\alpha \rightarrow 0$. Instead of this procedure it is common to keep α finite, in which case no further cut-off is needed since α itself plays the role of the cut-off. This defines a particular model, and the relationship between this model and others with different choices of cut-off will be discussed in §9.

§6. THE LUTHER-EMERY SOLUTION OF THE BACKWARD SCATTERING PROBLEM

It is possible to solve the Tomonaga-Luttinger model exactly by neglecting the large momentum transfer interactions $g_{1\perp}$ and g_3 . When these interactions are present, the Ward identities cannot be used and the best that can be done is to apply the renormalization group approach to sum a subset of diagrams—if the fermion representation of the Hamiltonian is used. Alternatively, one can try to apply the bosonization transformation to explore the properties of the model. Luther and Emery (1974) realized, using the bosonized Hamiltonian, that for particular values of the couplings the backward scattering problem can again be solved exactly.

6.1. Calculation of the energy spectrum on the Luther-Emery line

In this section the total Hamiltonian, as given by eqns. (2.3) and (2.4), is used together with boson representation of fermion operators. Writing the forward scattering processes in terms of the densities, as in §5.3, implies the use of a momentum transfer cut-off. As mentioned already, the terms with $g_{1\parallel}$ and $g_{2\parallel}$ are equivalent—apart from a sign difference—in the model with bandwidth cut-off; they are not, however, strictly equivalent if a momentum transfer cut-off is used. The difference is not significant if the contribution of states far from the Fermi surface can be neglected. It is therefore usual to assume the same boson representation for the $g_{1\parallel}$ term as for the $g_{2\parallel}$ term and to use $g_{1\parallel}$ and g_2 as independent couplings. This means that in the expressions obtained for the Tomonaga model $g_{2\parallel}$ is replaced by $g_2 - g_{1\parallel}$ and $g_{2\perp}$ is replaced by g_2 .

The transformation of the large momentum transfer terms is more delicate. Let us first study the backward scattering term $g_{1\perp}$. Transforming this term from the momentum representation to real space, the non-local interaction

$$\sum_s \int dx_1 dx_2 dx_3 dx_4 g_{1\perp}(x_1, x_2, x_3 - x_4) \psi_{1s}^+(x_1 + x_3) \psi_{2,-s}^+(x_2 + x_4) \psi_{1,-s}(x_4) \psi_{2s}(x_3) \quad (6.1)$$

appears. The non-locality, the functional form of $g_{1\perp}$ depends on the choice of cut-off in momentum space. With any reasonable choice this interaction is short-range. Approximating this expression by a local interaction $g_{1\perp} \delta(x_1) \delta(x_2) \delta(x_3 - x_4)$, which is equivalent to having no cut-off in momentum space, the expression

$$\sum_s g_{1\perp} \int dx \psi_{1s}^+(x) \psi_{2,-s}^+(x) \psi_{1,-s}(x) \psi_{2s}(x) \quad (6.2)$$

can be written in boson representation as

$$\begin{aligned} & \frac{1}{(2\pi\alpha)^2} g_{1\perp} \int dx \left\{ \exp \left[\frac{2\pi}{L} \sum_p \frac{\exp(-\frac{\alpha}{2}|p| - ipx)}{p} \sqrt{2(\sigma_1(p) + \sigma_2(p))} \right] + \text{h.c.} \right\} \\ &= \frac{2}{(2\pi\alpha)^2} g_{1\perp} \int dx \cosh \left[\frac{2\pi}{L} \sum_p \frac{\exp(-\frac{\alpha}{2}|p| - ipx)}{p} \sqrt{2(\sigma_1(p) + \sigma_2(p))} \right]. \end{aligned} \quad (6.3)$$

The backward scattering term could be expressed entirely through the spin-density operators, even though the expression is highly non-linear.

The same bosonization transformation can be performed on the Umklapp terms in eqn. (2.4), leading to

$$\begin{aligned} & \frac{1}{(2\pi\alpha)^2} g_3 \int dx \left\{ \exp \left[\frac{2\pi}{L} \sum_p \frac{\exp(-\frac{\alpha}{2}|p| - ipx)}{p} \right. \right. \\ & \quad \times \left. \left. \sqrt{2(\rho_1(p) + \rho_2(p)) + ix(G - 4k_F)} \right] + \text{h.c.} \right\}. \end{aligned} \quad (6.4)$$

The Umklapp processes may play an important role in a system with a half-filled band. In this case, $G = 4k_F$ and eqn. (6.4) can be written as

$$\frac{2}{(2\pi\alpha)^2} g_3 \int dx \cosh \left[\frac{2\pi}{L} \sum_p \frac{\exp(-\frac{\alpha}{2}|p| - ipx)}{p} \sqrt{2(\rho_1(p) + \rho_2(p))} \right]. \quad (6.5)$$

The Umklapp term is expressed entirely in terms of the charge-density operators.

Using the results of §5.3 with eqns. (6.3) and (6.4), the total Hamiltonian can be separated into two parts: one containing the spin-density degrees of freedom, the other the charge-density degrees of freedom. Remembering that the couplings chosen here correspond to replacing $g_{2\parallel}$ by $g_2 - g_{1\parallel}$ and $g_{2\perp}$ by g_2 ,

$$H = H_\sigma + H_\rho, \quad (6.6)$$

where the spin-density part is

$$H_{\sigma} = \frac{2\pi v_{\sigma}}{L} \sum_{p>0} [\sigma_1(p)\sigma_1(-p) + \sigma_2(-p)\sigma_2(p)] - \frac{g_{1\parallel}}{L} \sum_{p>0} [\sigma_1(p)\sigma_2(-p) + \sigma_1(-p)\sigma_2(p)] + \frac{g_{1\perp}}{(2\pi\alpha)^2} \int dx \left\{ \exp \left[\frac{2\pi}{L} \sum_p \frac{\exp(-\frac{\alpha}{2}|p| - ipx)}{p} \sqrt{2(\sigma_1(p) + \sigma_2(p))} \right] + \text{h.c.} \right\} \quad (6.7)$$

and the charge-density part is

$$H_{\rho} = \frac{2\pi v_{\rho}}{L} \sum_{p>0} [\rho_1(p)\rho_1(-p) + \rho_2(-p)\rho_2(p)] + \frac{2g_2 - g_{1\parallel}}{L} \sum_{p>0} [\rho_1(p)\rho_2(-p) + \rho_1(-p)\rho_2(p)] + \frac{g_3}{(2\pi\alpha)^2} \int dx \times \left\{ \exp \left[\frac{2\pi}{L} \sum_p \frac{\exp(-\frac{\alpha}{2}|p| - ipx)}{p} \sqrt{2(\rho_1(p) + \rho_2(p)) + ix(G - 4k_F)} \right] + \text{h.c.} \right\}, \quad (6.8)$$

with

$$v_{\sigma} = v_F + \frac{1}{2\pi}(g_{4\parallel} - g_{4\perp}) \quad \text{and} \quad v_{\rho} = v_F + \frac{1}{2\pi}(g_{4\parallel} + g_{4\perp}). \quad (6.9)$$

Before proceeding to solve the model, a few remarks have to be made about the approximations involved in this transformed Hamiltonian. One approximation is to neglect the difference between the $g_{1\parallel}$ and $g_{2\parallel}$ processes. This difference disappears if a bandwidth cut-off or no cut-off at all is used. The other approximation is in the bosonization of the large momentum transfer terms. If the limit $\alpha \rightarrow 0$ is taken, as it should be, these terms contain no cut-off. It is known, however, that without cut-off non-physical divergences appear and so a cut-off must be introduced. Since in the Tomonaga model the procedure of identifying α with the cut-off and keeping it finite leads to results which are very similar to the ones obtained by using a momentum transfer cut-off, it is hoped that the same is true for the backward scattering model.

In the case of a half-filled band, the two parts of the Hamiltonian have exactly the same structure. For a non-half-filled band the charge-density part reduces to a Tomonaga Hamiltonian for which the solution is already known. The further discussion relates to the spin-density part, but all results can trivially be extended to the charge-density part as well, if Umklapp processes are important.

It was shown in §5.3 that the bilinear part of H_{σ} can be diagonalized by a canonical transformation. Using this transformation for the whole H_{σ} affects the

backward scattering term in a simple way; the exponent is multiplied by $\exp(\psi)$ (see eqn. (5.51) for ψ) and

$$\tilde{H}_\sigma = \frac{2\pi u_\sigma}{L} \sum_{p>0} [\sigma_1(p)\sigma_1(-p) + \sigma_2(-p)\sigma_2(p)] \\ + \frac{g_{1\perp}}{(2\pi\alpha)^2} \int dx \left\{ \exp \left[\frac{2\pi}{L} \sum_p \frac{\exp(-\frac{\alpha}{2}|p| - ipx)}{p} \sqrt{2 \exp(\psi) (\sigma_1(p) + \sigma_2(p))} \right] + \text{h.c.} \right\}, \quad (6.10)$$

where u_σ is now given by

$$u_\sigma = \left\{ \left[v_F + \frac{1}{2\pi} (g_{4\parallel} - g_{4\perp}) \right]^2 - \left(\frac{1}{2\pi} g_{1\parallel} \right)^2 \right\}^{1/2}. \quad (6.11)$$

Luther and Emery (1974) realized that in the particular case in which $\sqrt{2 \exp(\psi)} = 1$, this Hamiltonian is the boson representation of a bilinear Hamiltonian of spinless fermions. By introducing the spinless fermion operators c_k and d_k , which in their bosonized representations are related to σ_1 and σ_2 by the expressions

$$\psi_1(x) = \frac{1}{L^{1/2}} \sum_k c_k \exp(ikx) \leftrightarrow \frac{\exp(ik_F x)}{(2\pi\alpha)^{1/2}} \exp \left[\frac{2\pi}{L} \sum_p \frac{\exp(-\frac{\alpha}{2}|p| - ipx)}{p} \sigma_1(p) \right], \quad (6.12)$$

and

$$\psi_2(x) = \frac{1}{L^{1/2}} \sum_k d_k \exp(ikx) \leftrightarrow \frac{\exp(-ik_F x)}{(2\pi\alpha)^{1/2}} \\ \times \exp \left[-\frac{2\pi}{L} \sum_p \frac{\exp(-\frac{\alpha}{2}|p| - ipx)}{p} \sigma_2(p) \right], \quad (6.13)$$

eqn. (6.10) becomes equivalent to

$$\tilde{H}_\sigma = u_\sigma \sum_k k(c_k^+ c_k - d_k^+ d_k) + \frac{g_{1\perp}}{2\pi\alpha} \sum_k (c_{k+k_F}^+ d_{k-k_F} + d_{k-k_F}^+ c_{k+k_F}). \quad (6.14)$$

A difficulty arises from the equivalence being valid in the limit $\alpha \rightarrow 0$, but clearly this limit cannot be taken either in eqn. (6.7) or in eqn. (6.14). It is assumed that eqn. (6.14), with finite α , is equivalent to the original model with an appropriately chosen cut-off, although no formal proof exists.

The condition $\sqrt{2 \exp(\psi)} = 1$ can be written in the form

$$-\frac{g_{1\parallel}}{2\pi v_\sigma} = -\frac{g_{1\parallel}}{2\pi v_F + g_{4\parallel} - g_{4\perp}} = \frac{3}{5} \quad (6.15)$$

when eqn. (5.51) and the new notations $g_{2\parallel} \rightarrow g_2 - g_{1\parallel}$ and $g_{2\perp} \rightarrow g_2$ are taken into account. This shows that the backward scattering term of the Hamiltonian simplifies to a bilinear expression for a particular value of $g_{1\parallel}$.

The energy spectrum of the bilinear Hamiltonian in eqn. (6.14) is obtained if a Bogoliubov transformation

$$c_{k+k_F} = \cos \theta_k \alpha_1(k+k_F) - \sin \theta_k \alpha_2(k-k_F) \\ d_{k-k_F} = \sin \theta_k \alpha_1(k+k_F) + \cos \theta_k \alpha_2(k-k_F) \quad (6.16)$$

is performed to new operators $\alpha_1(k)$ and $\alpha_2(k)$. The transformed Hamiltonian is diagonal if

$$\tan 2\theta_k = \frac{g_{1\perp}}{2\pi\alpha u_\sigma k}, \quad (6.17)$$

and the spectrum for the two particles associated with $\alpha_1(k)$ and $\alpha_2(k)$ is

$$\begin{aligned} \varepsilon_1(k) &= u_\sigma k_F + \text{sign}(k - k_F)[u_\sigma^2(k - k_F)^2 + \Delta_\sigma^2]^{1/2}, \quad k \sim k_F \\ (6.18) \end{aligned}$$

$$\varepsilon_2(k) = u_\sigma k_F - \text{sign}(k + k_F)[u_\sigma^2(k + k_F)^2 + \Delta_\sigma^2]^{1/2}, \quad k \sim -k_F,$$

where

$$\Delta_\sigma = \frac{|g_{1\perp}|}{2\pi\alpha}. \quad (6.19)$$

At the particular value of the couplings given in eqn. (6.15) a gap is present in the excitation spectrum of the spin-density degrees of freedom, which has serious consequences for the response functions.

In the case of a half-filled band, when the charge-density part of the Hamiltonian has a form similar to that of the spin-density part, an analogous calculation (Emery *et al.* 1976) shows that the problem with Umklapp scattering is soluble for

$$\frac{2g_2 - g_{1\parallel}}{2\pi v_p} = \frac{2g_2 - g_{1\parallel}}{2\pi v_F + g_{4\parallel} + g_{4\perp}} = \frac{3}{5}. \quad (6.20)$$

The charge-density excitations have a gap which is given by

$$\Delta_p = \frac{|g_3|}{2\pi\alpha}, \quad (6.21)$$

there is no gap if the band is not half-filled.

6.2. Response functions of the Luther-Emery model

The response functions have already been considered in § 4.3, in connection with the renormalization group approach, and in § 5.2, where exact results were given for the Tomonaga-Luttinger model. The same response functions are treated here for the particular values of the couplings for which the Luther-Emery solution applies.

The response function defined by eqns. (4.40)–(4.45) can be expressed in terms of the ρ_i and σ_i operators using the bosonization transformations (5.56) and (5.57). To simplify the discussion only one term in $\mathcal{O}(k, t)$ will be considered. This will reflect the correct analytic behaviour of the whole response function. In real space and time representation the response functions

$$N(x, t) = -i\langle T\{\psi_{2\uparrow}^+(x, t)\psi_{1\uparrow}(x, t)\psi_{1\uparrow}^+(0, 0)\psi_{2\uparrow}(0, 0)\}\rangle. \quad (6.22)$$

$$\chi(x, t) = -i\langle T\{\psi_{2\downarrow}^+(x, t)\psi_{1\uparrow}(x, t)\psi_{1\uparrow}^+(0, 0)\psi_{2\downarrow}(0, 0)\}\rangle, \quad (6.23)$$

$$\Delta_s(x, t) = -i\langle T\{\psi_{2\downarrow}(x, t)\psi_{1\uparrow}(x, t)\psi_{1\uparrow}^+(0, 0)\psi_{2\downarrow}^+(0, 0)\}\rangle \quad (6.24)$$

and

$$\Delta_i(x, t) = -i\langle T\{\psi_{2\uparrow}(x, t)\psi_{1\uparrow}(x, t)\psi_{1\uparrow}^+(0, 0)\psi_{2\uparrow}^+(0, 0)\}\rangle, \quad (6.25)$$

when written in terms of the ρ_i and σ_i operators, have the forms

$$N(x, t) = -i \frac{\exp(2ik_F x)}{(2\pi\alpha)^2} S_\rho^+(x, t) S_\sigma^+(x, t), \quad (6.26)$$

$$\chi(x, t) = -i \frac{\exp(2ik_F x)}{(2\pi\alpha)^2} S_\rho^+(x, t) S_\sigma^-(x, t), \quad (6.27)$$

$$\Delta_s(x, t) = -i \frac{1}{(2\pi\alpha)^2} S_\rho^-(x, t) S_\sigma^+(x, t) \quad (6.28)$$

and

$$\Delta_t(x, t) = -i \frac{1}{(2\pi\alpha)^2} S_\rho^-(x, t) S_\sigma^-(x, t), \quad (6.29)$$

where

$$S_\rho^\pm(x, t) = \left\langle T \left\{ \exp(itH_\rho) \exp \left[\frac{2\pi}{L} \sum_p \frac{\exp(-\frac{\alpha}{2}|p| - ipx)}{p} \frac{1}{\sqrt{2}} (\rho_1(p) \pm \rho_2(p)) \right] \right. \right. \\ \times \exp(-itH_\rho) \exp \left[\left. \left. -\frac{2\pi}{L} \sum_p \frac{\exp(-\frac{\alpha}{2}|p|)}{p} \frac{1}{\sqrt{2}} (\rho_1(p) \pm \rho_2(p)) \right] \right\rangle_\rho \quad (6.30)$$

and

$$S_\sigma^\pm(x, t) = \left\langle T \left\{ \exp(itH_\sigma) \exp \left[\frac{2\pi}{L} \sum_p \frac{\exp(-\frac{\alpha}{2}|p| - ipx)}{p} \frac{1}{\sqrt{2}} (\sigma_1(p) \pm \sigma_2(p)) \right] \right. \right. \\ \times \exp(-itH_\sigma) \exp \left[\left. \left. -\frac{2\pi}{L} \sum_p \frac{\exp(-\frac{\alpha}{2}|p|)}{p} \frac{1}{\sqrt{2}} (\sigma_1(p) \pm \sigma_2(p)) \right] \right\rangle_\sigma. \quad (6.31)$$

The ρ and σ parts of the response functions can be calculated independently. For a non-half-filled band the large momentum transfer terms affect only H_σ and H_ρ is the same as in the Tomonaga model. Therefore S_σ^\pm is easily obtained from the charge-density part of the response functions of the Tomonaga model in eqns. (5.28) and (5.30), by identifying the cut-off Λ with $1/\alpha$, as

$$S_\sigma^\pm(x, t) = [(x - u_\rho t + i\alpha \operatorname{sign} t)(x + u_\rho t - i\alpha \operatorname{sign} t)]^{\gamma_\rho^\pm} \quad (6.32)$$

where γ_ρ is given by eqn. (5.27). With the present choice of couplings $g_{2\parallel} \rightarrow g_2 - g_{1\parallel}$ and $g_{2\perp} \rightarrow g_2$, and remembering that the Luther-Emery solution is obtained for $g_{1\parallel} = -\frac{6}{5}\pi v_\sigma = -\frac{3}{5}(2\pi v_F + g_{4\parallel} - g_{4\perp})$,

$$\gamma_\rho = \left[\frac{1 + \frac{1}{2\pi v_F} (g_{4\parallel} + g_{4\perp}) - \frac{1}{2\pi v_F} (2g_2 - g_{1\parallel})}{1 + \frac{1}{2\pi v_F} (g_{4\parallel} + g_{4\perp}) + \frac{1}{2\pi v_F} (2g_2 - g_{1\parallel})} \right]^{1/2} \\ = \left[\frac{1 + \frac{1}{2\pi v_F} (g_{4\parallel} + 4g_{4\perp}) - \frac{5g_2}{2\pi v_F}}{4 + \frac{1}{2\pi v_F} (4g_{4\parallel} + g_{4\perp}) + \frac{5g_2}{2\pi v_F}} \right]^{1/2} \quad (6.33)$$

In calculating the σ part of the response functions, the canonical transformation (5.46) diagonalizing the bilinear part of the Hamiltonian is performed first, which leads to

$$\begin{aligned} S_{\sigma}^{\pm}(x, t) = & \left\langle T \left\{ \exp(it\tilde{H}_{\sigma}) \exp \left[\frac{2\pi}{L} \sum_p \frac{\exp(-\frac{\pi}{2}|p| - ipx)}{p} \frac{1}{\sqrt{2}} \exp(\pm\psi) \right. \right. \right. \right. \\ & \times (\sigma_1(p) \pm \sigma_2(p)) \left. \left. \right] \exp(-it\tilde{H}_{\sigma}) \right. \\ & \times \exp \left[-\frac{2\pi}{L} \sum_p \frac{\exp(-\frac{\pi}{2}|p|)}{p} \frac{1}{\sqrt{2}} \exp(\pm\psi) (\sigma_1(p) \pm \sigma_2(p)) \right] \left. \right\} \rangle_{\sigma}. \end{aligned} \quad (6.34)$$

On the Luther–Emery line, where $\sqrt{2} \exp(\psi) = 1$, S_{σ}^{\pm} can be expressed in terms of the spinless fermion fields introduced in eqns. (6.12) and (6.13) to obtain

$$S_{\sigma}^{+}(x, t) = 2\pi\alpha \langle T\{[\psi_1(x, t)\psi_2^{+}(x, t)\exp(-2ik_Fx)]^{1/2} [\psi_2(0, 0)\psi_1^{+}(0, 0)]^{1/2}\} \rangle \quad (6.35)$$

and

$$S_{\sigma}^{-}(x, t) = (2\pi\alpha)^2 \langle T\{\psi_1(x, t)\psi_2(x, t)\psi_2^{+}(0, 0)\psi_1^{+}(0, 0)\} \rangle. \quad (6.36)$$

These expressions have been studied by Lee (1975), Gutfreund and Klemm (1976) and Finkelstein (1977). The low-frequency behaviour of the response functions is determined by the behaviour of S_{σ}^{\pm} at large x and t . The most important difference in the behaviour of S_{σ}^{+} and S_{σ}^{-} comes from the fact that S_{σ}^{+} corresponds to the propagation of a particle–hole pair in the spinless fermion representation, whereas S_{σ}^{-} describes the propagation of a pair of particles. In this respect the square root in the expression for S_{σ}^{+} is of minor importance. Since

$$\langle [\psi_2(0, 0)\psi_1^{+}(0, 0)]^{1/2} \rangle \neq 0, \quad (6.37)$$

but

$$\langle \psi_2^{+}(0, 0)\psi_1^{+}(0, 0) \rangle = 0, \quad (6.38)$$

in the limit $x, t \rightarrow \infty$ when $\langle A(x, t)B \rangle \approx \langle A(x, t) \rangle \langle B \rangle$, $S_{\sigma}^{+}(x, t)$ becomes constant while $S_{\sigma}^{-}(x, t)$ vanishes. Thus the low-frequency behaviour of the charge-density and singlet-superconductor responses which contain S_{σ}^{+} is completely determined by the ρ part, and Fourier-transforming S_{ρ}^{+} in eqn. (6.32) gives

$$N(\omega) \sim \omega^{\gamma_{\rho}-2} \quad (6.39)$$

and

$$\Delta_s(\omega) \sim \omega^{1/\gamma_{\rho}-2}. \quad (6.40)$$

Using eqn. (6.33) for γ_{ρ} , the charge-density response function is divergent if

$$g_2 > -\frac{6}{5}\pi v_F - \frac{3}{5}g_{4\parallel} = -\frac{3}{5}\pi(v_{\rho} + v_{\sigma}), \quad (6.41)$$

and the singlet-superconductor response is divergent if

$$g_2 < \frac{3}{5}g_{4\perp} = \frac{3}{5}\pi(v_{\rho} - v_{\sigma}). \quad (6.42)$$

The point $g_2 = -\frac{3}{5}\pi v_F$ divides the regions in which one or other of the response functions is more divergent.

The behaviour of the spin-density and triplet-superconductor responses is different. $S_{\sigma}^{-}(x, t)$ is an oscillatory function of t and vanishes when $x, t \rightarrow \infty$. In

Fourier representation, $S_\sigma^-(k, \omega)$ has Fourier components only for $|\omega| > 2\Delta_\sigma$, corresponding to the fact that the minimum energy needed to excite a pair of spinless fermions is $2\Delta_\sigma$. The response functions are convolutions of $S_\sigma^-(k_1, \omega_1)$ with $S_\rho^\pm(k - k_1, \omega - \omega_1)$. Due to the existence of a gap in $S_\sigma^-(k_1\omega)$ the divergence of S_ρ^\pm is not present in the total response function at small ω . Gutfreund and Klemm (1976) have also shown that these response functions are not divergent at the gap edge.

Similar calculations can be performed for a half-filled model. In this case the analysis given for S_σ^\pm is also valid for S_ρ^\pm . The response functions containing either S_σ^- or S_ρ^- cannot be divergent; the only divergence is in $N(k, \omega)$. Since both S_σ^+ and S_ρ^+ become constant for large x and t , Fourier transformation for small k and ω gives

$$N(\omega) \sim \omega^{-2}. \quad (6.43)$$

The $4k_F$ response function depends entirely on the charge-density degrees of freedom, so the same result is obtained as in the Tomonaga model if the band is not half-filled.

§ 7. SCALING TO THE EXACTLY SOLUBLE MODELS

We have seen in §§ 5 and 6 that the Fermi gas model can be solved exactly for particular values of the couplings, namely for $g_{1\perp} = g_3 = 0$ (in the Tomonaga–Luttinger model) and for $g_{1\parallel} = -\frac{3}{5}(2\pi v_F + g_{4\parallel} - g_{4\perp})$ or $-2g_2 + g_{1\parallel} = -\frac{3}{5}(2\pi v_F + g_{4\parallel} + g_{4\perp})$. Solving for other values of the couplings is not an easy task. A calculation of the eigenvalues of the Hamiltonian in the vicinity of the Luther–Emery limit was attempted by Schlottmann (1977 a, b), who found that the gap exists in H_σ for $g_{1\parallel} < 0$, although the derivation of this result contains approximations which restrict the validity of the calculation to the neighbourhood of the Luther–Emery line.

The renormalization group and scaling arguments presented in § 4 establish a relationship between the original problem and a set of problems in which the coupling constants have a somewhat different value. If an exactly soluble model appears among these equivalent systems, the physical behaviour of the original model can be predicted by using the scaling arguments. The scaling relations were derived in § 4 by neglecting g_3 and g_4 . In this section the scaling curves for the most general case—with five coupling constants—are studied. As before, a bandwidth cut-off will be used and the couplings are $g_{1\parallel}$, $g_{1\perp}$, $g_2 = g_{2\parallel} = g_{2\perp}$, g_3 and $g_4 = g_{4\perp}$; in this case $g_{4\parallel}$ gives no contribution.

The scaling relations are analogous to those given by eqns. (4.12)–(4.18) and must be complemented by relations for the vertices Γ_3 and Γ_4 shown in figs. 26. and 27. A lengthy but straightforward calculation (Kimura 1975, Sólyom 1975) leads to the following equations for the invariant couplings (the superscript R is neglected for convenience):

$$\frac{dg_{1\parallel}}{dx} = \frac{1}{x} \left\{ \frac{1}{\pi v_F} g_{1\perp}^2 + \frac{1}{2\pi^2 v_F^2} (g_{1\parallel} g_{1\perp}^2 + g_{1\perp}^2 g_4) + \dots \right\}, \quad (7.1)$$

$$\frac{dg_{1\perp}}{dx} = \frac{1}{x} \left\{ \frac{1}{\pi v_F} g_{1\parallel} g_{1\perp} + \frac{1}{4\pi^2 v_F^2} (g_{1\parallel}^2 g_{1\perp} + g_{1\perp}^3 + 2g_{1\parallel} g_{1\perp} g_4) + \dots \right\}, \quad (7.2)$$

$$\frac{d(g_{1\parallel} - 2g_2)}{dx} = \frac{1}{x} \left\{ \frac{1}{\pi v_F} g_3^2 + \frac{1}{2\pi^2 v_F^2} [(g_{1\parallel} - 2g_2) g_3^2 - g_3^2 g_4] + \dots \right\}, \quad (7.3)$$

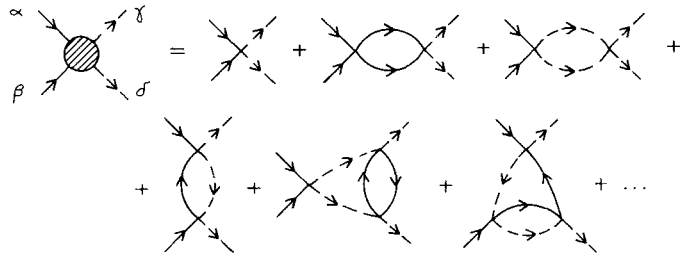
$$\begin{aligned} \frac{dg_3}{dx} = & \frac{1}{x} \left\{ \frac{1}{\pi v_F} (g_{1\parallel} - 2g_2) g_3 \right. \\ & \left. + \frac{1}{4\pi^2 v_F^2} [(g_{1\parallel} - 2g_2) g_3 + g_3^3 - 2(g_{1\parallel} - 2g_2) g_3 g_4] + \dots \right\} \quad (7.4) \end{aligned}$$

and

$$\frac{dg_4}{dx} = \frac{1}{x} \left\{ \frac{1}{4\pi^2 v_F^2} [-3g_{1\parallel} g_{1\perp}^2 + 3(g_{1\parallel} - 2g_2) g_3^2] + \dots \right\}, \quad (7.5)$$

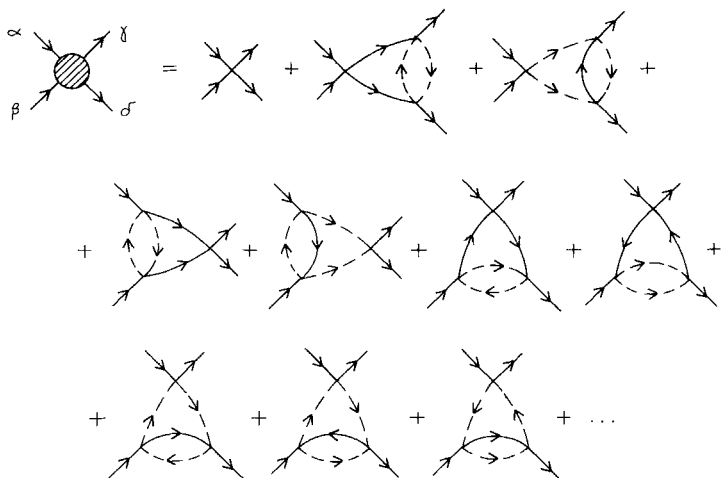
where x is the relative change of the cut-off. The combination $g_{1\parallel} - 2g_2$ is used instead of g_2 for later convenience.

Fig. 26



Low-order diagrams of the vertex $\Gamma_3 = g_3 \tilde{\Gamma}_3 (\delta_{\alpha\gamma} \delta_{\beta\delta} - \delta_{\alpha\delta} \delta_{\beta\gamma})$.

Fig. 27



Low-order diagrams of the vertex $\Gamma_4 = g_4 \tilde{\Gamma}_4 (\delta_{\alpha\gamma} \delta_{\beta\delta} - \delta_{\alpha\delta} \delta_{\beta\gamma})$. All the third-order diagrams are logarithmically divergent.

The scaling equations form a complicated set of coupled equations for which, generally, no analytic solution is possible. Considerable simplification is achieved if the effect of g_4 is treated approximately. It has been shown that, in a model with momentum transfer cut-off, the g_4 term leads to a Fermi velocity renormalization

$$v_F \rightarrow v_\sigma = v_F + \frac{1}{2\pi} (g_{4\parallel} - g_{4\perp}) \quad (7.6)$$

or

$$v_F \rightarrow v_p = v_F + \frac{1}{2\pi} (g_{4\parallel} + g_{4\perp})$$

in the spin- and charge-density parts of the Hamiltonian respectively. In a model with bandwidth cut-off, where $g_{4\parallel}$ has no effect, the Fermi velocities

$$v_\sigma = v_F - \frac{1}{2\pi} g_4 \quad (7.7)$$

and

$$v_p = v_F + \frac{1}{2\pi} g_4$$

are expected to appear. In fact, in the scaling equations the terms containing g_4 can be incorporated in the calculated order into the renormalized Fermi velocities, leading to

$$\frac{d g_{1\parallel}}{dx} = \frac{1}{x} \left\{ \frac{1}{\pi v_\sigma} g_{1\perp}^2 + \frac{1}{2\pi^2 v_\sigma^2} g_{1\parallel} g_{1\perp}^2 + \dots \right\}, \quad (7.8)$$

$$\frac{d g_{1\perp}}{dx} = \frac{1}{x} \left\{ \frac{1}{\pi v_\sigma} g_{1\parallel} g_{1\perp} + \frac{1}{4\pi^2 v_\sigma^2} (g_{1\parallel}^2 g_{1\perp} + g_{1\perp}^3) + \dots \right\}, \quad (7.9)$$

$$\frac{d (g_{1\parallel} - 2g_2)}{dx} = \frac{1}{x} \left\{ \frac{1}{\pi v_p} g_3^2 + \frac{1}{2\pi^2 v_p^2} (g_{1\parallel} - 2g_2) g_3^2 + \dots \right\}, \quad (7.10)$$

$$\frac{d g_3}{dx} = \frac{1}{x} \left\{ \frac{1}{\pi v_p} (g_{1\parallel} - 2g_2) g_3 + \frac{1}{4\pi^2 v_p^2} [(g_{1\parallel} - 2g_2)^2 g_3 + g_3^3] + \dots \right\}. \quad (7.11)$$

Two independent sets of equations are obtained; one for $g_{1\parallel}$ and $g_{1\perp}$ containing the Fermi velocity v_σ , the other for $g_{1\parallel} - 2g_2$ and g_3 containing the Fermi velocity v_p . The two sets have the same form if $g_{1\parallel} \rightarrow g_{1\parallel} - 2g_2$, $g_{1\perp} \rightarrow g_3$ and $v_\sigma \rightarrow v_p$. This is in agreement with the separation of the Hamiltonian into H_σ and H_p in the bosonized form. These equations agree with the scaling equations derived by Emery *et al.* (1976), using a somewhat different scaling approach by analogy with the scaling treatment of the Kondo problem by Anderson *et al.* (1970). The cut-off α is the scaling parameter in this approach.

In disagreement, however, with the separation of H_σ and H_p , the scaling equation (7.5) for g_4 couples all the other coupling constants. A renormalization of g_4 itself is not surprising; it is present also in the model described by Luther and Emery (1974). To clarify this point, the derivation of the scaling equations of the bosonized Hamiltonians is now briefly sketched. The Hamiltonian H_σ is transformed by the canonical transformation (5.46) to the form of eqn. (6.10). The parameters of the original Hamiltonian H_σ are the couplings $g_{1\parallel}$, $g_{1\perp}$ and $g_{4\parallel} - g_{4\perp}$ as well as the cut-off

α . After the canonical transformation, the couplings $g_{1\parallel}$ and $g_{4\parallel} - g_{4\perp}$ appear in two combinations: in u_σ given by eqn. (6.11) (which is the velocity of spin-wave excitations) and in the phase factor ψ (see eqn. (5.51)). Performing a scaling on α , $g_{1\perp}$ and ψ are renormalized, as given in the lowest order by Kosterlitz (1974), and in a higher order, as given by Emery *et al.* (1976), whereas the velocity u_σ remains invariant. Transforming the scaling equations obtained for $g_{1\perp}$, ψ and u_σ into equations for $g_{1\parallel}$, g_{\perp} and $g_{4\parallel} - g_{4\perp}$, eqns. (7.8) and (7.9) are recovered for $g_{1\parallel}$ and $g_{1\perp}$ with u_σ instead of v_σ . In the calculated order u_σ can be approximated by v_σ , and the two methods lead to the same results. For $g_{4\parallel} - g_{4\perp}$, however, from the condition of the invariance of u_σ is obtained

$$\frac{d(g_{4\parallel} - g_{4\perp})}{dx} = \frac{g_{1\parallel}}{2\pi v_F + g_{4\parallel} - g_{4\perp}} \frac{dg_{1\parallel}}{dx} = \frac{1}{x} \left\{ \frac{1}{2\pi^2 v_F^2} g_{1\parallel} g_{1\perp}^2 + \dots \right\}. \quad (7.12)$$

Similarly, scaling α in H_σ leads to the scaling relation for $g_{4\parallel} + g_{4\perp}$

$$\frac{d(g_{4\parallel} + g_{4\perp})}{dx} = \frac{g_{1\parallel} - 2g_2}{2\pi v_F + g_{4\parallel} + g_{4\perp}} \frac{dg_{1\parallel} - 2g_2}{dx} = \frac{1}{x} \left\{ \frac{1}{2\pi^2 v_F^2} (g_{1\parallel} - 2g_2) g_3^2 + \dots \right\} \quad (7.13)$$

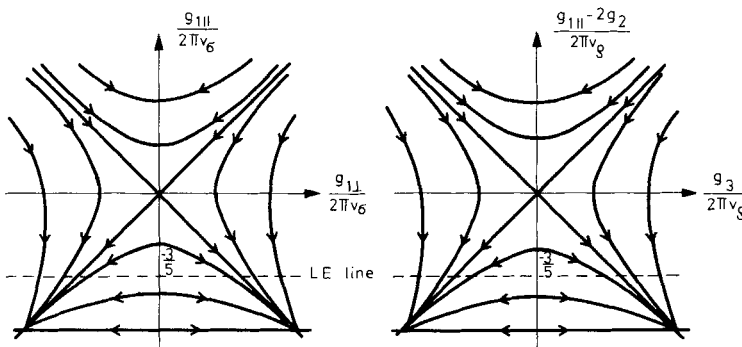
From these two equations, the scaling equation

$$\frac{dg_{4\perp}}{dx} = \frac{1}{x} \left\{ -\frac{1}{4\pi^2 v_F^2} g_{1\parallel} g_{1\perp}^2 + \frac{1}{4\pi^2 v_F^2} (g_{1\parallel} - 2g_2) g_3^2 + \dots \right\} \quad (7.14)$$

is obtained for $g_{4\perp}$. This equation is very similar to eqn. (7.5), apart from a factor of 3. There is, however, a fundamental difference. In the bosonized Hamiltonian, $g_{4\parallel}$ is also present and the separation of H_ρ and H_σ is complete if the combinations $g_{4\parallel} \pm g_{4\perp}$ are used. In the model with bandwidth cut-off, the $g_{4\parallel}$ coupling gives no contribution and the scaling equations are all coupled via $g_{4\perp}$. The difference comes from the different choice of the cut-off. This problem will be further discussed in § 9. See also note added in proof.

Neglecting now the renormalization of g_4 as a higher-order correction, the renormalization group equations for $g_{1\parallel}$ and $g_{1\perp}$ are identical to eqns. (4.31) and (4.32). The flow lines in the $(g_{1\parallel}, g_{1\perp})$ plane are shown in fig. 28. The Tomonaga-Luttinger model and the Luther-Emery model correspond to two crossing lines, the vertical line $g_{1\perp} = 0$ and the horizontal line $g_{1\parallel} = -\frac{6}{5}\pi v_\sigma$, respectively. Similar scaling curves are obtained in the $(g_{1\parallel} - g_2, g_3)$ plane for the dimensionless couplings

Fig. 28



Flow lines of scaling on the $(g_{1\parallel}, g_{1\perp})$ and $(g_{1\parallel} - 2g_2, g_3)$ planes. The dashed line is the Luther-Emery line.

$g_{1\parallel} - 2g_2)/2\pi v_\rho$ and $g_3/2\pi v_\rho$. The models for which $g_{1\parallel} \geq |g_{1\perp}|$ or $g_{1\parallel} - 2g_2 \geq |g_3|$ are equivalent to the Tomonaga model, at least in their σ or ρ parts, and the results of the Tomonaga model can be used to determine their behaviour.

The models for which $g_{1\parallel} < |g_{1\perp}|$ or $g_{1\parallel} - 2g_2 < |g_3|$ scale to a strong coupling fixed point, but before reaching this fixed point they pass through the Luther–Emery line. Thus the behaviour of these models can be inferred from the Luther–Emery solution, without having to rely on the approximations of §4.3.

§ 8. PHYSICAL PROPERTIES OF THE MODEL

It was shown in §7 that the weak-coupling Fermi gas model is equivalent to either the Tomonaga–Luttinger model or the Luther–Emery model. Thus the properties of the present model can be obtained from the known behaviour of these others. The possible ground states are discussed first, then various quantities such as susceptibility, specific heat and conductivity are considered.

8.1. Phase diagram of the Fermi gas model

Let us consider first a simple situation in which the couplings are spin-independent, $g_{1\parallel} = g_{1\perp} = g_1$, the band is not half-filled, i.e. g_3 gives no contribution, and the Fermi velocity renormalization due to g_4 is neglected. The domain of attraction of the Tomonaga fixed point ($g_2^* = 0$) is $g_1 \geq 0$. According to Fowler (1976), $g_1 - 2g_2$ is an exact invariant of the renormalization transformation, and therefore the fixed-point value of g_2 is $g_2^* = g_2 - \frac{1}{2}g_1$. It follows from the scaling relations for the response functions given by eqn. (4.50) that the ω -dependence of the response functions of the original model with couplings g_1 and g_2 is the same as that of the Tomonaga model with the fixed-point value $g_2^* = g - \frac{1}{2}g_1$. Inserting this value into the exponents in eqns (5.31)–(5.34), a singularity is obtained for small ω in the density responses if $g_2 - \frac{1}{2}g_1 > 0$ and in the pairing responses if $g_2 - \frac{1}{2}g_1 < 0$.

The behaviour of the system if $g_1 < 0$ can be determined by scaling to the Luther–Emery (LE) line. The spin-density and triplet-superconductor responses are not singular on the LE line, so they are non-singular for arbitrary $g_1 < 0$. The ω -dependence of the charge-density and singlet-superconductor responses is governed by the exponent γ_ρ (see eqns. (6.39) and (6.40)). The value of γ_ρ given on the LE line in eqn. (6.33) can be easily extended by using the invariance of $g_1 - 2g_2$ to give, for $g_4 = 0$,

$$\gamma_\rho = \left[\frac{1 - \frac{1}{2\pi v_F} (2g_2 - g_1)}{1 + \frac{1}{2\pi v_F} (2g_2 - g_1)} \right]^{1/2}. \quad (8.1)$$

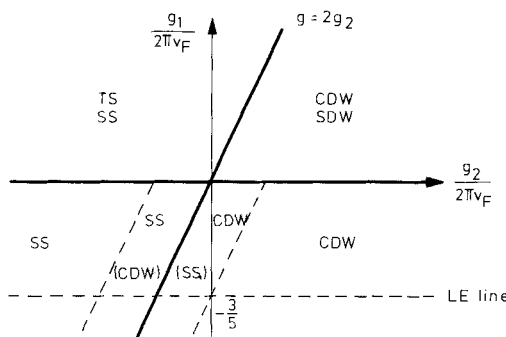
Inserting this value into eqns. (6.39) and (6.40), the charge-density response function is divergent if

$$2g_2 - g_1 > -\frac{6}{5}\pi v_F, \quad (8.2)$$

and the singlet-superconductor response is divergent if

$$2g_2 - g_1 < \frac{6}{5}\pi v_F. \quad (8.3)$$

Fig. 29



Phase diagram obtained by scaling to the exact solutions of the Tomonaga–Luttinger and Luther–Emery models. The response functions corresponding to the phases indicated in parentheses have a lower degree of divergence than the others.

The line $2g_2 - g_2 = 0$ divides the regions in which one or other of the response functions is more divergent. The phase diagram is shown in fig. 29 (Lee 1975). For weak couplings it coincides with the phase diagram obtained from the renormalization group treatment of §4.3.

The phase diagram becomes much more complicated if the couplings are spin-dependent, or if the band is half-filled and Umklapp processes are important. There are four different regions in the space of couplings limited by the demarcation planes $g_{1\parallel} - 2g_2 = |g_3|$ and $g_{1\parallel} = |g_{1\perp}|$. In region I, where $g_{1\parallel} \geq |g_{1\perp}|$ and $g_{1\parallel} - 2g_2 \geq |g_3|$, there is no gap in either the ρ or σ parts of the Hamiltonian; both H_ρ and H_σ are equivalent to the Tomonaga Hamiltonian. The scaling equations can be solved only approximately, leading to the fixed-point values

$$g_{1\parallel}^* \approx (g_{1\parallel}^2 - g_{1\perp}^2)^{1/2}, g_{1\perp}^* = 0, g_2^* \approx [(g_{1\parallel} - 2g_2)^2 - g_3^2]^{1/2} \text{ and } g_3^* = 0.$$

These values are to be used in the expressions for the Tomonaga model. All four response functions show a power-law behaviour for small ω , as given in eqns. (5.31)–(5.34), with exponents

$$\gamma_\sigma = \left[\frac{v_\sigma + \frac{1}{2\pi} g_{1\parallel}^*}{v_\sigma - \frac{1}{2\pi} g_{1\parallel}^*} \right]^{1/2} \approx \left[\frac{v_F - \frac{1}{2\pi} g_4 + \frac{1}{2\pi} (g_{1\parallel}^2 - g_{1\perp}^2)^{1/2}}{v_F - \frac{1}{2\pi} g_4 - \frac{1}{2\pi} (g_{1\parallel}^2 - g_{1\perp}^2)^{1/2}} \right]^{1/2} \quad (8.4)$$

and

$$\gamma_\rho = \left[\frac{v_\rho + \frac{1}{2\pi} (g_{1\parallel}^* - 2g_2^*)}{v_\rho - \frac{1}{2\pi} (g_{1\parallel}^* - 2g_2^*)} \right] \approx \left[\frac{v_F + \frac{1}{2\pi} g_4 + \frac{1}{2\pi} [(g_{1\parallel} - 2g_2)^2 - g_3^2]^{1/2}}{v_F + \frac{1}{2\pi} g_4 - \frac{1}{2\pi} [(g_{1\parallel} - 2g_2)^2 - g_3^2]^{1/2}} \right]^{1/2}. \quad (8.5)$$

Since both γ_σ and γ_ρ are greater than unity, the charge-density response function is not singular. The dominant singularity is in the triplet-superconductor response, although the spin-density and singlet-superconductor responses can also be divergent.

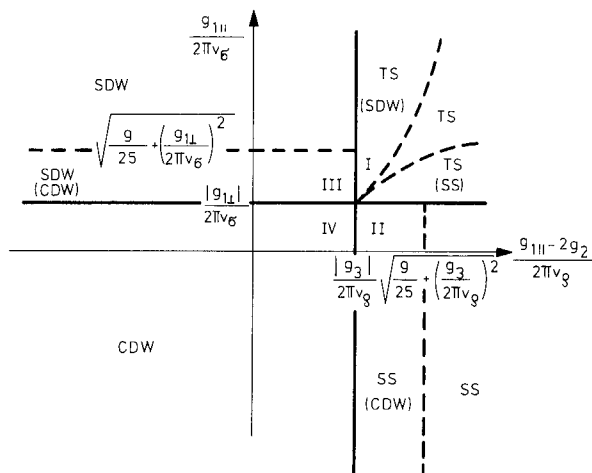
In region II, where $g_{1\parallel} < |g_{1\perp}|$ but $g_{1\parallel} - 2g_2 \geq |g_3|$, the models are equivalent to the Luther–Emery model. The σ part of the Hamilton scales to the LE line and there is a gap in the σ part of the excitation spectrum. The ρ part scales to a Tomonaga model and the Umklapp processes have no influence. As with the situation discussed in § 6.2, only the singlet-superconductor and charge-density wave responses can be divergent; their behaviour for small ω is given by eqns. (6.39) and (6.40) with γ_ρ given by eqn. (8.5). The dominant singularity is in the singlet-superconductor response.

In region III, where $g_{1\parallel} \geq |g_{1\perp}|$ but $g_{1\parallel} - 2g_2 < |g_3|$, the situation is reversed concerning the σ and ρ parts of the Hamiltonian. The gap is in the ρ part, and therefore only the charge- and spin-density responses containing S_ρ^+ can be divergent. The exponents are $\gamma_\sigma - 2$ and $1/\gamma_\sigma - 2$ for the charge- and spin-density responses respectively, with γ_σ given by eqn. (8.4). The dominant singularity is in the spin-density response.

Finally, in region IV, where $g_{1\parallel} < |g_{1\perp}|$ and $g_{1\parallel} - 2g_2 < |g_3|$, there is a gap in both the σ and ρ parts of the Hamiltonian. As discussed in § 6.2, only the charge-density response function is divergent, with an exponent of -2 .

The phase diagram has been constructed by Prigodin and Firsov (1976) for this most general case, and is shown in fig. 30.

Fig. 30

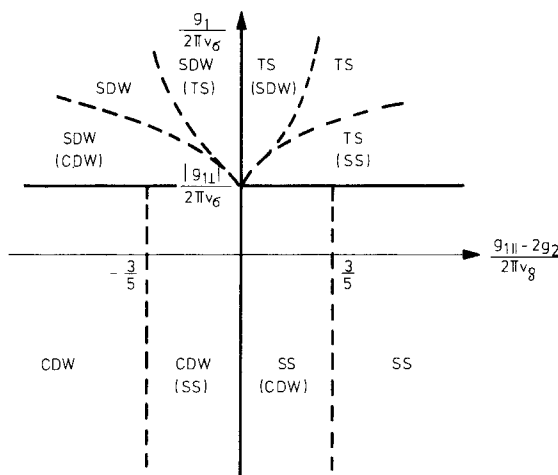


Phase diagram of the Fermi gas model for a half-filled band with spin-dependent couplings. The response functions corresponding to the phases indicated in parentheses have a lower degree of divergence than the others.

The situation is somewhat different if the band is not half-filled. In this case the ρ part is always equivalent to a Tomonaga model, $g_{1\parallel} - 2g_2$ is invariant and γ_ρ is given by

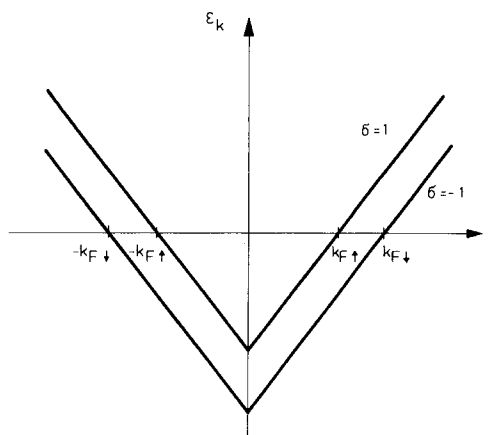
$$\gamma_\rho = \left[\frac{v_\rho + \frac{1}{2\pi}(g_{1\parallel} - 2g_2)}{v_\rho - \frac{1}{2\pi}(g_{1\parallel} - 2g_2)} \right]^{1/2} = \left[\frac{v_F + \frac{1}{2\pi}g_4 + \frac{1}{2\pi}(g_{1\parallel} - 2g_2)}{v_F + \frac{1}{2\pi}g_4 - \frac{1}{2\pi}(g_{1\parallel} - 2g_2)} \right]^{1/2}. \quad (8.6)$$

Fig. 31



Phase diagram of the Fermi gas model for a non-half-filled band with spin-dependent coupling. The response functions corresponding to the phases indicated in parentheses have a lower degree of divergence than the others.

Fig. 32



Dispersion relation of the Fermi gas model in an external magnetic field.

Depending on whether $g_{1\parallel} \geq |g_{1\perp}|$ or $g_{1\parallel} < |g_{1\perp}|$, the analysis given for regions I and II can be repeated, but with eqn. (8.6) instead of eqn. (8.5) for γ_p . The corresponding phase diagram is shown in fig. 31.

Gurgenishvili *et al.* (1977) studied the phase diagram produced in a magnetic field. The energy spectrum of free electrons is modified to

$$\epsilon_\sigma(k) = \epsilon_k + \sigma \mu H = v_F(|k| - k_{F\sigma}), \quad \sigma = \pm 1. \quad (8.7)$$

The energies are shifted differently for the two spin orientations, as shown in fig. 32, resulting in different Fermi points for the up- and down-spin bands.

The charge-density response function corresponds to the propagation of an electron-hole pair with the same spin. The singularity will appear at $2k_{F\uparrow}$ or $2k_{F\downarrow}$, i.e.

at $k = 2k_F \mp 2\mu H/v_F$. The charge-density wave state will therefore be a superposition of two charge-density waves. The spin-density response corresponds to the propagation of an electron-hole pair with different spin orientation, and the singularity appears at $k_{F\uparrow} + k_{F\downarrow} = 2k_F$. In the singlet superconductivity the Cooper pairs are formed from electrons with opposite spin, the total momentum of the pair will therefore be $\pm(k_{F\uparrow} - k_{F\downarrow}) = \mp 2\mu H/v_F$ and an inhomogeneous state appears. For triplet superconductivity the two electrons of the pair have the same spin and the total momentum of the pair is zero.

The response functions were calculated in the parquet approximation; the conclusions can, however, be formulated more generally. Since $2k_{F\uparrow}$ and $2k_{F\downarrow}$ are different, backward scattering of an up-spin electron with momentum $+k_{F\uparrow}$ on a down-spin electron with momentum $-k_{F\downarrow}$ will necessarily produce electrons which are far from the Fermi surface. In a sufficiently strong magnetic field, $\mu H \gg E_0 \exp(-\pi v_F/|g_1|)$, the contribution of these processes will be negligible, the backward scattering processes being frozen in. The forward scattering terms are not affected by the external field, so the model becomes equivalent to the Tomonaga model and the phase diagram is the same as in fig. 25.

The $4k_F$ response function, examined in §§4.3 and 5.2, depends only on the charge-density degrees of freedom, so the results obtained from the Tomonaga model are valid in the backward scattering model, provided the band is not half-filled. Singularity can appear for large negative values of $g_1 - 2g_2$.

This completes the determination of the possible ground states of a single chain. The ordered phase can occur only at $T=0$; it can, however, be stabilized at finite temperatures if a weak coupling between the chains is taken into account. This problem is discussed in § 12.

8.2. Uniform susceptibility, compressibility and specific heat

The uniform response functions have been considered by Dzyaloshinsky and Larkin (1971), Fukuyama *et al.* (1974a) and Kimura (1975) by using a parquet diagram summation or a renormalization group approach. They studied the uniform magnetic susceptibility, the charge-density response (which is related to the compressibility) and the specific heat. The existence of a gap in the excitation spectrum of the charge- or spin-density degrees of freedom will manifest itself in these quantities and may lead to unusual temperature dependences.

The long-wavelength susceptibilities of the Tomonaga model were obtained in eqn. (5.25). In the so-called k limit, i.e. for $k \rightarrow 0$ and $\omega/k \rightarrow 0$, they tend to a finite value; this is so for $g_{1\parallel} \geq |g_{\perp}|$ and $g_{1\parallel} - 2g_2 \geq |g_3|$. Since $N(0, 0)$ is related to the compressibility, both the magnetic susceptibility and the compressibility are finite in this region.

When $g_{1\parallel} < |g_{1\perp}|$, a gap appears in the spectrum of the spin degrees of freedom, and as a consequence the magnetic susceptibility shows an activated behaviour (Luther and Emery 1974):

$$\chi(0, 0) = \frac{1}{\pi u_{\sigma}} \left(\frac{2\pi\Delta_{\sigma}}{k_B T} \right)^{1/2} \exp \left[-\frac{\Delta_{\sigma}}{k_B T} \right]. \quad (8.8)$$

The value of the gap has been determined in § 6.1 for particular couplings only. Its calculation for arbitrary couplings is a delicate problem, which is dealt with in § 10. The magnetic susceptibility vanishes at $T=0$ and has a maximum at $k_B T = 2\Delta_{\sigma}$.

The compressibility shows an analogous activated behaviour for $g_{1\parallel} - 2g_2 < |g_3|$.

The activated behaviour in the specific heat appears only for a half-filled band in the region $g_{1\parallel} < |g_{1\perp}|$ and $g_{1\parallel} - 2g_2 < |g_3|$. Otherwise, there are always excitations which have no gap. The specific heat is then linear in temperature at low temperatures and is not affected by the singularity of the Green's function.

8.3. Temperature dependence of the conductivity

In the Fermi gas model, as described in § 2, the only way to achieve momentum relaxation is by Umklapp processes. In that region of temperatures where the kinetic equation can be used ($\tau T \gg 1$), the transport relaxation time coming from the electron-electron scattering (Gorkov and Dzyaloshinsky 1973) is

$$\tau_{ee}^{-1} \sim T |\Gamma_3(T)|^2, \quad (8.9)$$

where $\Gamma_3(T)$ is the renormalized vertex for Umklapp scattering defined in fig. 26. The pre-factor T is specific for the 1-d case and follows from phase space arguments, in contrast to the T^2 dependence in higher dimensions. The vertex Γ_3 can be calculated by the use of the renormalization group. The Lie equation for Γ_3 is

$$\begin{aligned} \frac{d \ln \Gamma_3(x)}{dx} = & \frac{1}{x} \left\{ \frac{1}{\pi v_p} (g_{1\parallel} - 2g_2) - \frac{i\pi}{2\pi^2 v_p^2} [(g_{1\parallel} - 2g_2)^2 + g_3^2] \right. \\ & \left. + \frac{1}{4\pi^2 v_p^2} (-g_{1\perp}^2 - 2g_{1\parallel}g_2 + 2g_2^2) + \dots \right\}, \end{aligned} \quad (8.10)$$

where $x = T/E_0$. Depending on the sign of $g_{1\parallel} - 2g_2$, the resistivity is increased or decreased compared to the linear dependence. The conductivity can be a monotonic function of temperature or can have a maximum, although the results obtained from eqns. (8.9) and (8.10) cannot be taken seriously if $|\Gamma_3(T)| > 1$.

Unfortunately, no better theory is available for the conductivity due to electron-electron scattering. One of the reasons is that the dominant contribution to the resistivity in 1-d conductors probably comes from other scattering mechanisms, such as electron-phonon scattering or scattering on impurities; moreover, the effect of disorder can be very important. A detailed discussion of these effects is outside the scope of the present review. A detailed study of the resistivity caused by impurities is presented in the review by Abrikosov and Ryzhkin (1978). Only a few remarks will be made here.

It is known from the work of Mott and Twose (1961) that a random potential, however weak, leads to localization of the states in 1-d systems. Berezinsky (1973) made a detailed calculation of the conductivity of a 1-d electron gas that took into account exactly the effect of impurities, but the electron-electron interaction was neglected. He showed that the d.c. conductivity vanishes, indicating that the electron states are in fact localized. The conductivity at finite frequencies depends on the amplitude of backward scattering on the impurity, and has a maximum at $\omega \sim 1/\tau_2$ where τ_2 is the corresponding collision time. This conductivity is roughly temperature-independent.

The interaction between electrons can give rise to an essential temperature dependence of the conductivity. Luther and Peschel (1974 b) and Mattis (1974 b) have shown that by treating the impurity scattering in the Born approximation, but considering the electron-electron interaction exactly, the conductivity of the

Tomonaga–Luttinger model is strongly temperature-dependent and can be enhanced compared to the non-interacting case. It can be divergent at $T=0$ for attractive g_2 interactions, and its temperature dependence is given by

$$\sigma(T) \sim \sigma_0(T) T^\gamma, \quad \gamma = \frac{g_2/2\pi v_F}{1 + g_2/\pi v_F}, \quad (8.11)$$

where $\sigma_0(T)$ is the conductivity for impurity scattering calculated in the Born approximation for the non-interacting system. In deriving this expression, Luther and Peschel used a relationship obtained by Götze and Wölfe (1972) between the momentum relaxation time and charge-density response function,

$$\tau^{-1} = \lim_{\omega \rightarrow 0} \frac{c}{\omega} U^2 v_F^2 \sum_{k, k'} (k - k')^2 \operatorname{Im} N(k - k', \omega), \quad (8.12)$$

where c is the impurity concentration and U is the impurity potential. The main contribution comes from the $2k_F$ part of the charge-density response. The results have been extended by Gorkov and Dzyaloshinsky (1973) and by Fukuyama *et al.* (1974 b) for the backward scattering model. Since the impurity scattering is treated in the Born approximation, localization effects are neglected. These calculations cannot, therefore, predict the correct low-temperature behaviour of the conductivity.

§ 9. DIFFERENT CHOICES OF THE CUT-OFF

It was emphasized in § 2, where the Fermi gas model was introduced, that the cut-off has to be properly given in order to have a well-defined theory. It was shown that there are two usual choices of the cut-off, depending on the physical interpretation. In one case, i.e. in the model with bandwidth cut-off, all the momenta are restricted to a band which is symmetric around the Fermi points. This cut-off procedure was used in the renormalization group treatment. The other choice is to have a momentum transfer cut-off, i.e. to limit the momentum p in eqn. (2.4) to small values. In fact, the transferred momentum is small in the g_2 and g_4 terms, whereas it is about $2k_F$ for the g_1 and g_3 terms. These latter processes can be interpreted as coming from phonon-mediated effective electron–electron scattering processes in which a phonon with momentum $2k_F$ is exchanged. Physically, it would be more appropriate to have a cut-off on the energy transfer, but this model is less easy to treat.

In the Tomonaga model where the large momentum transfer terms are neglected, a cut-off $k_c \sim \Lambda$ on p allows a consistent treatment, as shown in § 5. It was pointed out by Chui *et al.* (1974) that, in a model with phonon-mediated electron–electron interactions where the backward scattering terms are important, two cut-offs should appear: a bandwidth cut-off E_0 and an energy-transfer cut-off ω_D . While a model with bandwidth cut-off is properly defined, a model with energy transfer cut-off is not well defined if backward scattering terms are present, and a bandwidth cut-off should necessarily be introduced. The energy transfer cut-off is replaced for simplicity by a momentum transfer cut-off k_c , where $\omega_D = 2v_F k_c$. The results obtained for models with two characteristic energies are reviewed in this section.

A different cut-off procedure is used if the bosonized Hamiltonian is considered. In this case the parameter α is kept finite and is identified with the cut-off. Following Grest (1976) and Theumann (1977), the problem of whether α can be taken as a physical cut-off will be discussed in § 9.2. See also note added in proof.

9.1. Scaling theories with two cut-offs

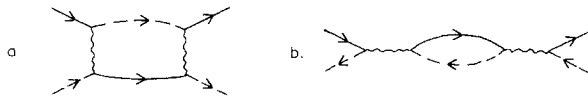
The phonon-mediated attractive electron-electron interaction which is used in the BCS theory of superconductivity is usually taken in an energy range of width $2\omega_D$ around the Fermi energy, where ω_D is the Debye energy. This cut-off is usually smaller than the real bandwidth, but the latter plays no role in a 3-d system where only the Cooper-pair diagrams are singular. In a 1-d system, when electron-hole bubbles should also be given equal consideration, both cut-offs appear in logarithmic contributions. Figure 33 shows two typical diagrams. In the Cooper pair diagram of fig. 33 (a) the momenta in the intermediate state are limited to the neighbourhood of the incoming momenta if the momentum transfer is restricted to a range $2k_c$ around $2k_F$ and the analytic contribution is

$$-\frac{g_1^2}{2\pi v_F} \left(\ln \frac{\omega}{\omega_D} - \frac{i\pi}{2} \right) \delta_{\alpha\bar{\alpha}} \delta_{\beta\bar{\beta}}. \quad (9.1)$$

The transferred momentum of the electron-hole bubble of fig. 33 (b) does not appear in the integration, the momenta in the intermediate state are not limited by the transfer cut-off and therefore a bandwidth cut-off has to be used, leading to

$$\frac{g_1^2}{\pi v_F} \left(\ln \frac{\omega}{E_0} - \frac{i\pi}{2} \right) \delta_{\alpha\bar{\alpha}} \delta_{\beta\bar{\beta}}. \quad (9.2)$$

Fig. 33



(a) Cooper pair and (b) electron-hole polarization diagrams in the lowest order. The wavy line represents a phonon exchange.

The model with two cut-offs, a cut-off k_c for the momentum transfer and another cut-off E_0 for the bandwidth, has been studied by Grest *et al.* (1976) using the renormalization group. These authors, by extending a suggestion by Chui *et al.* (1974), showed that this problem can be mapped onto a one-cut-off problem by eliminating the phase space between the energies ω_D and E_0 . The new couplings of the one-cut-off problem are

$$\bar{g}_1 = \frac{g_1}{1 - \frac{g_1}{\pi v} \ln \frac{\omega_D}{E_0}}, \quad \bar{g}_2 = g_2, \quad (9.3)$$

and the Fermi velocity v_F is replaced by

$$v = v_F - \frac{g_1}{2\pi} - \frac{g_1^2}{2\pi^2 v} \ln \frac{\omega_D}{E_0} + \dots \quad (9.4)$$

The apparent divergence of \bar{g}_1 is cured if this Fermi velocity renormalization is taken into account. The scaling equations derived in §4.3 can be used to calculate the response functions. The low-frequency behaviour of the response functions of the two-cut-off model is the same as that of a one-cut-off model, provided the values \bar{g}_1 and \bar{g}_2 are taken for the bare couplings.

An alternative two-cut-off model has been considered by Sólyom and Szabó (1977). Since the momentum transfer cut-off is only an approximation for the energy transfer cut-off in the phonon-mediated electron-electron coupling, they made a different approximation by using a bandwidth cut-off at ω_D for this interaction. The direct electron-electron interaction is also considered, with a bandwidth cut-off at E_0 . It is shown that, (as in the model of Grest *et al.* (1976)), this model can also be mapped onto a one-cut-off model with effective \bar{g}_1 and \bar{g}_2 couplings. The physical behaviour of the system is therefore the same as discussed in § 8.

9.2. Relationship between the physical cut-offs and the cut-off of the bosonized Hamiltonian

The overall behaviour of the Fermi gas model is similar whether a bandwidth cut-off or a momentum transfer cut-off is used. There are certainly differences in detail, as already mentioned in § 2 and § 9.1. In the solution of the backward scattering model in § 6 a different cut-off procedure was used,—that of keeping the parameter α of the bosonization transformation finite to obtain a non-singular result for the energy spectrum. It can be shown that this procedure reproduces the results of the Tomonaga model with only a slight difference. In the expressions (5.19), (5.28) and (5.30) obtained for the Green's function and response functions by direct diagram summation, the free Green's function contains a bandwidth cut-off $\delta \sim 1/k_0$, whereas the correction terms contain only $\Lambda \sim k_c$. Calculating the same quantities in the boson representation, the Tomonaga Hamiltonian can be bosonized without using eqns. (5.56) and (5.57). These operator identities are used only to express the fermion operators of the Green's function and response functions in terms of the boson operators. Finite α leads to an expression for $G_+(x, t)$ similar to eqn. (5.19), where α appears instead of both δ and Λ^{-1} ; the same is true for the response functions. This shows that in the Tomonaga model, where exact results are available, α corresponds exactly neither to a bandwidth cut-off nor to a momentum transfer cut-off, but appears in place of both of them.

The situation is more complicated in the backward scattering model. Here no exact solutions are available without the bosonization transformation, and therefore no definite statement can be made. Calculations made by Grest (1976) and Theumann (1977) indicate, however, that keeping α finite poses some problems. Grest compared the perturbational expressions of the charge-density response function obtained in a model with bandwidth cut-off (see § 4.3), in one with both momentum transfer and bandwidth cut-off (see § 9.1) and in one with the bosonization transformation (see § 6.2). These are denoted by N_S (Sólyom 1973), N_G (Grest *et al.* 1976) and N_{LE} (Luther and Emery 1974) respectively. The results are

$$N_S(\omega) = \frac{1}{\pi v_F} \ln \frac{\omega}{E_0} \left[1 + \frac{1}{2\pi v_F} (g_{1\parallel} + g_{1\perp} - g_2) \ln \frac{\omega}{E_0} + \dots \right], \quad (9.5)$$

$$\begin{aligned} N_G(\omega) = & \frac{1}{\pi v_F} \ln \frac{\omega}{E_0} \left[1 + \frac{1}{2\pi v_F} (g_{1\parallel} + g_{1\perp}) \ln \frac{\omega}{E_0} + \dots \right] \\ & - \frac{1}{2\pi^2 v_F^2} g_2 \ln^2 \frac{\omega}{\omega_D} + \dots, \end{aligned} \quad (9.6)$$

and

$$N_{\text{LE}}(\omega) = \frac{1}{\pi v_F} \ln \frac{\omega\alpha}{v_F} \left[1 + \frac{g_{1\perp}}{2\pi v_F} \ln \frac{\omega\alpha}{v_F} \right] \\ + \frac{1}{2\pi^2 v_F^2} (g_{1\parallel} - g_2) \ln^2 \frac{\omega\alpha}{2v_F} + \dots \quad (9.7)$$

The terms proportional to $g_{1\parallel}$ and $g_{1\perp}$ correspond to the same diagram and differ only in the spin orientations on the lines. The corresponding contribution should be the same and it should be proportional to the square of the contribution of the simple electron-hole bubble. This is not true in the Luther-Emery solution. The extra factor of 2 in the argument of $\ln^2(\omega\alpha/2v_F)$ indicates that the use of α may lead to non-physical results in the next-to-leading logarithmic contributions already. A similar situation was noticed by Wilson (1975) when he compared his exact results with the results obtained with the bosonization transformation in the Kondo problem.

Theumann (1977) studied the problem of under what conditions the transformations that allow the Luther-Emery solution to be obtained can be performed. She showed that the canonical transformation (5.46) preserves the anticommutation relation of the fermion fields only if the limit $\alpha \rightarrow 0$ is taken first. The momentum transfer cut-off Λ appearing in the canonical transformation through $\phi(p)$ and $\psi(p)$ cannot be identified with $1/\alpha$, since normalization factors would appear in the anticommutators. On the other hand, the backward scattering term can be written as a bilinear expression of spinless fermions for the particular value $g_{1\parallel} = -\frac{3}{5}(2\pi v_F + g_{4\parallel} - g_{4\perp})$ only if the limiting process is inverted, as in the Luther-Emery solution, and $\Lambda \rightarrow \infty$ first while keeping α finite.

There are, however, other physical arguments which suggest that the choice of a finite α may be a reasonable cut-off procedure. Lee (1975) pointed out that the binding energy of a singlet pair in a model with linear dispersion and a bandwidth cut-off at $E_0 = v_F/\alpha$ is

$$2\Delta = \frac{v_F}{\alpha} \left[\exp\left(\frac{\pi v_F}{g}\right) - 1 \right]^{-1}. \quad (9.8)$$

In the limit of strong coupling, Δ reduces to the value obtained by Luther and Emery (1974) showing that using α leads to physically correct results. Without making strong statements, the only conclusion can be that the results obtained for the bosonized Hamiltonian should always be considered with some caution.

§ 10. SOLUTION OF THE MODEL BELOW THE LUTHER-EMERY LINE

The aim of this paper until now has been to find exact solutions for particular cases of the Fermi gas model and to use scaling arguments to extend these results for arbitrary values of the couplings. Luther (1976, 1977) has shown that an alternative approach is possible. He pointed out that an exactly soluble model, the 1-d anisotropic Heisenberg model, can be transformed to a form equivalent to the backward scattering model. Knowing the energy spectrum of the 1-d spin model (Johnson *et al.* 1973), that of the 1-d Fermi gas can also be obtained. New features appear below the Luther-Emery line, and it is this region that is of most interest.

Luther (1977) started from the boson representation of the Fermi gas Hamiltonian. As in § 6.1, two transformations are performed on H_σ , first a canonical transformation given by eqns. (5.46) and (5.48), then a transformation to the spinless fermions introduced in eqns. (6.12) and (6.13). Leaving ψ undetermined for the moment, the first transformation leads to

$$\begin{aligned} \tilde{H}_\sigma = & \frac{2\pi v_F}{L} \sum_{p>0} \left\{ \left[1 + \frac{1}{2\pi v_F} (g_{4\parallel} - g_{4\perp}) \right] \cosh 2\psi(p) - \frac{1}{2\pi v_F} g_{1\parallel} \sinh 2\psi(p) \right\} \\ & \times [\sigma_1(p)\sigma_1(-p) + \sigma_2(-p)\sigma_2(p)] \\ & + \frac{2\pi v_F}{L} \sum_{p>0} \left\{ \left[1 + \frac{1}{2\pi v_F} (g_{4\parallel} - g_{4\perp}) \right] \sinh 2\psi(p) - \frac{1}{2\pi v_F} g_{1\parallel} \cosh 2\psi(p) \right\} \\ & \times [\sigma_1(p)\sigma_2(-p) + \sigma_1(-p)\sigma_2(p)] \\ & + \frac{g_{1\perp}}{(2\pi\alpha)^2} \int dx \left\{ \exp \left[\frac{2\pi}{L} \sum_p \frac{\exp(-\frac{\alpha}{2}|p| - ipx)}{p} \sqrt{2 \exp(\psi) (\sigma_1(p) + \sigma_2(p))} \right] + \text{h.c.} \right\} \end{aligned} \quad (10.1)$$

The spinless fermion representation can be used for the backward scattering term if $\sqrt{2 \exp(\psi)} = 1$. Fixing ψ at this value, the Hamiltonian can be written in terms of c_k and d_k , introduced in eqns. (6.12) and (6.13), as

$$\begin{aligned} \tilde{H}_\sigma = & \frac{2\pi v'}{L} \sum_{k>0} [\sigma_1(k)\sigma_1(-k) + \sigma_2(-k)\sigma_2(k)] \\ & - \frac{1}{L} \sum_k \left\{ \frac{5}{4} g_{1\parallel} + \frac{3}{2} \pi v_F \left[1 + \frac{1}{2\pi v_F} (g_{4\parallel} - g_{4\perp}) \right] \right\} \sigma_1(k)\sigma_2(-k) \\ & + \frac{g_{1\perp}}{2\pi\alpha} \sum_k (c_{k+k_F}^+ d_{k-k_F}^- + d_{k-k_F}^+ c_{k+k_F}^-), \end{aligned} \quad (10.2)$$

where

$$\sigma_1(k) = \sum_p c_{p+k}^+ c_p, \quad \sigma_2(k) = \sum_p d_{p+k}^+ d_p \quad (10.3)$$

and

$$v' = \frac{5}{4} \left[v_F + \frac{1}{2\pi} (g_{4\parallel} - g_{4\perp}) \right] + \frac{3}{8\pi} g_{1\parallel}. \quad (10.4)$$

This Hamiltonian corresponds to a one-dimensional interacting spinless fermion system. The interaction vanishes on the Luther–Emery line, and the problem can be solved, as shown by Luther and Emery (1974). Apart from an attempt by Schlottmann (1977 a, b), no direct solution is known for other values of the couplings. However, Luther produced a remarkable solution by noticing the analogy of this model to the spin- $\frac{1}{2}$ 1-d anisotropic Heisenberg model.

The Hamiltonian of an anisotropic Heisenberg model on a chain with N sites is

$$H_{XYZ} = - \sum_{\alpha=1}^N J_\alpha S_j^\alpha S_{j+1}^\alpha, \quad (10.5)$$

where j denotes the lattice sites on the chain, α stands for the component indices x , y and z , and the exchange coupling J_α can be different for the three components. This model is also called X - Y - Z model. The $S=\frac{1}{2}$ spin problem is conveniently transformed to a spinless fermion problem by using the Jordan-Wigner transformation

$$\begin{aligned} S_j^+ &= S_j^x + iS_j^y = a_j^+ \prod_{l=1}^{j-1} \exp(i\pi a_l^+ a_l), \\ S_j^- &= S_j^x - iS_j^y = a_j \prod_{l=1}^{j-1} \exp(-i\pi a_l^+ a_l), \\ S_j^z &= a_j^+ a_j - \frac{1}{2}. \end{aligned} \quad (10.6)$$

The spin operators expressed in terms of spinless fermions obey the correct commutation relations.

With a cyclic boundary condition for the chain, i.e. taking $S_{N+1} = S_1$, it is found that

$$\begin{aligned} H_{XYZ} = & -\frac{1}{4}(J_x + J_y) \sum_{j=1}^{N-1} (a_j^+ a_{j+1} + a_{j+1}^+ a_j) \\ & -\frac{1}{4}(J_x - J_y) \sum_{j=1}^{N-1} (a_j^+ a_{j+1}^+ + a_{j+1} a_j) \\ & -J_z \sum_{j=1}^N (a_j^+ a_j - \frac{1}{2}) (a_{j+1}^+ a_{j+1} - \frac{1}{2}) \\ & -\frac{1}{4}(J_x + J_y)(a_N^+ a_1 + a_1^+ a_N) \exp\left(i\pi \sum_{l=1}^N a_l^+ a_l\right) \\ & -\frac{1}{4}(J_x - J_y)(a_N^+ a_1^+ + a_1 a_N) \exp\left(i\pi \sum_{l=1}^N a_l^+ a_l\right). \end{aligned} \quad (10.7)$$

The last two terms can be merged into the first two by extending the summation up to N if

$$\mathcal{N} = \sum_{l=1}^N a_l^+ a_l$$

is an even number. If it is odd, the Hamiltonian should be treated somewhat differently. This complication will be laid aside for the time being, but its consequences are examined later in this section.

Introducing the Fourier-transformed operators with

$$a_k = \frac{1}{\sqrt{N}} \sum_{j=1}^N \exp(ikja) a_j \quad \text{and} \quad -\frac{\pi}{a} \leq k \leq \frac{\pi}{a}, \quad (10.8)$$

where a is the lattice constant, the Hamiltonian can be written in the form

$$\begin{aligned} H_{XYZ} = & -\frac{1}{2}(J_x + J_y) \sum_k \cos(ka) a_k^+ a_k \\ & -\frac{J_z}{N} \sum_k \cos(ka) \rho(k) \rho(-k) \\ & + \frac{1}{4}(J_x - J_y) \sum_k [\exp(ika) a_k^+ a_k^+ + \exp(-ika) a_k a_k] \end{aligned} \quad (10.9)$$

where

$$\rho(k) = \sum_p a_{p+k}^+ a_p. \quad (10.10)$$

In zero magnetic field the total magnetization

$$\langle S^z \rangle = \sum_{j=1}^N \langle S_j^z \rangle = 0.$$

Using eqn. (10.6), this means that the number of fermions,

$$\mathcal{N} = \sum_{j=1}^N a_j^+ a_j,$$

is $N/2$, corresponding to a half-filled band. The Fermi points are at $k_F = \pm \pi/2a$. The dispersion relation of the free fermions is the same as that shown in fig. 1. Assuming that particles lying near the Fermi surface play an important role, the wave-vectors in the region $k \sim \pm k_F$ contribute in the first and third terms, while the regions around 0 and $2k_F$ should be considered in the second term of eqn. (10.9). Approximating the dispersion relation by two linear spectra, as given in fig. 2, the particles corresponding to the two branches are distinguished by the indices 1 and 2, referring to the regions around $+k_F$ and $-k_F$ respectively. Further approximations are made in the second and third terms, where $\cos(ka)$ and $\exp(ika)$ are approximated by their first terms in the expansion around $k=0$ and $k=2k_F$ and $k=\pm k_F$ respectively. The Hamiltonian, when written in terms of the operators $a_{1,k+k_F}$ and $a_{2,k-k_F}$, and

$$\rho_1(k) = \sum_p a_{1,p+k}^+ a_{1,p}$$

and

$$\rho_2(k) = \sum_p a_{2,p+k}^+ a_{2,p}$$

has the form

$$\begin{aligned} H_{XYZ} = & \frac{1}{2}(J_x + J_y) a \sum_k k (a_{1,k+k_F}^+ a_{1,k+k_F} - a_{2,k-k_F}^+ a_{2,k-k_F}) \\ & - \frac{2J_z}{N} \sum_{k>0} [\rho_1(k)\rho_1(-k) + \rho_2(-k)\rho_2(k)] \\ & - \frac{4J_z}{N} \sum_k \rho_1(k)\rho_2(-k) \\ & + i\frac{1}{2}(J_x - J_y) \sum_k (a_{1,k+k_F}^+ a_{2,-k-k_F}^+ + a_{1,k+k_F} a_{2,-k-k_F}). \end{aligned} \quad (10.11)$$

The momentum summation is cut off at $1/a$. After a further transformation, $a_{2,k-k_F} \rightarrow ia_{2,-k-k_F}^+$, and using the fact that the kinetic energy term can be written in terms of ρ as in the Tomonaga-Luttinger model, it is found that

$$\begin{aligned} H_{XYZ} = & a \left\{ \frac{2\pi}{L} \left[\frac{1}{2}(J_x + J_y) - \frac{1}{\pi} J_z \right] \sum_{k>0} [\rho_1(k)\rho_1(-k) + \rho_2(-k)\rho_2(k)] \right. \\ & + \frac{4J_z}{L} \sum_k \rho_1(k)\rho_2(-k) \\ & \left. + \frac{1}{2a} (J_x - J_y) \sum_k (a_{1,k+k_F}^+ a_{2,k-k_F} + a_{2,k-k_F}^+ a_{1,k+k_F}) \right\}, \end{aligned} \quad (10.12)$$

This Hamiltonian is the same as the one in eqn. (10.2), if measured in units of a . The correspondences between the coefficients are given by

$$a \left[\frac{1}{2}(J_x + J_y) - \frac{1}{\pi} J_z \right] = \frac{5}{4} \left[v_F + \frac{1}{2\pi} (g_{4\parallel} - g_{4\perp}) \right] + \frac{3}{8\pi} g_{1\parallel}, \quad (10.13)$$

$$a4J_z = -\frac{5}{4}g_{1\parallel} - \frac{3}{2}\pi \left[v_F + \frac{1}{2\pi} (g_{4\parallel} - g_{4\perp}) \right] \quad (10.14)$$

and

$$\frac{1}{2}(J_x - J_y) = \frac{g_{1\perp}}{2\pi\alpha}. \quad (10.15)$$

The two soluble cases of the Fermi gas model correspond to simple situations in the X - Y - Z model. In the Tomonaga model, $g_{1\perp} = 0$, corresponding to $J_x = J_y$, which is the Heisenberg–Ising or X - X - Z model. The right-hand side of eqn. (10.14) vanishes on the Luther–Emery line, i.e. the Luther–Emery model corresponds to $J_z = 0$, which is the X - Y model.

The low-lying excited states of the X - Y - Z model have been determined exactly by Johnson *et al.* (1973) by using Baxter’s relation (Baxter 1971, 1972) between the energy levels of the X - Y - Z Hamiltonian and the eigenvalues of the eight-vertex transfer matrix. Using the correspondence in eqns. (10.13)–(10.15), the energy spectrum of the 1-d Fermi gas model can also be obtained.

Before writing down the results, it is appropriate to comment on the exactness of this correspondence. In the course of the transformations leading to eqn. (10.12), two approximations were made. First, the Hamiltonian was simplified by neglecting in eqn. (10.7) the phase factors

$$\exp \left(i\pi \sum_{l=1}^N a_l^+ a_l \right).$$

This factor equals 1 if the number of particles is even, and -1 is the number of particles is odd. The Hamiltonian has to be treated separately in the two subspaces. Since the evenness and oddness of the number of particles is invariant under the further transformations, the Hamiltonian has to be treated separately in the subspaces in which the number of spin-wave quasi-particles is even or odd. As a consequence, the excited states of the system are obtained by adding pairs of quasi-particles to the ground state. The gap in the excitation spectrum is twice as big as the gap in the single spin-wave energy, but states with a single spin-wave are not eigenstates of the X - Y - Z Hamiltonian. The equivalence with the Fermi gas model was obtained for the simplified Hamiltonian, so there is no restriction in the Fermi gas model that only pairs of quasi-particles can be excited.

An important approximation was made in eqn. (10.9) when $\cos(ka)$ and $\exp(ika)$ were expanded and only the first terms were considered. Luther (1976) argues that a continuum version of the X - Y - Z model can be introduced in the limit $a \rightarrow 0$, and the steps leading to eqn. (10.12) are exact in the continuum limit. The continuum version of the Jordan–Wigner transformation was constructed by Luther and Peschel (1975). There are, of course, important renormalizations of the coupling constants and it is usually difficult to consider this renormalization explicitly. Luther (1976) suggested a neat way of avoiding this problem. As mentioned before, the X - Y - Z

model ($J_x = J_y$) corresponds to the Tomonaga model. The correlation functions can be calculated for the X - X - Z model (Johnson *et al.* 1973). On the other hand, these quantities are known for the Tomonaga model as well. The corresponding problems should have the same exponent. The exponents appearing in the calculation for the Tomonaga model are expressed in terms of γ_σ , given by eqn. (5.26), which can be written as

$$\gamma_\sigma = \left[\frac{v_\sigma + \frac{1}{2\pi} g_{1\parallel}}{v_\sigma - \frac{1}{2\pi} g_{1\parallel}} \right]^{1/2} = \left[\frac{v_F + \frac{1}{2\pi} (g_{4\parallel} - g_{4\perp}) + \frac{1}{2\pi} g_{1\parallel}}{v_F + \frac{1}{2\pi} (g_{4\parallel} - g_{4\perp}) - \frac{1}{2\pi} g_{1\parallel}} \right]^{1/2} \quad (10.16)$$

if $g_{1\parallel}$ and g_2 are used instead of $g_{2\parallel}$ and $g_{2\perp}$. Calculating the response functions for the Heisenberg-Ising model, the corresponding exponents are obtained in the form

$$\gamma_\sigma = 1 - \frac{\mu}{\pi} = 1 - \frac{1}{\pi} \arccos \left(-\frac{J_z}{J_x} \right). \quad (10.17)$$

Using the identification given by eqns. (10.13) and (10.14) for $J_x = J_y$, the two expressions are not equivalent. This apparent contradiction is resolved by taking into account the fact that eqns. (10.13)–(10.15) were obtained without performing the renormalization necessary in the continuum limit. In this limit, when $a \rightarrow 0$, the renormalization should lead to identical exponents. Thus the renormalized parameters of the spin model in the continuum limit should be identified with the parameters of the Fermi gas by equating eqns. (10.16) and (10.17). It should be noted near the LE line, where J_z is small, the expansions of eqns. (10.16) and (10.17) agree to first order, indicating that in the weak coupling limit of the spinless fermion problem, states lying far from the Fermi surface, in a region where the dispersion is not linear, do not contribute essentially.

A further consequence of the continuum limit is that the anisotropy $(J_x - J_y)/(J_x + J_y)$ should tend to zero as $a \rightarrow 0$. One can therefore use the excitation spectrum valid in the limit of small anisotropy; $l^2 = (J_x^2 - J_y^2)/(J_x^2 - J_z^2) \rightarrow 0$. In this limit Johnson *et al.* (1973) found that in the lattice theory there is a gap in the spin-wave spectrum with

$$\Delta = 4\pi \frac{\sin \mu}{\mu} |J_x| \left(\frac{l}{4} \right)^{\pi/\mu}, \quad (10.18)$$

where μ is given by eqn. (10.17). In the continuum limit J_x and l should be replaced by their renormalized values. The renormalized value of J_x diverges as $1/a$ and, at the same time, l should tend to zero as $a^{\mu/\pi}$, to have a finite gap as $a \rightarrow 0$. It follows from eqn. (10.15) that the quantity corresponding to the anisotropy $J_x - J_y$ is $g_{1\perp}$; Luther (1977) therefore concludes that the value of the gap in the Fermi gas problem is

$$\Delta = \frac{4\pi v_\sigma \sin \mu}{\alpha} \left(\frac{g_{1\perp}}{8\pi v_\sigma} \right)^{\pi/2\mu}, \quad (10.19)$$

where now $\mu = \pi(1 - \gamma_\sigma)$ is given by eqn. (10.16). The identification of μ and l with the corresponding expressions in the Fermi gas model is not rigorous in a mathematical sense. It is, however, very reasonable physically to use this identification, although certain problems arise. The exponent $\pi/2\mu$ diverges when $g_{1\parallel} \rightarrow 0$, i.e. the gap

vanishes on the line $g_{1\parallel} = 0$ if $|g_{1\perp}| < 8\pi v_\sigma$. This contradicts the result obtained in the renormalization group treatment, according to which the scaling trajectories go through the $g_{1\parallel} = 0$ line, as shown in fig. 28. This discrepancy is either a consequence of treating the cut-off in a particular way or is due to the ambiguities in taking the continuum limit. The results are probably correct in the vicinity of the LE line where the renormalizations are unimportant.

Although the expression of μ in terms of the Fermi gas parameters depends on the cut-off prescription, it is expected that the analogy with the X - Y - Z model allows a qualitatively correct description. There is a gap in the excitation spectrum for any $g_{1\parallel} < 0$. On the LE line itself the gap determined in § 6.1 is reproduced. Here we have to take into account that, as discussed earlier in this paragraph, the gap of the X - Y - Z model is twice the single particle gap.

Completely new features appear below the Luther-Emery line, i.e. for $g_{1\parallel} < -\frac{6}{5}\pi v_\sigma$. In this region, which corresponds to $J_z > 0$ in the X - Y - Z model, bound states appear in addition to the free state solutions. In the limit of weak anisotropy, the energies of these excitations are given by

$$\Delta_n^2(k) = \Delta_n^2 + c^2 k^2, \quad (10.20)$$

where

$$\Delta_n = \Delta \sin\left(\frac{n\pi}{2} \frac{\pi - \mu}{\mu}\right), \quad n = 1, 2, \dots, < \frac{\mu}{\pi - \mu}. \quad (10.21)$$

These new states first appear at $g_{1\parallel} = -\frac{6}{5}\pi v_\sigma$, where $\mu = \pi/2$. In the X - Y - Z model these are bound spin-wave states since, for a slightly stronger coupling, their energy is lower than the energy of two free spin-waves. The binding energy increases with stronger coupling. At $\mu = \frac{2}{3}\pi$, then at $\mu = \frac{3}{4}\pi$ etc., further bound states will appear.

In the Fermi gas model, where no distinction should be made between states with an even or odd number of particles, the bound states appear at twice the single particle gap, but can descend below it for a sufficiently strong coupling.

The appearance of bound states in the strong coupling regime will give rise to significant modifications in the response functions if compared with a model in which only free states are present. It is expected that the correlation function critical exponents will be modified. In the scaling treatment in § 7, where scaling to the LE line was used to obtain information about the region above the LE line, there was no indication that scaling cannot be continued to couplings below this line. Nevertheless, since the appearance of bound states is not compatible with the simple scaling ideas suggested for this model in § 4.2, it is believed that this scaling no longer holds in the strong coupling regime.

One should not, however, over-emphasize the results obtained for the Fermi gas model by using this analogy with the X - Y - Z model. This latter model is related directly to the spinless fermion model. It has been mentioned that the transformations leading from the original Fermi gas model to the spinless fermion model are not exact if α in the bosonization transformation is identified with the cut-off and kept finite.

§ 11. RELATIONSHIP BETWEEN THE FERMI GAS MODEL AND OTHER MODELS

As shown in § 10, the spin- $\frac{1}{2}$ X - Y - Z chain is equivalent to the Fermi gas model and the known solution of the spin model can be used to help to solve the Fermi gas

model. A remarkable feature of this particular model is that equivalence to several other models—including 1-d and 2-d spin models, field theoretical models and the two-dimensional Coulomb gas—can be found. By using these relationships a large class of models can be studied, most of which are of interest in their own right.

11.1. The two-dimensional Coulomb gas

Chui and Lee (1975) recognized that the 1-d Fermi gas model is equivalent to the 2-d classical plasma with a long-range logarithmic Coulomb potential. They started from the bosonized form of the Hamiltonian as given in eqns. (6.6)–(6.8). For a non-half-filled band the charge-density part is a Tomonaga model Hamiltonian and only the spin-density part will be considered. A similar equivalence holds for H_ρ if Umklapp processes are not negligible.

After a canonical transformation, \tilde{H}_σ takes the form given in eqn. (6.10). If the backward scattering term is treated as a perturbation, the partition function $Z = \langle \exp(-\beta \tilde{H}_\sigma) \rangle$ can be written as $Z = Z_0 \cdot \Delta Z$ where Z_0 is the partition function of the system without backward scattering and

$$\begin{aligned} \Delta Z = & \sum_n \left[\frac{g_{1\perp}}{(2\pi\alpha)^2} \right]^{2n} \int_0^{\beta} d\tau_{2n} \cdots \int_0^{\tau_3} d\tau_2 \int_0^{\tau_2} d\tau_1 \\ & \times \int_0^L \left(\prod_{i=1}^{2n} dx_i \right) \sum_Q \left\langle \prod_{i=1}^{2n} \exp \{ s_Q(i) \sqrt{2} \exp(\psi) [\phi_1(\tau_i, x_i) + \phi_2(\tau_i, x_i)] \} \right\rangle_{H_0}, \end{aligned} \quad (11.1)$$

where

$$\phi_j(x) = \frac{2\pi}{L} \sum_k \frac{\exp(-\frac{\alpha}{2}|k| - ikx)}{k} \sigma_j(k), \quad (11.2)$$

the time dependence is defined in the usual way and $s_Q = \pm 1$, depending on whether the term written out in eqn. (6.10) or its complex conjugate is taken. The summation over Q goes over all possibilities in taking one of the two terms. The average over the non-interacting Hamiltonian leads to (Schulz 1977)

$$\begin{aligned} \Delta Z = & \sum_n \left[\frac{g_{1\perp}}{(2\pi\alpha)^2} \right]^{2n} \int_0^{\beta} d\tau_{2n} \cdots \int_0^{\tau_3} d\tau_2 \int_0^{\tau_2} d\tau_1 \\ & \times \int_0^L \left(\prod_{i=1}^{2n} dx_i \right) \sum_Q \exp \left\{ -2 \exp(2\psi) \sum_{i>j=1}^{2n} s_Q(i) s_Q(j) g(x_i - x_j, u_\sigma \tau_i - u_\sigma \tau_j) \right\} \end{aligned} \quad (11.3)$$

with

$$g(x, y) = \int_0^\infty dq \frac{\exp(-\alpha q)}{q} [(1 + n_q) \exp(iqx - q|y|) + n_q \exp(iqx + q|y|) - 1 - 2n_q] + \text{h.c.} \quad (11.4)$$

where

$$n_q = [\exp(\beta u_\sigma q) - 1]^{-1}. \quad (11.5)$$

By using the symmetry properties of the g function, and taking into account that the number of possible combinations in the summation over Q is $(2n)!/(n!)^2$, since an equal number of terms with $s_Q(i) = 1$ and $s_Q(i) = -1$ should be present,

$$\Delta Z = \sum_n \frac{1}{(n!)^2} \left[\frac{g_{1\perp}}{u_\sigma (2\pi\alpha)^2} \right]^{2n} \int_0^L \int_0^{u_\sigma \beta} \left(\sum_{i=1}^{2n} dx_i dy_i \right) \times \exp \left\{ -2 \exp(2\psi) \sum_{i>j=1}^{2n} s_i s_j g(x_i - x_j, y_i - y_j) \right\}. \quad (11.6)$$

It is possible to arrange the terms with $s_i = \pm 1$ so that $s_i = 1$ for $i = 1, \dots, n$ and $s_i = -1$ for $i = n+1, \dots, 2n$.

Following Chui and Lee (1975), one can recognize in eqn. (11.6) the grand partition function of a classical real gas of two kinds of particles with equal masses but opposite charges moving in a two-dimensional area $lu_\sigma\beta$ and interacting via a potential proportional to $g(x, y)$. In the limit $\alpha \rightarrow 0$, this potential is the two-dimensional Coulomb potential on the surface of a cylinder of length L and circumference $u_\sigma\beta$. In the zero temperature limit the usual logarithmic 2-d Coulomb potential with soft-core cut-off is recovered as

$$\frac{1}{2}g(x, y) \rightarrow -\frac{1}{2} \ln \frac{(\alpha + |y|)^2 + x^2}{\alpha^2}. \quad (11.7)$$

By comparing eqn. (11.6) with the grand partition function of the 2-d Coulomb plasma, the fugacity $z = \exp(-\beta_{pl}\mu)$, where μ is the chemical potential and β_{pl} the inverse of the plasma temperature, is found to correspond to

$$\exp(-\beta_{pl}\mu) = \frac{g_{1\perp}}{4\pi^2 u_\sigma}, \quad (11.8)$$

and the charge e is related to ψ by the relation

$$\beta_{pl}e^2 = 4 \exp(2\psi) = 4 \left[\frac{v_\sigma + \frac{g_{1\parallel}}{2\pi}}{v_\sigma - \frac{g_{1\parallel}}{2\pi}} \right]^{1/2}. \quad (11.9)$$

With this identification all that needs to be known about the Coulomb plasma can be translated to the Fermi gas model, and vice versa.

The properties of the 2-d Coulomb gas have been studied extensively in recent years. Hauge and Hemmer (1971) and Kosterlitz and Thouless (1973) pointed out that this system has a metal-insulator transition at a finite temperature. It is interesting to remark that, according to Chui and Weeks (1976) and Zittartz (1978), the neutral Coulomb gas in more than two dimensions is a conductor at any temperature, whereas it is insulating at any temperature in less than two dimensions. The phase transition occurs only in the two-dimensional system. At low temperatures particles of opposite charges are bound into pairs, but at high temperatures the system shows the usual properties of a free-particle plasma. Contrary to this result, Kosterlitz (1977) found a metal-insulator transition for $d \leq 2$. This difference arises from a different formulation of the renormalization transformation.

Zittartz and Huberman (1976) calculated the wave-vector and temperature-dependent dielectric function $\epsilon(q, T)$ in the low density limit. Instead of a metallic and an insulating phase, they found three different temperature regimes.

- (1) At low temperatures, i.e. for $\beta_{pl}e^2 > 4$ ($T < e^2/4k_B$), the system behaves as an insulator and $\epsilon(q, T)$ has a finite value as $q \rightarrow 0$. All charges are bound into pairs.
- (2) In an intermediate temperature range $2 < \beta_{pl}e^2 < 4$ ($e^2/4k_B < T < e^2/2k_B$) the pairs begin to break up, the system goes continuously into a metallic-like state, the dielectric function is singular for small q ($q\alpha \ll 1$, where α is a cut-off, i.e. the minimum distance between the particles). According to a suggestion of Everts and Koch (1977), which was verified by Grinstein *et al.* (1978), the behaviour of $\epsilon(q, T)$ is different for $q\xi \ll 1$ and $q\xi \gg 1$, where ξ is a correlation length given by $\xi = \alpha(4\pi z\beta_{pl}e^2)^{-v}$, with $v = 2/(4 - \beta_{pl}e^2)$

$$\epsilon(q, T) = \begin{cases} 1 + \frac{C(T)}{(q\xi)^2} & \text{if } q\xi \ll 1 \\ 1 + \frac{D(T)}{(q\xi)^{2/v}} & \text{if } q\xi \gg 1. \end{cases} \quad (11.10)$$

- (3) In the high-temperature region, i.e. for $\beta_{pl}e^2 < 2$ ($T > e^2/2k_B$) all the charges are free and the fully screened Debye–Hückel dielectric function of a plasma is recovered as

$$\epsilon(q, T) = 1 + \frac{C(T)}{(q\xi)^2}. \quad (11.11)$$

The transitions between the three regions are continuous. The metallic screening characteristic for the high-temperature region is preserved in the intermediate temperature range for very large distance (very small q). As the temperature approaches $e^2/4k_B$, v goes to infinity, and in the low-density limit the correlation length diverges as well. No metallic screening can be seen and the system becomes insulating. This result shows that the metal–insulator transition is smooth and that the phase transition is of continuous order (Müller-Hartmann and Zittartz 1974, 1975).

These three temperature regimes correspond to three regions in the space of couplings of the 1-d Fermi gas. Since the investigation of the Coulomb plasma is possible in the low-density limit, i.e. for $z \rightarrow 0$, the corresponding results in the 1-d Fermi gas are related to the neighbourhood of the $g_{1\perp} = 0$ line. Using the equivalence expressed in eqn. (11.9), the low-temperature region corresponds to $g_{1\parallel} > 0$, the high-temperature region to $g_{1\parallel} < -\frac{6}{5}\pi v_\sigma$ and the intermediate temperature region to $-\frac{6}{5}\pi v_\sigma < g_{1\parallel} < 0$. The boundaries obtained earlier in the 1-d Fermi gas can be recognized in these values. The region $g_{1\parallel} > 0$ ($g_{1\perp} \approx 0$) scales to the Tomonaga model and the correlation functions show a simple power-law behaviour with a continuously varying exponent. In the 2-d Coulomb gas the corresponding critical exponents vary continuously with temperature.

The gap in the region $g_{1\parallel} < 0$ is related to the screening length in the plasma, which in turn is inversely proportional to the number of free charges. The Debye–Hückel theory of the plasma can be applied in this region. In the usual approximations of this theory the free energy can be calculated, leading to (Schulz 1977)

$$F = E_0 - \frac{L}{u_\sigma} \frac{4 - \beta_{pl}e^2}{8\pi\beta_{pl}e^2} \Delta^2 - \frac{L}{u_\sigma} \sqrt{\frac{2}{\pi}} T^{3/2} \Delta^{1/2} \exp(-\Delta/T), \quad (11.12)$$

where the gap Δ is given by

$$\Delta \sim \frac{1}{\alpha} \left(\frac{g_{1\perp}}{2\pi v_F} \right)^{2/(4-\beta_{pl}e^2)} \quad (11.13)$$

The exponent in this expression agrees with the one in eqn. (10.19) if the equivalence in eqn. (11.9) is used; the numerical factors are somewhat different.

The analogy shows clearly that the behaviour of the 1-d Fermi gas is different below and above the LE line $g_{1\parallel} = -\frac{6}{5}\pi v_\sigma$. Unfortunately, this analogy does not indicate the existence of a set of bound states for $g_{1\parallel} < -\frac{6}{5}\pi v_\sigma$.

The analogy with the 2-d Coulomb gas also allows the response functions of the Fermi gas to be calculated. Chui and Lee (1975) have shown that, for example, the spin-density part $S_\sigma^+(x, t)$ of the singlet-superconductor response $\Delta_s(x, t)$ (see eqn. (6.28)) is related to the screened interaction of two charges $\pm\frac{1}{2}e$ embedded in the Coulomb gas. This interaction can be determined from the knowledge of the dielectric constant in the low-density limit, leading to the result already known for the response function (Gutfreund and Huberman 1977). The magnetic susceptibility has been studied by Everts and Koch (1977). Unfortunately the temperature dependence of this quantity does not produce the dependence expected for the 1-d Fermi system, showing that the analogy to the Coulomb gas is of limited use in studying the behaviour of the 1-d Fermi gas.

11.2. Spin models

In §10 it has been shown that the spin- $\frac{1}{2}$ X - Y - Z chain problem can be transformed by a Jordan-Wigner transformation to a spinless fermion problem which in the continuum limit is equivalent to the spinless fermion representation of the spin part of the backward scattering problem. This analogy has been used to solve the latter problem for $g_{1\parallel} < 0$.

It is remarkable that the Fermi gas model is related not only to the spin chain problem but also to two-dimensional spin problems. Unfortunately this relationship is rather controversial, and various approximate treatments lead to completely different mappings between the 2-d X - Y model and the 1-d Fermi gas. Following Kosterlitz and Thouless (1973), Villain (1975), Zittartz (1976 a, b) and José *et al.* (1977) used the analogy between the X - Y model and the 2-d Coulomb gas to describe the low temperature behaviour of the X - Y model. On the other hand, Luther and Scalapino (1977) mapped the 2-d X - Y model directly onto the 1-d Fermi gas and transcribed the results known for the Fermi gas to the corresponding quantities in the X - Y model. The main ideas of the various mappings are now briefly sketched.

The low-temperature behaviour of the classical planar rotator model (X - Y model) defined by the Hamiltonian

$$H = - \sum_{ij} J_{ij} \mathbf{S}_i \cdot \mathbf{S}_j = - \sum_{ij} J_{ij} \cos(\varphi_i - \varphi_j), \quad (11.14)$$

where \mathbf{S}_i is a 2-d classical vector of unit length at the lattice site R_i , and φ_i is the polar angle of this vector, has been studied by Wegner (1967) and Berezinsky (1970). They used a harmonic approximation, i.e. they replaced $\cos \varphi$ by $1 - \frac{1}{2}\phi^2$ and studied the properties of this model, which can be called a harmonic rotator model. This is equivalent to taking only spin-wave excitations, and the correlation functions can be calculated giving

$$\langle \mathbf{S}_i \cdot \mathbf{S}_j \rangle \sim |R_i - R_j|^{-\eta}, \quad \eta = \frac{T}{4\pi J} \quad (11.15)$$

if first-neighbour interaction is assumed. The magnetization in an external magnetic field h is given by

$$\langle m \rangle \sim h^{n/(4-n)} \quad (11.16)$$

and the zero-field susceptibility diverges for $T < 8\pi J$.

Berezinsky (1970) emphasized that these results cannot be easily extended to high temperatures. The spin configurations that may be important here are those in which the spins make a full turn of 2π and the neglect of the 2π periodicity of the original interaction in the harmonic approximation can have serious consequences. Kosterlitz and Thouless (1973) pointed out that these spin configurations (called vortex configurations) are metastable and should be present at any finite temperature in a 2-d X - Y model. The energy of a vortex configuration is a logarithmic function of its size. The interaction energy between two vortices is also logarithmic. Assuming that the spin-waves and the vortices do not interact, Kosterlitz and Thouless proposed, in a rather intuitive way, a Hamiltonian

$$H = J \int d^2r (\nabla \varphi(r))^2 - 2\pi J \sum_{i \neq j} q_i q_j \ln \left| \frac{r_i - r_j}{a} \right| + \pi^2 J \sum_i q_i^2, \quad (11.17)$$

where the first term corresponds to the spin-wave excitations, $\varphi(r)$ is the phase at the point r , the second term describes the interaction of vortices situated at r_i and r_j , q_i is the vorticity and a is the lattice constant, and the last term corresponds to the chemical potential.

It can be seen that the vortex part of the Hamiltonian is equivalent to the 2-d Coulomb gas; the same logarithmic potential appears here. It is a plausible assumption that only vortices of unit strength are present since the creation of vortices with $|q_i| < 1$ is energetically unfavourable. With this assumption, the identification of the parameters gives

$$4\pi\beta_{XY}J = \beta_{pl}e^2 \quad \text{and} \quad \pi^2J = \mu, \quad (11.18)$$

where β_{XY} is the inverse temperature of the X - Y model and β_{pl} is the inverse temperature of the 2-d Coulomb gas. Using eqns. (11.8) and (11.9), the relationship between the X - Y model and the 1-d Fermi gas is expressed as

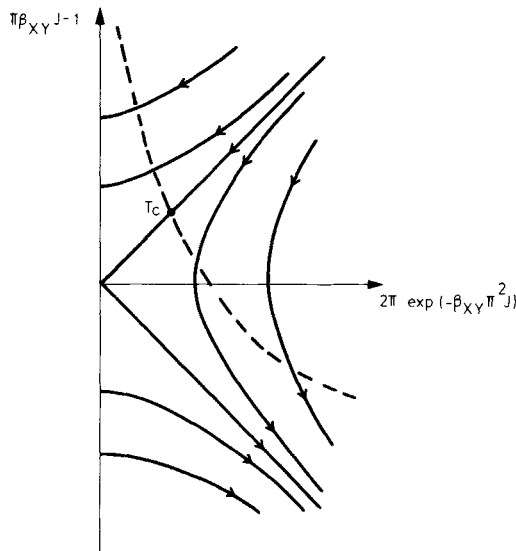
$$4\pi\beta_{XY}J = 4 \left[\frac{\frac{v_\sigma + \frac{1}{2\pi}g_{1\parallel}}{v_\sigma - \frac{1}{2\pi}g_{1\parallel}}}{\frac{1}{v_\sigma - \frac{1}{2\pi}g_{1\parallel}}} \right]^{1/2}$$

and

$$\exp(-\beta_{XY}\pi^2J) = \frac{g_{1\perp}}{4\pi^2 u_\sigma}. \quad (11.19)$$

The properties of this model were studied by Kosterlitz (1974), who used a cut-off scaling on the partition function. These scaling equations agree with the corresponding scaling equations of the 1-d Fermi gas model in the weak coupling case. In accord with the two distinct regions $g_{1\parallel} \geq |g_{1\perp}|$ and $g_{1\parallel} < |g_{1\perp}|$, the X - Y model behaves very

Fig. 34

Scaling curves of the 2-d X - Y model. The dashed line is the locus of the original X - Y model.

differently for $\pi\beta_{XY}J - 1 > 2\pi \exp(-\beta_{XY}\pi^2 J)$ and $\pi\beta_{XY}J - 1 < 2\pi \exp(-\beta_{XY}\pi^2 J)$. The critical temperature is obtained from

$$\frac{\pi J}{k_B T_c} - 1 = 2\pi \exp\left(-\frac{\pi^2 J}{k_B T_c}\right). \quad (11.20)$$

In the low-temperature region, i.e. for $T < T_c$, the vortices are bound into pairs, as, in the Coulomb gas, the particles with opposite charges are bound into pairs, and they can be scaled out when the lattice constant is scaled to larger values. The problem is then equivalent to a spin-wave problem and the correlation functions decay according to a power law, as in eqn. (11.15). The dependence of η on the physical (unrenormalized) T and J can be obtained from the scaling curves shown in fig. 34.

The X - Y model at T_c is equivalent to a model without vortices ($2\pi \exp(-\beta_{XY}\mu) = 0$) and $\beta_{XY}J - 1 = 0$. Substituting this value in the exponent of eqn. (11.15) gives $\eta = \frac{1}{4}$ at T_c . For temperatures $T < T_c$, $\eta < \frac{1}{4}$ and η vanishes at $T = 0$. Equivalence with the spin-wave problem indicates that the susceptibility is divergent in the whole temperature range $T \leq T_c$.

The vortices have a very drastic effect on the behaviour of the X - Y model at $T > T_c$. The vortex pairs begin to break up, resulting in an exponential decay of the correlation function. If the analogy with the 2-d Coulomb gas were complete, a further transition should occur at $\pi\beta_{XY}J - 1 = -\frac{3}{5}$, and in the high-temperature region all the vortices should already be free. It is very probable that the analogy breaks down in the high-temperature region and that a reliable description of the high-temperature behaviour of the X - Y model cannot be obtained in this way.

The analogy in the low-temperature region has been further developed by Villain (1975) and José *et al.* (1977). While the introduction of vortices by Kosterlitz and

Thouless was done intuitively, Villain has shown that a modified form of the X - Y model, in which $\cos \varphi$ is replaced by a mathematically more tractable expression (which is, however, 2π -periodic and thus allows the possibility of vortex states), can indeed be transformed into a decoupled system of spin-waves and vortices. The difference between this model and the one treated before is that everywhere in eqns. (11.17)–(11.20) J should be replaced by $A(J)$, given by

$$A(J) = J \left(1 - \frac{k_B T}{4J} + \dots \right), \quad (11.21)$$

which in the low-temperature region coincides with J . The physical picture and the values of the exponents at T_c are the same as in the model of Kosterlitz and Thouless (1973).

José *et al.* (1977) pointed out that the Villain model, or something very similar to it, can be obtained from the original X - Y model by using the Migdal recursion relation (Migdal 1975). This justifies the use of the Villain model to study the properties of the X - Y model. Thus it is possible to show that the above-mentioned treatment of the X - Y model gives a reasonable description at low temperatures but cannot be trusted above T_c .

Zittartz (1976 a, b) approached the problem of the 2-d X - Y model in a different way. He relaxed the restriction $0 \leq \varphi_i \leq 2\pi$ by allowing the angles to vary in the interval $(-\infty, \infty)$. Furthermore, he introduced a term $\frac{1}{2}\lambda(\varphi_i - \varphi_j)^2$ which favours small angular differences. The Hamiltonian

$$H_\lambda = \sum_{ij} J_{ij} [1 - \cos(\varphi_i - \varphi_j) + \frac{1}{2}\lambda(\varphi_i - \varphi_j)^2] - h \sum_i \cos \varphi_i, \quad (11.22)$$

where h is the external magnetic field, is not 2π -periodic, but averages of 2π -periodic functions calculated with H_λ should lead to the correct expressions in the limit $\lambda \rightarrow 0$. In zero field, Zittartz finds spin-wave excitations only with the dispersion relation

$$\epsilon_k = 2a^2 A(J, T) k^2, \quad (11.23)$$

where a is the lattice constant and

$$A(J, T) = J \left(1 - \frac{T}{2J} + \dots \right) \quad (11.24)$$

at low temperatures and it vanishes at high temperatures.

As a consequence of the k^2 dispersion, the correlation functions show a power-law behaviour for large distances, as in spin-wave theory, unless $A(J, T)$ vanishes at a finite temperature T' above which the decay is exponential. In the harmonic rotator (spin-wave) model, where $\cos \varphi$ is approximated by $1 - \frac{1}{2}\varphi^2$, $A(J, T)$ is equal to J and is independent of T , so the correlations are always power-law-like. Zittartz (1976) assumes that in the X - Y model, T' exists and $A(J, T) = 0$ for any $T > T'$. In the low-temperature region $T < T'$, he obtains for the two-angle correlation function

$$\langle \varphi_i \varphi_j \rangle \sim |R_i - R_j|^{-\eta}, \quad (11.25)$$

where now

$$\eta = \frac{T}{4\pi A(J, T)}. \quad (11.26)$$

The results obtained for the singular part of the free energy and for the magnetization are also similar to the results of the spin-wave theory;

$$\langle m \rangle \sim h^{n/(4-n)}. \quad (11.27)$$

At very low temperatures, where $A=J$, the results of the spin-wave theory are reproduced. However, according to Zittartz, eqns. (11.25) and (11.27) are valid in the whole temperature interval $0 < T < T'$. There are two characteristic temperatures in this temperature range. Below T_2 , defined by $\eta(T_2)=2$, the susceptibility is divergent, while above it the susceptibility is finite. Above T_2 higher derivatives of the free energy with respect to the magnetic field can be divergent. When the temperature reaches T_∞ , defined by $\eta(T_\infty)=4$, the free energy is infinitely many times differentiable. The correlation length in zero magnetic field is divergent for any $T < T_\infty$ and behaves for a finite field as

$$\zeta \sim h^{-2/(4-n)} \quad (11.28)$$

In contrast to this behaviour, the phase transition found by Kosterlitz (1974), Villain (1975) and José *et al.* (1977) occurs at $\eta(T_c)=\frac{1}{4}$. Above this temperature the correlation length is finite, although it does not have the usual power law behaviour,

$$\xi \sim \exp[-b(T-T_c)^{1/2}] \quad (11.29)$$

The disagreement probably stems from the failure of Zittartz's method to account for the vortex excitations.

It is interesting that Zittartz (1976 a, b) found an analogy between his model and the 2-d Coulomb gas. This analogy is, however, very different from the one suggested by Kosterlitz and Thouless (1973) and described above. The partition function in a finite magnetic field h can be written as

$$Z = Z_0 \cdot \Delta Z, \quad (11.30)$$

where Z_0 is the partition function in the absence of field and ΔZ corresponds to the excess free energy due to the field. Expanding ΔZ in powers of h , Zittartz found an expression similar to eqn. (11.6) and the following correspondence holds:

$$\begin{aligned} \frac{h}{2T} &= \exp(-\beta_{pl}\mu) = \frac{g_{1\perp}}{4\pi^2 u_\sigma}, \\ \eta(T) &= \beta_{pl}e^2 = 4 \left[\frac{\frac{1}{2\pi}g_{1\parallel}}{\frac{1}{v_\sigma - 2\pi g_{1\parallel}}} \right]^{1/2} \end{aligned} \quad (11.31)$$

This analogy holds only for ΔZ . The scaling relations of the 2-d Coulomb gas and 1-d Fermi gas predict that h is a relevant perturbation if $\eta(T) < 4$, i.e. if $T < T_\infty$ ($g_{1\perp}$ is relevant if $g_{1\parallel} < 0$), and it is irrelevant if $T > T_\infty$, in agreement with the result of José *et al.* (1977). Although, formally, low temperatures in Zittartz's model correspond to high temperatures in the Coulomb gas and vice versa, this analogy is of no help in the study of the $X-Y$ model, because Z_0 —for which this analogy does not hold—will determine its behaviour.

A completely different approach to the study of the critical behaviour of the 2-d $X-Y$ model has been proposed by Luther and Scalapino (1977). They criticized the

separation of spin-wave and vortex excitations explicitly made by Kosterlitz and Thouless (1973). This separation is also a feature of the Villain model. Luther and Scalapino argue that the separation is not valid near the critical point, and in contrast to Zittartz's treatment it is not sufficient to consider elementary excitations with quadratic dispersion. They transform the Hamiltonian of the 2-d X - Y model in a series of transformations to a 1-d fermion problem and then use the known properties of this problem to determine the correlation functions of the 2-d X - Y model.

Universality of critical behaviour suggests that, near T_c the 2-d X - Y model and a two-component, 2-d Ginzburg-Landau model have the same properties, and one can study the model in which the free energy functional is

$$F\{\psi\} = \int dx dy \left[a|\psi(r)|^2 + b|\psi(r)|^4 + c_x \left| \frac{\partial \psi}{\partial x} \right|^2 + c_y \left| \frac{\partial \psi}{\partial y} \right|^2 \right], \quad (11.32)$$

where ψ is a complex two-dimensional field and the partition function can be expressed as the functional integral

$$Z = \int \mathcal{D}\psi \exp(-\beta F\{\psi\}). \quad (11.33)$$

The transfer-matrix method allows the d -dimensional functional integral to be reduced to a $(d-1)$ -dimensional quantum mechanical problem as shown by Scalapino *et al.* (1972) and Stoeckly and Scalapino (1975). The free energy and the order parameter correlation function of the original problem can be obtained from the ground-state energy and low-lying excitations of the transfer Hamiltonian. Stoeckly and Scalapino (1975) have shown that in the particular case of a complex (two-component) 2-d Ginzburg-Landau model, the transfer Hamiltonian corresponds to a 1-d set of linearly coupled anharmonic oscillators. This problem can be approximated if only low-lying states of the oscillators are considered, in which case the equivalent Hamiltonian is a spin-1 chain problem,

$$H = \Delta \sum_i (J_i^z)^2 - \sum_i (J_i^+ J_{i+1}^- + J_i^- J_{i+1}^+), \quad (11.34)$$

with J a spin-1 operator and $\Delta = (b/|a|)^2 \beta^2 c_x c_y$. The most serious approximation in the whole consideration of Luther and Scalapino is probably the one in which only the three lowest eigenstates of the individual oscillators are kept. *A priori*, it is not clear that the vortices are correctly described in this approximation.

Luther and Scalapino (1977) argue that in the low-lying states of this system every site is in the triplet state, there J can be replaced by $J = L + S$ where both L and S are spin- $\frac{1}{2}$ operators. They then show that, by using a continuum version of the Jordan-Wigner transformation, the transfer Hamiltonian can be expressed in terms of two spinless fermion fields corresponding to the two spin- $\frac{1}{2}$ operators. Finally, the two spinless fermion fields are combined into one fermion field with spin. Introducing the charge and spin densities, the transfer Hamiltonian takes the form

$$H = H_0 + H_1, \quad (11.35)$$

with

$$H_0 = \frac{2\pi v_0}{L} \sum_{k>0} \left[\rho_1(k)\rho_1(-k) + \rho_2(-k)\rho_2(k) \right] + \frac{V_{\parallel}}{L} \sum_k \rho_1(k)\rho_2(-k) \quad (11.36)$$

and

$$H_1 = \frac{2\pi v_1}{L} \sum_{k>0} [\sigma_1(k)\sigma_1(-k) + \sigma_2(-k)\sigma_2(k)] \\ + \frac{U_{\parallel}}{L} \sum_k \sigma_1(k)\sigma_2(-k) \\ + \frac{U_{\perp}}{(2\pi\alpha)^2} \int dx \left\{ \exp \left[\frac{2\pi}{L} \sum_k \frac{\exp(-\frac{\alpha}{2}|k| - ikx)}{|k|} (\sigma_1(k) + \sigma_2(k)) \right] + \text{h.c.} \right\}. \quad (11.37)$$

Formally, this is the same as the Hamiltonian of the backward scattering model in eqns. (6.6)–(6.8). The velocities and coupling constants are given by

$$\left. \begin{aligned} 2\pi v_0 &= \frac{17\pi}{4} + \frac{\Delta}{2}, & V_{\parallel} &= -\frac{15\pi}{4} + \frac{\Delta}{2} \\ 2\pi v_1 &= \frac{17\pi}{4} - \frac{\Delta}{2}, & U_{\parallel} &= -\frac{15\pi}{4} - \frac{\Delta}{2}, \end{aligned} \right\} \quad (11.38)$$

and

$$U_{\perp} = -\frac{\pi}{2}.$$

Since the Hamiltonian is the sum of two commuting terms, the correlation functions factorize as

$$\langle \psi(r)\psi^*(r') \rangle = C_0(r-r')C_1(r-r'), \quad (11.39)$$

where $C_0(r-r')$ and $C_1(r-r')$ are calculated with H_0 and H_1 respectively. H_0 is a Tomonaga model Hamiltonian and the correlation functions show a power-law behaviour. Using the results of §5 we obtain

$$C_0(r-r') \sim |r-r'|^{-n_0(T)}, \quad (11.40)$$

with

$$\eta_0(T) = \left[\frac{2\pi v_0 + V_{\parallel}}{2\pi v_0 - V_{\parallel}} \right]^{1/2}. \quad (11.41)$$

The temperature dependence is incorporated into Δ , and it varies smoothly with temperature and decreases with decreasing T . At high temperatures $\Delta > \pi/2$, $U_{\parallel} < -2\pi v_1$ and H_1 corresponds to a strongly attractive backward scattering model. This model cannot be studied by the conventional methods reviewed in this paper because, for strong enough couplings, the renormalized Fermi velocities become complex. Using the equivalence to the X-Y-Z model, the Fermi gas model with $U_{\parallel} < -2\pi v_1$ can be mapped to a problem with $U_{\parallel} > -2\pi v_1$ (Luther 1977), so in this case too a gap exists in the excitation spectrum and there are also bound states. The finite excitation energy gives rise to an exponential decay in $C_1(r-r')$. With decreasing temperatures, Δ approaches $\pi/2$, U_{\parallel} tends to $-2\pi v_1$, the energy of the bound states approaches zero and eventually, at $\Delta=\pi/2$, the system becomes degenerate. This defines the critical temperature T_c . Above T_c , $C_1(r-r')$ is expected to behave as

$$C_1(r-r') = |r-r'|^{-n_1} f((r-r')/\xi). \quad (11.42)$$

At T_c , $\eta_1=0$, the correlation length ζ diverges and $C_1(r-r')$ becomes constant. The critical behaviour is determined only by η_0 , which at T_c ($\Delta=\pi/2$) takes the value $\eta_0(T_c)=1/\sqrt{8}$. This result differs from the one obtained by Kosterlitz (1974). One way to understand this is to suppose that the critical behaviour is non-universal, that it depends on the details of the particular model; the classical X - Y model and the two-component 2-d Ginzburg-Landau model do not belong to the same universality class. José *et al.* (1977) suggested another explanation. It is possible that the 2-d planar model has two phase transitions, since the one studied by Kosterlitz (1974), Villain (1975) and José *et al.* (1977) occurred at a lower temperature than that studied by Luther and Scalapino (1977). The energy spectrum of the backward scattering model allows such an explanation because degeneracy occurs, not only at $U_{\parallel}=-2\pi v_1$, but also at $U_{\parallel}=|U_{\perp}|$. The low-temperature phase transition could be associated with this point in the fermion representation. Finally, it is possible that the discrepancy arises from the approximations made in the transfer Hamiltonian.

11.3. Field-theoretical models

A further analogy (Heidenreich *et al.* 1975) can be obtained for the spin-density part of the Hamiltonian by using eqn. (6.10). Introducing the field variable

$$\phi(x)=\frac{-i}{\sqrt{(4\pi)}}\frac{2\pi}{L}\sum_k \frac{\exp(-\frac{\alpha}{2}|k|-ikx)}{|k|}(\sigma_1(k)+\sigma_2(k)) \quad (11.43)$$

and the canonical momentum

$$\pi(x)=\frac{1}{\sqrt{(4\pi)}}\frac{2\pi}{L}\sum_k \exp(-\frac{\alpha}{2}|k|-ikx)(\sigma_1(k)-\sigma_2(k)) \quad (11.44)$$

which obey the canonical commutation relation

$$[\pi(x), \phi(x')] = -i\delta(x-x'), \quad (11.45)$$

the first term of eqn. (6.10) can be written in terms of π and ϕ as a usual free-field Hamiltonian; the second term with the Hermitian conjugate gives a cosine, thus leading to

$$H=\int dx u_{\sigma} \left\{ \frac{1}{2} [\pi^2(x) + (\nabla\phi(x))^2] + 2 \frac{g_{1\perp}}{(2\pi\alpha)^2 u_{\sigma}} \cos [\sqrt{(4\pi)}\sqrt{2} \exp(\psi)\phi(x)] \right\}. \quad (11.46)$$

This is just the same as the Hamiltonian of the sine-Gordon theory (Coleman 1975) measured in units of u_{σ} :

$$H=\int dx \left\{ \frac{1}{2} [\pi^2(x) + (\nabla\phi(x))^2] - \frac{\alpha_0}{\beta^2} \cos \beta\phi(x) \right\}, \quad (11.47)$$

with

$$\frac{\alpha_0}{\beta^2} = -2 \frac{g_{1\perp}}{(2\pi\alpha)^2 u_{\sigma}} \quad (11.48)$$

and

$$\beta=\sqrt{(8\pi)\exp(\psi)} \quad \text{or} \quad \beta^2=8\pi \left[\frac{v_{\sigma}+\frac{1}{2\pi}g_{1\parallel}}{v_{\sigma}-\frac{1}{2\pi}g_{1\parallel}} \right]^{1/2} \quad (11.49)$$

The cut-offs are defined in a different way in the two theories. Bergcan *et al.* (1978) have shown that the cut-off α in the boson representation of the backward scattering model and the cut-off Λ in the sine-Gordon theory, as defined by Coleman, should satisfy the relation

$$\alpha\Lambda = c^{-1/2}, \quad (11.50)$$

where $c^{1/2} = 0.89$ is related to Euler's constant. If this relationship is satisfied, both theories show similar behaviour for small space-like separations.

On the other hand, Coleman (1975) pointed out the equivalence of the sine-Gordon theory to the zero-charge sector of the massive Thirring model defined by the Lagrangian density

$$\mathcal{L} = \bar{\psi} i\gamma_\mu \partial^\mu \psi - \frac{1}{2} g j^\mu j_\mu - m' \bar{\psi} \psi, \quad (11.51)$$

where ψ is a two-component spinor,

$$\bar{\psi} = \psi^+ \gamma_0, \quad j^\mu = \bar{\psi} \gamma^\mu \psi \quad (11.52)$$

and the γ matrices in one space and one time dimension can be expressed by the Pauli matrices

$$\gamma_0 = \sigma_x = \begin{pmatrix} 0 & 1 \\ 1 & 0 \end{pmatrix} \quad \text{and} \quad \gamma_1 = i\sigma_y = \begin{pmatrix} 0 & 1 \\ -1 & 0 \end{pmatrix}. \quad (11.53)$$

The equivalence holds in a term-by-term comparison of the perturbation series if the following identification is made between the coupling constants:

$$\frac{\beta^2}{4\pi} = \frac{1}{1 + \frac{1}{\pi}g}. \quad (11.54)$$

Recent work by Schroer and Truong (1977) indicates that this equivalence holds for $0 \leq \beta^2 \leq 4\pi$ ($g > 0$) only. According to eqn. (11.49) this region corresponds to $-2\pi v_s \leq g_{11} \leq -\frac{6}{5}\pi v_s$, i.e. to the region below the Luther-Emery line. It has been shown that in this range of couplings bound states appear within the gap. The same result was obtained by Dashen *et al.* (1975) who studied the sine-Gordon theory by using a semi-classical WKB method. They obtained soliton solutions with mass

$$M = \frac{8\sqrt{\alpha_0}}{\beta^2} \left(1 - \frac{\beta^2}{8\pi} \right) \quad (11.55)$$

and bound solution states at masses

$$M_n = 2M \sin \left[\frac{\beta^2}{2} \frac{n\pi}{1 - \frac{\beta^2}{8\pi}} \right], \quad n = 1, 2, \dots, < \frac{1 - \frac{\beta^2}{8\pi}}{\frac{\beta^2}{8\pi}}. \quad (11.56)$$

Comparing this result with eqn. (10.21), the same structure appears, since in eqns. (10.16) and (11.49) the argument of the sine function is the same. The soliton mass is not correctly obtained in the semi-classical approach. It is interesting to remark that Bergcan *et al.* (1978) obtained almost the same expression for the soliton mass using a variational approach as the one obtained from the correspondence with the $S=\frac{1}{2} X-Y-Z$ chain.

At $\beta^2 = 4\pi$ or $g = 0$ the sine-Gordon equation describes the zero-charge sector of a free massive Dirac field. This is again in agreement with the result of Luther and Emery (1974) who found that at $g_{1\parallel} = -\frac{6}{5}\pi v_\sigma$ the backward scattering model can be transformed to a free spinless fermion problem.

The properties of the sine-Gordon theory for β^2 around 8π depend on the way the model is defined. Coleman (1975) eliminates all ultra-violet divergences by an appropriate normal-ordering operation with an arbitrary mass m , which is then chosen so that the coefficient before the cosine should be finite. This leads to β^2 being unrenormalized and the theory having no ground state for $\beta^2 > 8\pi$. This region corresponds to $g_{1\parallel} > 0$ irrespective of the value of $g_{1\perp}$, whereas on the basis of symmetry considerations the dividing line between the gapless region and the region with gap should be $g_{1\parallel} = |g_{1\perp}|$. Similar discrepancy is present in the relationship between the Fermi gas and the $S=\frac{1}{2} X-Y-Z$ chain.

Wiegmann (1978) pointed out that this discrepancy can be eliminated if the sine-Gordon theory is defined on a lattice. In this case no instability arises, β^2 becomes renormalized and the scaling trajectories around 8π agree, after the identification given by eqns. (11.48) and (11.49), with the scaling curves obtained earlier in the $(g_{1\parallel}, g_{1\perp})$ plane.

11.4. The Hubbard model

The discussion in this paper of the various properties of the 1-d Fermi gas has so far been based on the model Hamiltonian given by eqns. (2.3) and (2.4). An alternative approach is to start from the Hubbard model (Hubbard 1963) which, in its simplest form,

$$H = t \sum_{i, \sigma} (c_{i\sigma}^\dagger c_{i+1\sigma} + c_{i+1\sigma}^\dagger c_{i\sigma}) + U \sum_i c_{i\uparrow}^\dagger c_{i\uparrow} c_{i\downarrow}^\dagger c_{i\downarrow}, \quad (11.57)$$

describes hopping between nearest-neighbour sites, labelled by i , and Coulomb repulsion between electrons of opposite spin if they are on the same site; $c_{i\sigma}^\dagger$ ($c_{i\sigma}$) is a creation (annihilation) operator for an electron of spin σ in the Wannier state localized at the i th lattice site. This model can be solved exactly in one dimension, as was shown by Lieb and Wu (1968). They found that in the case of a half-filled band the ground state is insulating for any non-zero U and is antiferromagnetic. Each site is occupied by one electron and the spins are alternating.

Writing this Hamiltonian in Bloch state representation

$$c_k = \frac{1}{\sqrt{N}} \sum_{i=1}^N \exp(-ikR_i) c_i, \quad (11.58)$$

and approximating the spectrum $2t \cos(ka)$ by linear spectra around $\pm k_F$, a Hamiltonian of the form described in § 2 is obtained. All the couplings, $g_{1\parallel}, g_{1\perp}, g_2, g_3$ and g_4 , are equal since they are all related to the single coupling U of the Hubbard model. When all the couplings are equal and positive, $g_{1\parallel} - 2g_2 < g_3$ and, as shown in §§ 6 and 7, a gap appears in the charge-density excitation spectrum, but not in the spectrum of spin-density excitations. According to the discussion in § 8.1, a spin-density wave and a charge-density wave, both with wave-vector $2k_F$, are formed. This is in agreement with the result of Lieb and Wu (1968) that the ground state is antiferromagnetic and insulating.

Generalizing the Hubbard model taking into account the Coulomb interaction between electrons on neighbouring sites allows for unequal values of the Fermi gas

couplings. This model cannot be solved exactly, but there is large literature on various approximate treatments of the extended Hubbard model. Only a few works which can be related to the models discussed in this review are mentioned here. In all the considerations earlier in this paper it was assumed that the interaction energies are small compared to the bandwidth, $g_i/2\pi v_F \ll 1$, or, in the language of the Hubbard model, $U \ll t$. Efetov and Larkin (1975) and Emery (1976 b) studied the opposite limit, i.e. a 1-d electron gas with strong ‘on-site’ interaction. They assumed that the largest energy in the problem is U and that the hopping term and the nearest-neighbour Coulomb interaction V are small in comparison. The model they considered is defined by the Hamiltonian

$$\begin{aligned} H = & U \sum_i c_{i\uparrow}^+ c_{i\uparrow} c_{i\downarrow}^+ c_{i\downarrow} + t \sum_{i,\sigma} (c_{i\sigma}^+ c_{i+1\sigma} + c_{i+1\sigma}^+ c_{i\sigma}) \\ & + V \sum_{i,\sigma,\sigma'} c_{i\sigma}^+ c_{i\sigma} c_{i+1\sigma'}^+ c_{i+1\sigma'} . \end{aligned} \quad (11.59)$$

The ‘on-site’ Coulomb interaction U is usually taken to be positive, corresponding to repulsion between electrons on the same site, but in strongly polarizable molecules the direct Coulomb repulsion can be reduced and the indirect interaction can lead to $U < 0$. In this case electrons of opposite spin form pairs and the sites are either doubly occupied or unoccupied. By making a second-order perturbational calculation, an effective Hamiltonian can be introduced in the space of paired states the

$$\begin{aligned} H' = & -\frac{t^2}{|U|} \sum_{i,\sigma} [c_{i\sigma}^+ c_{i+1\sigma} c_{i+1\sigma}^+ c_{i\sigma} + c_{i+1\sigma}^+ c_{i+1\sigma} c_{i\sigma} c_{i\sigma}^+ c_{i+1\sigma} \\ & + c_{i\sigma}^+ c_{i+1\sigma} c_{i,-\sigma}^+ c_{i+1,-\sigma} + c_{i+1\sigma}^+ c_{i\sigma} c_{i\sigma}^+ c_{i+1,-\sigma} c_{i,-\sigma}] \\ & + V \sum_{i,\sigma,\sigma'} c_{i\sigma}^+ c_{i\sigma} c_{i+1\sigma'}^+ c_{i+1\sigma'} . \end{aligned} \quad (11.60)$$

Introducing the pair operators

$$b_i = c_{i\uparrow} c_{i\downarrow} \quad \text{and} \quad b_i^+ = c_{i\downarrow}^+ c_{i\uparrow}^+ , \quad (11.61)$$

and the operators

$$n_i = \frac{1}{2}(c_{i\uparrow}^+ c_{i\uparrow} + c_{i\downarrow}^+ c_{i\downarrow} - 1) \quad \text{and} \quad (11.62)$$

$$\sigma_i = \frac{1}{2}(c_{i\uparrow}^+ c_{i\uparrow} - c_{i\downarrow}^+ c_{i\downarrow}) ,$$

the effective Hamiltonian H' has the form

$$\begin{aligned} H' = & \frac{2t^2}{|U|} \sum_i [-b_i^+ b_{i+1} - b_{i+1}^+ b_i + 2n_i n_{i+1} + 2\sigma_i \sigma_{i+1} - \frac{1}{2}] \\ & + 4V \sum_i (n_i n_{i+1} + n_i + \frac{1}{4}) . \end{aligned} \quad (11.63)$$

The operators σ_i give zero acting on doubly occupied or unoccupied sites and can be ignored. The commutation relations of the b_i and n_i operators

$$\left. \begin{aligned} [b_i, b_j^+] &= [b_i, b_j] = 0 \text{ if } i \neq j, \\ b_i^2 &= 0, [n_i, b_j^+] = b_j^+ \delta_{ij} \text{ and } [n_i, b_j] = -b_j \delta_{ij}, \end{aligned} \right\} \quad (11.64)$$

are the same as the commutation relations of spin- $\frac{1}{2}$ operators with the identification

$$\left. \begin{aligned} b_i &= S_i^- \\ b_i^+ &= S_i^+ \\ n_i &= S_i^z. \end{aligned} \right\} \quad (11.65)$$

and

Thus the Hamiltonian given by eqn. (11.63) is equivalent to a spin- $\frac{1}{2}$ anisotropic Heisenberg model Hamiltonian

$$\begin{aligned} H' = & \frac{4t^2}{|U|} \sum_i [S_i^z S_{i+1}^z - \frac{1}{2}(S_i^+ S_{i+1}^- + S_i^- S_{i+1}^+)] \\ & + 4V \sum_i S_i^z S_{i+1}^z + 4V \sum_i S_i^z. \end{aligned} \quad (11.66)$$

This is the model which has already been shown in § 10, to be equivalent to the 1-d fermion gas. Using the results of Johnson *et al.* (1973), Fowler (1978) studied the behaviour of this generalized Hubbard model. He concluded from this analogy that the ground state is a charge-density wave state for $V>0$, whereas for $V<0$ a superconducting state is stabilized at $T=0$.

Emery (1967 b) pointed out that in the strongly repulsive case ($U>0$) with a half-filled band when all sites are singly occupied, the generalized Hubbard model can again be mapped onto a spin- $\frac{1}{2}$ Heisenberg chain problem, now with the identification

$$\left. \begin{aligned} S_i^+ &= c_{i\downarrow} c_{i\uparrow}^+, \\ S_i^- &= c_{i\uparrow} c_{i\downarrow}^+, \\ S_i^z &= \frac{1}{2}(c_{i\uparrow}^+ c_{i\downarrow} - c_{i\downarrow}^+ c_{i\uparrow}), \end{aligned} \right\} \quad (11.67)$$

and

and the ground state is a transverse or longitudinal spin-density wave state.

11.5. Summary of the relationships between the various models

Not all the models that can be related to the 1-d Fermi gas model have yet been mentioned. The 2-d Coulomb gas and the 2-d X - Y model can be further related to roughening models. Knops (1977) and, independently, José *et al.* (1977) have shown that a general 2-d planar model

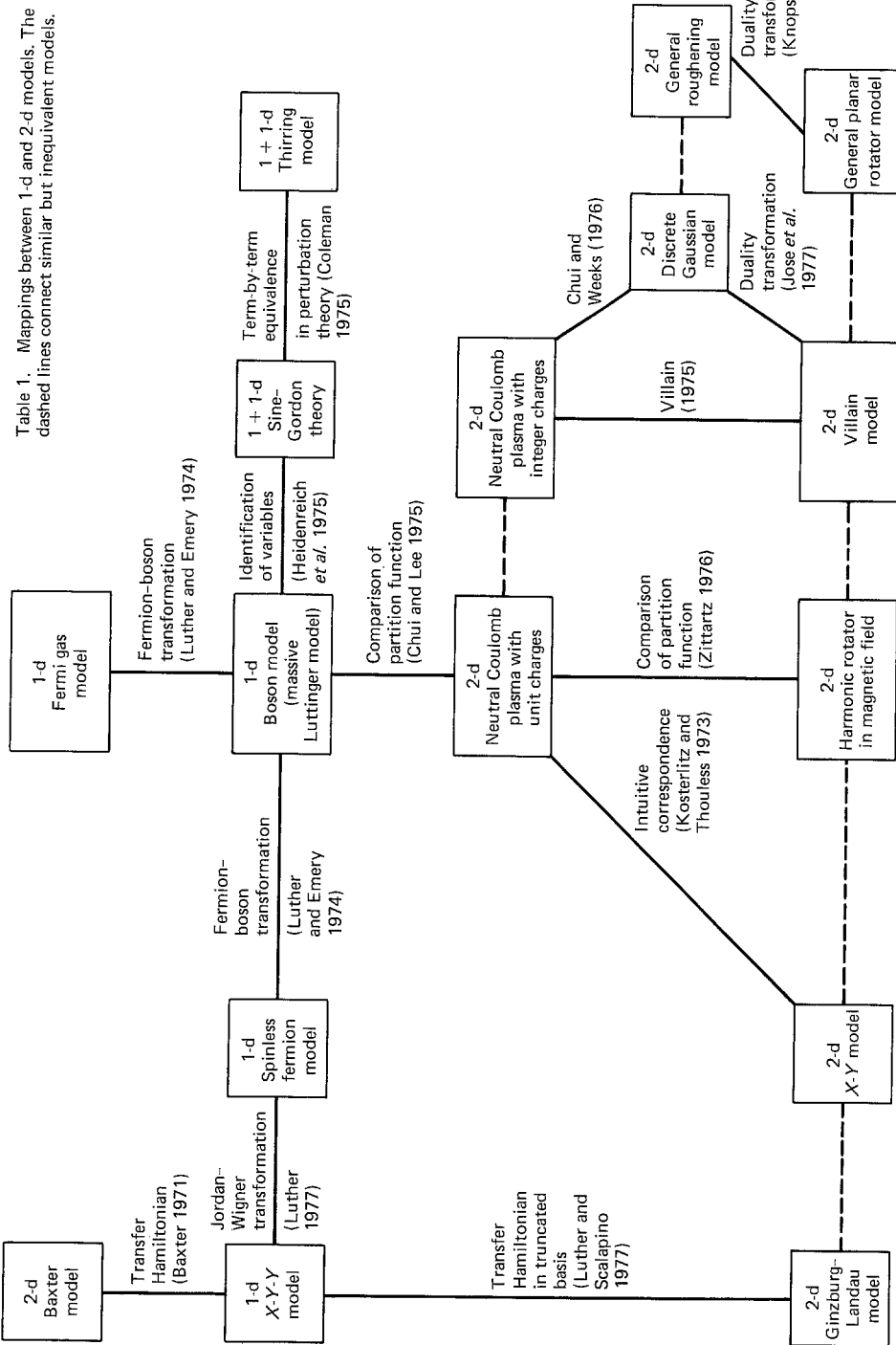
$$H = - \sum_{ij} V(\varphi_i - \varphi_j), \quad (11.68)$$

where $-\pi \leq \varphi_i \leq \pi$ is the polar angle at site R_i , with an arbitrary potential V , can be transformed by a duality transformation into a general 2-d roughening model

$$\tilde{H} = - \sum_{ij} \tilde{V}(h_i - h_j), \quad (11.69)$$

where h_i takes on all integral values, provided

$$\exp(-\beta \tilde{V}(h)) = \frac{1}{2\pi} \int_{-\pi}^{\pi} d\varphi \exp[-ih\varphi - \beta V(\varphi)], \quad (11.70)$$



where $\tilde{\beta}$ is the inverse temperature in the dual model. The Villain model (Villain 1975) corresponds to a particular choice of $V(\varphi)$ for which $\tilde{V}(h)$ is quadratic; the dual model is called the discrete Gaussian model.

On the other hand, the discrete Gaussian model can be mapped (Chui and Weeks 1976) onto a neutral Coulomb gas with arbitrary integral charges. Villain (1975) obtained the relationship between his model and the Coulomb gas directly. When studying the properties of the Coulomb gas, only particles with unit charge are considered, which is probably a reasonable approximation to make at low temperatures.

The various models mentioned in this section and the transformations by which they can be related to each other are shown in table 1. Table 2 summarizes the relationship between the parameters of the various models, and indicates the behaviour of the systems in the different regimes.

§ 12. SYSTEM OF WEAKLY COUPLED CHAINS

So far in this paper, the model has been treated in a strictly one-dimensional way. The so-called ‘one-dimensional conductors’, on which many experimental studies are now being made, are in fact real three-dimensional systems. Their one-dimensional or quasi-one-dimensional character arises from their particular structure, namely they consist of weakly coupled linear chains. It would be natural to assume that this weak coupling does not greatly affect the behaviour of the system. It is known, however, that there are very important dimensionality effects in one-dimensional systems and a weak inter-chain coupling, however weak it is, can have drastic effects. It is therefore of great interest how a system of weakly coupled chains behaves and existing experimental data should be compared with the results obtained for coupled chains. In this respect the single-chain problem serves as an example where the different approaches have been elaborated and then these methods are easily applied to the coupled-chain problem. As with the strictly one-dimensional case, some models of the coupled-chain problem can be solved exactly, but unfortunately none of these correspond to a physically relevant situation. Usually therefore, either a leading logarithmic (or next-to-leading logarithmic) approximation is made in both the intra-chain and inter-chain couplings, or the single-chain problem is considered as a zeroth-order approximation and the inter-chain couplings taken into account in a mean-field approximation. In this section the main results obtained for a system of weakly coupled chains are presented.

There are various interaction mechanisms that can couple the one-dimensional chains. The phonon-mediated coupling has been treated by several authors (Rice and Strässler 1973 b, Bjelis *et al.* 1974, Dieterich 1974, Leung 1975, Brazovsky and Dzyaloshinsky 1976, Brazovsky *et al.* 1977, Barišić 1978). This problem will not be dealt with in this paper, which is concerned only with electron-electron interactions. Retardation effects, which can be important in phonon-mediated effective electron-electron interactions, will not be considered here.

If the effect of phonons is not taken into account, two types of electronic interaction are usually considered to couple the chains. One is a Coulomb-type two-body interaction between electrons on different chains, the other is a direct hopping of electrons between the chains. The two mechanisms will be considered successively, starting first with the case when there is no hopping between the chains.

As in the earlier treatment of the single-chain problem, first the backward scattering is neglected and an exact solution is found for the generalized Tomonaga

Table 2. Relationship in the behaviour and between the parameters of the various models.

Model	Parameters and their relationships	Region I	Region II	Region III
Spin-density part of the 1-d Fermi gas model	$g_{1\parallel}, g_{1\perp}, v_\sigma = v_F + \frac{1}{2\pi}(g_{4\parallel} - g_{4\perp})$ or $u_\sigma = \left[v_\sigma^2 - \left(\frac{1}{2\pi} g_{1\parallel} \right)^2 \right]^{1/2}$	$ g_{1\parallel} \geq g_{1\perp} $ This region scales to the Tomonaga model with $g_{1\perp} = 0$. There is no gap in the excitation spectrum.	$-\frac{6\pi v_\sigma}{3} \leq g_{1\parallel} < g_{1\perp} $ This region scales to a strong coupling regime. There is a gap in the excitation spectrum.	$-2\pi v_\sigma \leq g_{1\parallel} < -\frac{6\pi v_\sigma}{3}$ There are bound states in the excitation spectrum.
Charge-density part of the 1-d Fermi gas model	$g_{1\parallel} - 2g_2, g_3, v_\rho = v_F + \frac{1}{2\pi}(g_{4\parallel} + g_{4\perp})$ or $u_\rho = \left\{ v_\rho^2 - \left[\frac{1}{2\pi} \left(g_{1\parallel} - 2g_2 \right) \right]^2 \right\}^{1/2}$	$ g_{1\parallel} - 2g_2 \geq g_3 $ This region scales to the Tomonaga model with $g_3 = 0$. There is no gap in the excitation spectrum.	$-\frac{6\pi v_\rho}{3} \leq g_{1\parallel} - 2g_2 < g_3 $ This region scales to a strong coupling regime. There is a gap in the excitation spectrum.	$-2\pi v_\rho \leq g_{1\parallel} - 2g_2 < -\frac{6\pi v_\rho}{3}$ There are bound states in the excitation spectrum.
2-d Coulomb gas	$\exp(-\beta_p u) = \frac{g_{1\perp}}{4\pi^2 v_\rho}, \beta_p e^2 = 4 \left[v_\sigma + \frac{1}{2\pi} g_{1\parallel} \right]^{1/2}$	$\beta_p e^2 \geq 4$ Insulating phase in the low-temperature region.	$2 \leq \beta_p e^2 < 4$ Metallic behaviour only for large distances in an intermediate temperature region.	$0 \leq \beta_p e^2 < 2$ Metallic phase in the high temperature region.
1-d X-Z model	$\frac{1}{2}(J_x - J_y) = \frac{g_{1\perp}}{2\pi\alpha}, 4J_z a = -\frac{5}{4}g_{1\parallel} - \frac{3}{2}\pi v_\sigma, \left[a \frac{1}{2}(J_x + J_y) - \frac{1}{\pi} \right] = \frac{5}{4}v_\sigma + \frac{3}{8\pi}g_{1\parallel}$	Extension of the analogy to this region is questionable.	$J_z \leq 0$ There is a gap in the spin-wave spectrum.	$J_z > 0$ There exist bound spin-wave states.

2-d X-Y model	$\exp(-\beta_{XY}\pi^2 J) = \frac{g_{1\perp}}{4\pi^2 u_\sigma}$, $4\pi\beta_{XY}J = 4 \left[\frac{v_\sigma + \frac{1}{2\pi}g_{1\parallel}}{\frac{1}{2\pi}g_{1\parallel}} \right]^{1/2}$	$\pi\beta_{xy}J - 1 > 2\pi \exp(-\beta_{xy}\pi^2 J)$ The vortices are bound into pairs in the low-temperature region.	$\pi\beta_{xx}J - 1 \leq 2\pi \exp(-\beta_{xx}\pi^2 J)$ The vortices become free in the high-temperature region.	Extension of the analogy to this region is questionable.
2-d Harmonic rotator model	$\frac{h}{2T} = \frac{g_{1\perp}}{4\pi^2 u_\sigma}$ $\eta(T) \equiv \frac{T}{4\pi A(J, T)} = 4 \left[\frac{v_\sigma + \frac{1}{2\pi}g_{1\parallel}}{\frac{1}{2\pi}g_{1\parallel}} \right]^{1/2}$	$\eta(T) \geq 4$ The magnetic field is an irrelevant perturbation in the high-temperature region.	$2 \leq \eta(T) < 4$ The susceptibility is finite; the magnetic field is a relevant perturbation in an intermediate temperature region.	$0 \leq \eta(T) < 2$ The susceptibility is divergent in the low temperature region.
Sine-Gordon theory	$\frac{x_0}{\beta^2} = -2 \frac{g_{1\perp}}{(2\pi\alpha)^2 u_\sigma}$ $\beta^2 = 8\pi \left[\frac{1}{v_\sigma + \frac{1}{2\pi}g_{1\parallel}} \right]^{1/2}$	$\beta^2 \geq 8\pi$ The theory is meaningful only on a lattice.	$4\pi \leq \beta^2 < 8\pi$ The solitons have finite mass.	$0 \leq \beta^2 < 4\pi$ There exist bound soliton states.
Thirring model	$g = \frac{4\pi^2}{\beta^2} - \pi$	$g \leq -\frac{\pi}{2}$	$-\frac{\pi}{2} < g \leq 0$	$g > 0$

model. The various ways of treating the backward scattering are then presented and, finally the effect of inter-chain hopping is also considered. The crossover from 1-d to 3-d behaviour is briefly reviewed.

12.1. Chains coupled by inter-chain forward scattering

The Tomonaga model for a single chain can be solved exactly, as was shown in §5, because the Hamiltonian of the Tomonaga model can be written as a bilinear expression of the charge and spin densities respectively, and an exact diagonalization is possible. The Ward identities used in §5 are the consequences of this simple form of the Hamiltonian. For a system of coupled chains the same situation occurs if the inter-chain interaction has forward scattering components only. By using the same procedure as in §5 the Green's function and response functions can be calculated exactly.

The Hamiltonian is best written in a mixed representation with an index λ , denoting the chain on which the electron moves, and an index k , denoting the momentum along the chain. In this notation the Hamiltonian can be written as

$$H = H_0 + H_{\text{int}}, \quad (12.1)$$

where

$$H_0 = \sum_{\lambda, k, \alpha} \varepsilon_k a_{\lambda k \alpha}^+ a_{\lambda k \alpha} + \sum_{\lambda, k, \alpha} \varepsilon_k b_{\lambda k \alpha}^+ b_{\lambda k \alpha}, \quad (12.2)$$

$$\begin{aligned} H_{\text{int}} = & \frac{1}{L} \sum_{\substack{\lambda, \mu \\ k_1, k_2, p \\ \alpha, \beta}} (g_{2\parallel\lambda\mu} \delta_{\alpha\beta} + g_{2\perp\lambda\mu} \delta_{\alpha, -\beta}) a_{\lambda k_1 \alpha}^+ b_{\mu k_2 \beta}^+ b_{\mu k_2 + p \beta} a_{\lambda k_1 - p \alpha} \\ & + \frac{1}{2L} \sum_{\substack{\lambda, \mu \\ k_1, k_2, p \\ \alpha, \beta}} (g_{4\parallel\lambda\mu} \delta_{\alpha\beta} + g_{4\perp\lambda\mu} \delta_{\alpha, -\beta}) (a_{\lambda k_1 \alpha}^+ a_{\mu k_2 \beta}^+ a_{\mu k_2 + p \beta} a_{\lambda k_1 - p \alpha} \\ & + b_{\lambda k_1 \alpha}^+ b_{\mu k_2 \beta}^+ b_{\mu k_2 + p \beta} b_{\lambda k_1 - p \alpha}), \end{aligned} \quad (12.3)$$

$g_{\lambda\mu}$ is the coupling strength for the interaction of electrons moving on chains λ and μ , and it is assumed that the chains are equivalent, i.e. that the dispersion relation is the same on all the chains. The cut-off will be on the momentum transfer p and therefore $g_{4\parallel}$ is also kept.

The calculational procedure of §5 can be repeated with a few trivial notational changes. The Ward identities in eqns. (5.16)–(5.17) and the generalized relations shown in figs. 22 and 23 are again valid for vertices which have the same chain index on the two fermion legs. The effective interactions can be introduced by the same diagrammatic equations (see figure 17). In these equations a summation over intermediate chain indices has to be performed. In the Fourier-transformed form a momentum component q perpendicular to the chain direction appears and in this momentum representation the effective couplings have the same form as before (see eqns. (5.9)–(5.15)) except that everywhere g should be replaced by the q -dependent g

$$g_j(q) = \sum_{\lambda} g_{j\lambda\mu} \exp[-iq(R_{\lambda} - R_{\mu})], \quad j=2\parallel, 2\perp, 4\parallel, 4\perp, \quad (12.4)$$

where R_λ and R_μ give the positions of the chains. The renormalized velocities u_σ and u_ρ also depend on q and are given by

$$u_\sigma^2(q) = \left[v_F + \frac{1}{2\pi} (g_{4||}(q) - g_{4\perp}(q)) \right]^2 - \left[\frac{1}{2\pi} (g_{2||}(q) - g_{2\perp}(q)) \right]^2 \quad (12.5)$$

and

$$u_\rho^2(q) = \left[v_F + \frac{1}{2\pi} (g_{4||}(q) + g_{4\perp}(q)) \right]^2 - \left[\frac{1}{2\pi} (g_{2||}(q) + g_{2\perp}(q)) \right]^2. \quad (12.6)$$

Since the Green's function is diagonal in the chain index, the solution of the Dyson equation has a product form

$$\begin{aligned} G_{+\lambda}(x, t) &= \frac{1}{2\pi} \frac{x - v_F t + i/\Lambda(t)}{x - v_F t + i\delta(t)} \\ &\times \prod_q \left\{ \frac{1}{(x - u_\sigma(q)t + i/\Lambda(t))^{1/2} (x - u_\rho(q)t - i/\Lambda(t))^{1/2}} \right. \\ &\times [\Lambda^2(t)(x - u_\sigma(q)t + i/\Lambda(t))(x + u_\sigma(q)t - i\Lambda(t))]^{-\alpha_\sigma(q)} \\ &\times [\Lambda^2(t)(x - u_\rho(q)t + i/\Lambda(t))(x + u_\rho(q)t - i/\Lambda(t))]^{-\alpha_\rho(q)} \left. \right\}^{1/N}, \end{aligned} \quad (12.7)$$

with

$$\alpha_\sigma(q) = \frac{1}{4u_\sigma(q)} \left[v_F + \frac{1}{2\pi} (g_{4||}(q) - g_{4\perp}(q)) - u_\sigma(q) \right], \quad (12.8)$$

and

$$\alpha_\rho(q) = \frac{1}{4u_\rho(q)} \left[v_F + \frac{1}{2\pi} (g_{4||}(q) + g_{4\perp}(q)) - u_\rho(q) \right]. \quad (12.9)$$

The product has to be taken for all the perpendicular momenta in the Brillouin zone; N is the number of chains, i.e. the number of possible values of q . If the q dependence of the velocities can be neglected, the Green's function has the same form as for a single chain (see eqn. (5.19)), but with α_σ and α_ρ replaced by α'_σ and α'_ρ , respectively, with

$$\alpha'_\sigma = \frac{1}{N} \sum_q \frac{1}{4u_\sigma} \left[v_F + \frac{1}{2\pi} (g_{4||}(q) - g_{4\perp}(q)) - u_\sigma \right] \quad (12.10)$$

and

$$\alpha'_\rho = \frac{1}{N} \sum_q \frac{1}{4u_\rho} \left[v_F + \frac{1}{2\pi} (g_{4||}(q) + g_{4\perp}(q)) - u_\rho \right]. \quad (12.11)$$

A similar result is valid for the response functions. Considering again the same response functions as for the single-chain problem, i.e. charge-density wave, spin-density wave, and singlet and triplet Cooper pair response functions, they are all diagonal in the chain index and the response functions are obtained in product form. Neglecting again the q dependence in u_σ and u_ρ , the response functions have the same

form as in eqns. (5.28) and (5.30), but the exponents β_σ and β_p are replaced by β'_σ and β'_p , given by

$$\beta'_\sigma = \frac{1}{N} \sum_q \frac{1}{4\pi u_\sigma} (g_{2\parallel}(q) - g_{2\perp}(q)), \quad (12.12)$$

$$\beta'_p = \frac{1}{N} \sum_q \frac{1}{4\pi u_p} (g_{2\parallel}(q) + g_{2\perp}(q)). \quad (12.13)$$

This result shows that, at least for the weak coupling case when the q dependence of u_σ and u_p can be neglected, the inter-chain forward scattering alone does not change the structure of the response functions compared to the single-chain problem, it only renormalizes the exponents. An excitation of a charge- or spin-density wave or a Cooper pair has no response on other chains, which act as if they were decoupled. Therefore this system may have no phase transition at any finite temperature.

This result was first obtained by Klemm and Gutfreund (1976), who used the bosonization transformation, which in this model leads to the same result as the diagrammatic approach. Furthermore, the bosonization transformation allows the model in which the intrachain backward scattering is included to be solved. The Luther–Emery solution can be used for a particular value of the strength of this process. The inter-chain forward scattering gives rise only to a renormalization of the exponents, but the singularities are not shifted to finite temperature, and no real phase transition can occur with inter-chain forward scattering.

12.2. Chains coupled by inter-chain backward scattering

Since the inter-chain forward scattering does not lead to correlation between different chains, the inter-chain backward scattering or hopping must be considered as possible mechanisms giving rise to three-dimensional ordering. The treatment of backward scattering is difficult enough for the single chain problem, but a similar treatment of the system of chains is even more complicated. There are two usual approaches, which are extensions of two approaches used in the single-chain problem.

The Fermi gas model of a system of coupled chains can be obtained by a simple extension of the model described in § 2. If there is no hopping between the chains, the dispersion relation in the quasi-1-d case is like the one in the 1-d problem. The logarithmic contributions appearing in the perturbational calculation are the consequences of the linear dispersion, and so this problem is again a logarithmic one. The parquet approximation has been shown to be a usual approximate treatment of logarithmic problems. Gorkov and Dzyaloshinsky (1974) studied the properties of the system of coupled chains in this approximation. In this way only the leading logarithmic corrections are properly collected, but next-to-leading and subsequent corrections may be equally important. These corrections can be accounted for straightforwardly by using the renormalization group approach, as in § 4. This method was applied to the present problem by Mihály and Sólyom (1976). A detailed discussion of the effect of various couplings and of the possible phase transitions was presented by Lee *et al.* (1977).

In an alternative treatment of the system of coupled chains the linear dispersion relation allows the bosonization transformation to be used in the same way as for a single chain. Klemm and Gutfreund (1976) applied this technique, using the Luther–

Emery solution of the single-chain problem (see § 6) and treating the inter-chain backward scattering in mean field approximation, although the effect of fluctuations has also been estimated.

The Hamiltonian of even the single-chain problem contains so many coupling constants in the most general spin-dependent case, that it is difficult to handle. A generalization of the model to a system of coupled chains will increase the number of coupling constants enormously. In all the treatments so far a much simpler Hamiltonian is used in which spin dependence, Umklapp processes and g_4 -type processes are neglected, leaving a problem with intra-chain and inter-chain backward and forward scatterings, respectively. The Hamiltonian is written in the form

$$H = H_0 + H_{\text{int}}, \quad (12.14)$$

where

$$H_0 = \sum_{\lambda, k, \alpha} v_F (|k| - k_F) (a_{\lambda, k, \alpha}^+ a_{\lambda k \alpha} + b_{\lambda k \alpha}^+ b_{\lambda k \alpha}) \quad (12.15)$$

and

$$\begin{aligned} H_{\text{int}} = & \frac{1}{L} \sum_{\substack{\lambda, \mu \\ k_1, k_2, p \\ \alpha, \beta}} [g_{1\lambda\mu} a_{\lambda k_1 \alpha}^+ b_{\mu k_2 \beta}^+ a_{\mu k_2 + 2k_F + p\beta} b_{\lambda k_1 - 2k_F - p\alpha} \\ & + g_{2\lambda\mu} a_{\lambda k_1 \alpha}^+ b_{\mu k_2 \beta}^+ b_{\mu k_2 + p\beta} a_{\lambda k_1 - p\alpha}]. \end{aligned} \quad (12.16)$$

Again it is assumed that the chains are equivalent and that the Fermi velocities are equal on all the chains. In the case of TTF-TCNQ (see § 13), the two types of chains have inverted bands with $v_{\text{TTF}} \approx -v_{\text{TCNQ}}$. Making an electron-hole transformation on one type of chain, the Fermi velocity changes sign and the sign of the coupling constants of the interactions coupling two different types of chain is also changed. Therefore, without losing generality, it may be assumed that the velocities are equal and that the couplings can have any sign.

Since the problem defined by this Hamiltonian is a logarithmic one due to the linear dispersion, the renormalization group treatment allows a consistent calculation of leading, next-to-leading, etc. logarithmic terms. In the same way as for the single-chain problem, the cut-off scaling can be formulated as a multiplicative renormalization (Mihály and Sólyom 1976), and the Lie equations for the invariant couplings can be obtained, straightforwardly by generalizing eqns. (4.31)–(4.33), as

$$\begin{aligned} \frac{d g_{1\lambda\mu}}{dx} = & \frac{1}{x} \left\{ \frac{1}{\pi v_F} \sum_v g_{1\lambda v} g_{1v\mu} + \frac{1}{\pi v_F} g_{1\lambda\mu} (g_{2\lambda\mu} - g_{2\lambda\lambda}) \right. \\ & + \frac{1}{2\pi^2 v_F^2} g_{1\lambda\mu} \left[g_{1\lambda\lambda} (g_{2\lambda\mu} - g_{2\lambda\lambda}) \right. \\ & \left. \left. + \sum_v (g_{1\lambda v}^2 + g_{2\lambda v}^2 - g_{2\lambda v} g_{2v\mu}) \right] + \dots \right\} \end{aligned} \quad (12.17)$$

and

$$\begin{aligned} \frac{d g_{2\lambda\mu}}{dx} = & \frac{1}{x} \left\{ \frac{1}{2\pi v_F} g_{1\lambda\mu}^2 + \frac{1}{4\pi^2 v_F^2} g_{1\lambda\mu}^2 g_{1\lambda\lambda} \right. \\ & + \frac{1}{2\pi^2 v_F^2} \sum_v g_{1\lambda v}^2 (g_{2\lambda\mu} - g_{2v\mu}) + \dots \right\}. \end{aligned} \quad (12.18)$$

In the Lie equations for the invariant couplings, x is the ratio of the new and old cut-offs. When the invariant couplings are used to calculate the temperature-dependent response functions, the argument x of the invariant couplings has to be identified with the argument T/E_0 of the response functions. Keeping this identification in mind, the temperature dependence of the invariant couplings is now discussed.

Keeping only the second-order terms, the parquet equations of Gorkov and Dzyaloshinsky (1974) are recovered. In this approximation, as well as in the better one in which the third-order terms are also taken into account, two different regimes are found which lead to two very different solutions.

The renormalization-group equations have fixed points such that $g_{1\lambda\mu}^*=0$ and $g_{2\lambda\mu}^*$ have non-universal values. This corresponds to a system of Tomonaga chains coupled by inter-chain forward scattering only. This model was treated in § 12.1 and, as was shown, it has no real phase transition.

The physically more interesting solution is a fixed point with strong attractive inter-chain backward scattering. In order to find this fixed point, the forward scattering terms in eqn. (12.17) are neglected. The reason for this is that, as has been shown, forward scattering alone does not lead to real phase transition, and it can also be seen from eqns. (12.17) and (12.18) that, for a large number of interacting chains, the enhancement of the backward scattering is much stronger during the renormalization than that of the forward scattering. Near the fixed point, eqn. (12.17) can be approximated as

$$\frac{dg_{1\lambda\mu}}{dx} = \frac{1}{x} \left\{ \frac{1}{\pi v_F} \sum_v g_{1\lambda v} g_{1v\mu} + \frac{1}{2\pi^2 v_F^2} g_{1\lambda\mu} \sum_v g_{1\lambda v}^2 + \dots \right\}. \quad (12.19)$$

Starting with intra-chain and nearest-neighbour inter-chain bare interactions, the renormalization will generate interactions between next-nearest neighbours and further neighbours. Near the fixed point the renormalized interaction can be long-range, and therefore it is not sufficient to restrict the summation in eqn. (12.19) to a few neighbours only. It is useful to transform eqn. (12.19) by Fourier transformation into

$$\frac{dg_1(q)}{dx} = \frac{1}{x} \left\{ \frac{1}{\pi v_F} g_1^2(q) + \frac{1}{2\pi^2 v_F^2} g_1(q) \frac{1}{N} \sum_{q'} g_1^2(q') + \dots \right\}, \quad (12.20)$$

where q is the wave-vector perpendicular to the chain directions and N is the number of chains.

For particular values of the bare coupling constants, this equation can have a solution where the q and x dependences are separable, i.e. all the inter-chain couplings are enhanced in the same way as the intra-chain coupling. This can happen for long-range bare inter-chain interaction only (Gorkov and Dzyaloshinsky 1974), and the situation is not very interesting physically.

In the more physically meaningful situation when the unrenormalized inter-chain interaction is of short range, the q and x dependences are not separable. The shape of $g_1(q)$ changes in the course of renormalization when the cut-off is scaled down (the temperature is decreased). In that region where $g_1(q)$ is negative and renormalization leads to a strengthening of the attractive interaction, a dip develops in $g_1(q)$ at some value q_0 of the perpendicular wave-vector. The position of q_0 is approximately determined by the minimum of the Fourier transform of the bare coupling. The depth of this dip decreases with decreasing temperature and diverges

at a temperature T_c , which is the transition temperature. Near q_0 and T_c the solution of eqn. (12.20) can be written in the form (Gorkov and Dzyaloshinsky 1974, Mihály and Sólyom 1976)

$$g_1(q, x) \sim \frac{1}{\ln \frac{T_c}{T}} \frac{\kappa^2(x)}{(q - q_0)^2 + \kappa^2(x)}, \quad (12.21)$$

where $\kappa^2(x)$ decreases with decreasing temperature and vanishes at T_c . In the parquet approximation $\kappa^2(x = T/E_0) = \ln T/T_c$, while if next corrections are also considered, this form is somewhat modified.

Assuming that the bare inter-chain coupling is attractive and acts between nearest-neighbour chains only, $g_1(q)$ for the bare coupling ($x = 1$) is a combination of cosine curves with its minimum at $q_0 = 0$. The singularity in the invariant coupling will appear at $q_0 = 0$, which means that at the phase transition point all the far distant neighbours are equally strongly coupled attractively. If, however, the coupling between the nearest-neighbour chains is repulsive, the cosine functions in $g_1(q)$ have their minima at $q_0 = (\pm \pi/a, \pm \pi/a)$ i.e. at the zone boundary of the Brillouin zone. At the fixed point the couplings between the chains are alternatively repulsive or attractive.

In order to determine what kinds of phase transition can take place in this system, the temperature dependence of the response functions has to be studied. Mihály and Sólyom (1976) investigated the charge-density wave, spin-density wave and singlet-superconductor responses. Lee *et al.* (1977) extended these investigations to the triplet-superconductor and excitonic responses and inter-chain Cooper pairing. These temperature-dependent response functions can be obtained by analytic continuation to the upper half-plane of the correlation functions

$$R(k, q, \omega_v) = - \int_0^{1/T} d\tau \exp(i\omega_v \tau) \sum_{\lambda\mu} \exp[iq(R_\lambda - R_\mu)] \langle T_\tau \{O_\lambda(k, \tau) O_\mu(k, 0)\} \rangle, \quad (12.22)$$

where for the charge-density wave response $N(k, q, \omega_v)$,

$$O_\lambda(k, \tau) = \sum_\alpha \frac{1}{L^{1/2}} \sum_p c_{\lambda p\alpha}^+(\tau) c_{\lambda p+k\alpha}(\tau), \quad (12.23)$$

for the spin-density wave response $\chi(k, q, \omega_v)$,

$$O_\lambda(k, \tau) = \frac{1}{L^{1/2}} \sum_p c_{\lambda p\uparrow}^+(\tau) c_{\lambda p+k\downarrow}(\tau), \quad (12.24)$$

for the singlet-superconductor response $\Delta_s(k, q, \omega_v)$,

$$O_\lambda(k, \tau) = \frac{1}{L^{1/2}} \sum_p c_{\lambda p\uparrow}(\tau) c_{\lambda k-p\downarrow}(\tau), \quad (12.25)$$

for the triplet-superconductor response $\Delta_t(k, q, \omega_v)$,

$$O_\lambda(k, \tau) = \frac{1}{L^{1/2}} \sum_p c_{\lambda p\uparrow}(\tau) c_{\lambda k-p\uparrow}(\tau), \quad (12.26)$$

for the excitonic response $X_{\alpha\alpha'}(k, q, \omega_v)$,

$$\mathcal{O}_{\lambda\alpha\alpha'}(k, \tau) = \frac{1}{L^{1/2}} \sum_p c_{\lambda p\alpha}^+(\tau) c_{\lambda+1 p+k\alpha'}(\tau), \quad (12.27)$$

and for the inter-chain Cooper pairing $A_{\alpha\alpha'}(k, q, \omega_v)$,

$$\mathcal{O}_{\lambda\alpha\alpha'}(k, \tau) = \frac{1}{L^{1/2}} \sum_p c_{\lambda p\alpha}(\tau) c_{\lambda+1 k-p\alpha'}(\tau). \quad (12.28)$$

In the expressions p and k are momenta parallel to the chain direction and q is the perpendicular momentum. The density responses are most singular for $k=2k_F$, and the pairing responses for $k=0$. In what follows, k is fixed at these values, but q and ω are kept as variables.

As in the 1-d model, the response functions do not obey Lie equations if the cut-off is used as a scaling parameter. It can be assumed, however, using the perturbational expression for the response functions, that auxiliary quantities $R \sim x \cdot dR/dx$, with $x=\omega/E_0$, can be defined that satisfy the scaling equations. The Lie equations for the appropriately normalized auxiliary quantities are obtained from the perturbational expressions as

$$\frac{d \ln \bar{N}(q, x)}{dx} = \frac{1}{x} \left\{ \frac{2}{\pi v_F} g_1(q) - \frac{1}{\pi v_F} \frac{1}{N} \sum_{q'} g_2(q') + \dots \right\}, \quad (12.29)$$

$$\frac{d \ln \bar{\chi}(q, x)}{dx} = \frac{1}{x} \left\{ -\frac{1}{\pi v_F} \frac{1}{N} \sum_{q'} g_2(q') + \dots \right\}, \quad (12.30)$$

$$\frac{d \ln \bar{\Delta}_s(q, x)}{dx} = \frac{1}{x} \left\{ \frac{1}{\pi v_F} \frac{1}{N} \sum_{q'} [g_1(q') + g_2(q')] + \dots \right\}, \quad (12.31)$$

$$\frac{d \ln \bar{\Delta}_t(q, x)}{dx} = \frac{1}{x} \left\{ -\frac{1}{\pi v_F} \frac{1}{N} \sum_{q'} [g_1(q') - g_2(q')] + \dots \right\}, \quad (12.32)$$

$$\frac{d \ln \bar{X}_{\alpha\alpha'}(q, x)}{dx} = \frac{1}{x} \left\{ \frac{1}{\pi v_F} \frac{1}{N} \sum_{q'} [g_1(q') + g_2(q')] f(q') + \dots \right\} \quad (12.33)$$

and

$$\frac{d \ln \bar{A}_{\alpha\alpha'}(q, x)}{dx} = \frac{1}{x} \left\{ -\frac{1}{\pi v_F} \frac{1}{N} \sum_{q'} g_2(q') f(q') + \dots \right\}, \quad (12.34)$$

where $f(q')$ depends on the arrangements of the chains. For a two-dimensional square lattice of chains, $f(q) = \cos(q_x a) + \cos(q_y a)$, where a is the distance between the chains. It is easily seen in the perturbational series that, except for $N_{\lambda\mu}(k, \omega_v)$, all the response functions involve a δ function in the chain index, i.e. apart from $N(k, q, \omega_v)$, all the response functions are independent of q . The inter-chain correlation exists for charge-density fluctuations only, for all other perturbations the chains are effectively decoupled. Thus it is expected that if a phase transition occurs in this system, it will be to a charge-density wave state. The analysis of the Lie equations for the response function confirms that only the charge-density wave response functions develops a true singularity, i.e. only the charge-density wave state can be stabilized

by the inter-chain backward scattering. This can easily be understood since the spin-exchange between the chains which would favour a three-dimensional spin ordering has been neglected, as has also the tunnelling of Cooper pairs from one chain to the other, which would stabilize a three-dimensional superconducting state.

Lee *et al.* (1977) studied the behaviour of the $4k_F$ as well as the uniform response functions. A strong inter-chain backward scattering can couple the $4k_F$ charge-density waves on different chains and could explain the observation of strong $4k_F$ correlations (Pouget *et al.* 1976, Kagoshima *et al.* 1976). However, the inter-chain interactions are weak and become stronger only near the three-dimensional ordering. In this situation the $4k_F$ correlation should be a harmonic of the $2k_F$ charge-density correlation. This is not in agreement with experimental observations of $4k_F$ correlations at high temperatures, where the $2k_F$ correlations are still very weak. No generally accepted theory exists as yet to explain the $4k_F$ correlations.

Using different methods, Klemm and Gutfreund (1976) studied the same model and arrived at essentially the same conclusions. The Hamiltonian was transformed to a bosonized form by using the fermion–boson transformation (see eqns. (5.56) and (5.57)). The intra-chain interactions are taken into account exactly by using the Luther–Emery solution and its extension to general values of the intra-chain backward scattering. The effect of inter-chain backward scattering is considered in mean field approximation. Klemm and Gutfreund found that a nearest-neighbour inter-chain backward scattering gives rise to a phase transition at finite temperatures into a charge-density wave state. This occurs for those values of the intra-chain interactions for which the charge-density wave response function of a single chain is divergent at $T=0$.

12.3. Simultaneous treatment of backward and forward scattering

As has been shown, real three-dimensional ordering can take place if inter-chain backward scattering is present in the system. More precisely, the phase transition to the charge-density wave state occurs if the inter-chain backward scattering is renormalized to a strong coupling fixed point, and no transition occurs if the backward scattering tends to zero in the renormalization procedure. It is very simple to obtain the domains of attraction of the two fixed points if forward scattering is neglected. The two fixed points are $g_{1\lambda\mu}^*=0$, i.e. $g_1^*(q)=0$, and $|g_{1\lambda\mu}^*|=2\pi v_F$ which means that $g_1^*(q)$ is singular for some value of q . The first fixed point is reached if the unrenormalized $g_1(q)$ is positive for all q and the strong-coupling fixed point is reached if the unrenormalized $g_1(q)$ is negative for some values of q . Assuming strong intra-chain and weak nearest-neighbour inter-chain interactions, the condition for a phase transition to occur is that there should be attractive intra-chain backward scattering. In this section the effect of inter-chain forward scattering on the domain of attraction of the fixed points is considered.

As a first step, Lee *et al.* (1977) studied the problem of two coupled chains in the lowest order of the renormalization group approach. Denoting by $g_{1\lambda}$ and $g_{2\lambda}$ ($\lambda=1, 2$) the coupling constants of the intra-chain backward and forward scattering for the two chains (λ is the chain index), and by w_1 and w_2 the coupling constants of the inter-chain backward and forward scattering respectively, the Lie equations (12.17) and (12.18) for the renormalized couplings have the form

$$\frac{dg_{1\lambda}}{dx} = \frac{1}{x} \left\{ \frac{1}{\pi v_F} (g_{1\lambda}^2 + w_1^2) + \dots \right\}, \quad (12.35)$$

$$\frac{d g_{2\lambda}}{dx} = \frac{1}{x} \left\{ \frac{1}{2\pi v_F} g_{1\lambda}^2 + \dots \right\}, \quad (12.36)$$

$$\frac{d w_1}{dx} = \frac{1}{x} \left\{ \frac{1}{\pi v_F} (g_{1\lambda} w_1 + g_{1\mu} w_1 + w_1 w_2 - \frac{1}{2} w_1 g_{2\lambda} - \frac{1}{2} w_1 g_{2\mu}) + \dots \right\} \quad (12.37)$$

and

$$\frac{d w_2}{dx} = \frac{1}{x} \left\{ \frac{1}{2\pi v_F} w_1^2 + \dots \right\}. \quad (12.38)$$

For two equivalent chains ($g_{1\lambda}$ and $g_{2\lambda}$ are independent of the chain index λ), the renormalization group equations have two fixed points:

- (1) $g_1^* = 0$, $w_1^* = 0$, g_2^* and w_2^* have non-universal values at the fixed point, and
- (2) $g_1^* \rightarrow -\infty$, $|w_1^*| \rightarrow +\infty$ and $g_1^* - 2g_2^* + 2w_2^* \rightarrow -\infty$ with $g_1^*/(g_1^* - 2g_2^* + 2w_2^*) = 1$ and $|w_1^*(g_1^* - 2g_2^* + 2w_2^*)| = -1$.

A better theory, taking into account higher-order corrections in the Lie equations, may modify the value of the strong-coupling fixed point. The important feature is that, as in the single chain problem or in the problem with inter-chain backward scattering alone, there are two different regimes: one which is scaled onto a fixed point with forward scattering only (Tomonaga chains coupled by inter-chain forward scattering) and one which is scaled onto the strong-coupling fixed point.

The domain of attraction of the strong-coupling fixed point in the single-chain problem is $g_1 < 0$. In the case of two coupled chains this domain is larger. In addition to the region $g_1 < 0$, the regions defined by

$$g_1 > 0 \text{ and } g_1 - 2g_2 + 2w_2 < 0$$

and

$$g_1 > 0, g_1 - 2g_2 + 2w_2 > 0 \quad \text{and} \quad g_1(g_1 - 2g_2 + 2w_2) < w_1^2$$

also scale onto the strong-coupling fixed point. The effect of forward scattering is that it can renormalize the originally repulsive intra-chain backward scattering to attractive couplings. Similar conclusions can be drawn for two coupled inequivalent chains. The response functions of the two-chain problem have been studied by Klemm *et al.* (1977).

It is not possible to treat the N -chain problem analytically. However, it is reasonable to expect that the forward scattering has a similar effect and that the strong-coupling attractive fixed point can be reached, even from repulsive initial couplings. This was verified by Lee *et al.* (1977) by solving the scaling equations (12.17) and (12.18) numerically. They found that, even by starting from a repulsive δ -function interaction, the coupling constants scale onto the strong-coupling attractive fixed point. This behaviour was also noticed by Menyhárd (1977 a) and Obukhov (1977). Lee *et al.* (1977) calculated the response functions by a numerical integration of the Lie equation. It may happen that the spin-density wave response function is more strongly enhanced than the charge-density wave response function over a large temperature range, but the true singularity develops only in the charge-density wave response function. This confirms that, near the fixed point, the forward scattering can be neglected compared to the backward scattering and the earlier analysis of the possible phase transitions is true, but the approach to the fixed point is strongly influenced by the forward scattering.

12.4. Crossover from 1-d to 3-d behaviour

The treatments mentioned so far in this paper have concentrated on what states are stabilized for a given set of coupling constants. Menyhárd (1977 b) examined the problem of quasi-1-d systems from a different point of view. She assumed a weak interchain coupling—weak compared with the intra-chain couplings, $|\sum_{\lambda \neq \mu} g_{1\lambda\mu}| \ll |g_{1\lambda\lambda}|$ and $|\sum_{\lambda \neq \mu} g_{2\lambda\mu}| \ll |g_{2\lambda\lambda}|$ —and studied how the behaviour of the system changes from 1-d-like to 3-d as the temperature is decreased. By using the approximation mentioned above, and assuming further that $g_{2\lambda\mu}$ ($\lambda \neq \mu$) does not contribute essentially to the renormalization, the Lie equations (12.17) and (12.18) for the invariant couplings have the form

$$\begin{aligned} \frac{dg_{1\lambda\mu}}{dx} = & \frac{1}{x} \left\{ \frac{1}{\pi v_F} \sum_{\substack{\lambda \neq \nu \\ \mu \neq \nu}} g_{1\lambda\nu} g_{1\nu\mu} + \frac{1}{\pi v_F} g_{1\lambda\mu} (2g_{1\lambda\lambda} - g_{2\lambda\lambda}) \right. \\ & \left. + \frac{1}{2\pi^2 v_F^2} g_{1\lambda\mu} (g_{1\lambda\lambda}^2 + g_{2\lambda\lambda}^2 - g_{1\lambda\lambda} g_{2\lambda\lambda}) + \dots \right\}, \quad \lambda \neq \mu, \end{aligned} \quad (12.39)$$

$$\frac{dg_{2\lambda\mu}}{dx} = 0, \quad \lambda \neq \mu, \quad (12.40)$$

$$\frac{dg_{1\lambda\lambda}}{dx} = \left\{ \frac{1}{\pi v_F} g_{1\lambda\lambda}^2 + \frac{1}{2\pi^2 v_F^2} g_{1\lambda\lambda}^3 + \dots \right\}. \quad (12.41)$$

and

$$\frac{dg_{2\lambda\lambda}}{dx} = \left\{ \frac{1}{2\pi v_F} g_{1\lambda\lambda}^2 + \frac{1}{4\pi^2 v_F^2} g_{1\lambda\lambda}^3 + \dots \right\}. \quad (12.42)$$

The second and third terms on the right-hand side of eqn. (12.39) can be recognized as the coupling constant combination which appears in the Lie equation determining the charge-density response function of a single chain (see eqn. (4.52)). Denoting by N_{1d} this response function and by \bar{N}_{1d} the auxiliary function

$$\bar{N}_{1d} = \pi v_F x \frac{d N_{1d}}{dx}, \quad x = T/E_0, \quad (12.43)$$

eqn. (12.39) can be solved in the form

$$g_{1t}(q, x) = \frac{g_{1t}^{(0)}(q) \bar{N}_{1d}(x)}{1 - g_{1t}^{(0)}(q) \bar{N}_{1d}(x)}, \quad (12.44)$$

where $g_{1t}^{(0)}(q)$ is the bare coupling and the Fourier transform is defined by

$$g_{1t}(q, x) = \sum_{\lambda \neq \mu} g_{1\lambda\mu}(x) \exp[iq(R_\lambda - R_\mu)]. \quad (12.45)$$

Thus g_{1t} characterizes the interchain (transverse) coupling. The mean-field transition temperature is obtained from the pole of eqn. (12.44). It gives a crude approximation for the ordering temperature, but indicates that T_c depends strongly on the inter-chain couplings as well as on the fluctuations within the chains. Above T_c , but close to it, the system behaves like a real 3-d system. Far above T_c the denominator in eqn. (12.44) is near to unity, $g_{1t}(q, x) \approx g_{1t}^{(0)}(q) \bar{N}_{1d}(x)$, i.e. the

singularity of $g_{11}(q, x)$ seems to be at $x=0$ and the system behaves effectively as a 1-d system. In between, a crossover temperature can be defined at which the renormalized inter-chain and intra-chain coupling constants become of the same order of magnitude. Above this T_{cross} , the system shows 1-d fluctuations with no correlation between the chains; below T_{cross} , the 3-d nature of the system becomes perceptible.

12.5. The effect of inter-chain hopping

The inter-chain scattering of electrons is only one mechanism which can couple the chains in quasi-1-d systems. The other mechanism is a direct hopping (tunnelling) of electrons from one chain to the other. The Hamiltonian describing the hopping is

$$H_h = \sum_{\lambda\mu} t_{\lambda\mu} a_{\lambda k\alpha}^+ a_{\mu k\alpha}. \quad (12.46)$$

It gives rise to a change in the energy spectrum, which in the case of $t_{\lambda\mu} \ll \epsilon_F$ can be written as

$$\epsilon(k, q) - \epsilon_F = v_F(|k| - k_F) + w(q), \quad (12.47)$$

where k and q are the momentum components parallel and perpendicular, respectively, to the chain direction. In the nearest-neighbour, tight-binding approximation for a square lattice with lattice constant a ,

$$w(q) = 2t[\cos(q_x a) + \cos(q_y a)]. \quad (12.48)$$

In the absence of hopping ($t=0$), the Fermi surface is flat. The hopping will distort this flat surface and the curvature is proportional to the rate of hopping. At a temperature T the electrons which are in a range of width $k_B T$ around the Fermi surface will contribute essentially to the scattering. If the distortion of the Fermi surface is within this range, to a first approximation the hopping will play no role. It becomes important only if the distortion of the Fermi surface is larger than the thermal smearing, in which case the 1-d character of the system is lost and a 3-d behaviour is obtained.

The renormalization-group treatment is again very suitable for the study of this crossover. Looking first at the elementary bubbles of the parquet diagrams, the Cooper-pair diagram is not sensitive to the hopping, as was noticed by Dzyaloshinsky and Kac (1968), and in the logarithmic approximation the same result is obtained as in the 1-d case (see eqn. (3.1)). The zero-sound channel with external momentum $k=2k_F$ is, however, modified and instead of eqn. (3.2) the integral can be approximated by

$$\frac{1}{2\pi v_F} \ln \frac{(\omega^2 + t^2)^{1/2}}{E_0} \approx \frac{1}{2\pi v_F} \ln \frac{\max\{\omega, t\}}{E_0}. \quad (12.49)$$

In the finite-temperature formalism ω is replaced by T .

In the renormalization-group treatment the cut-off is scaled down until a fixed point or singularity is reached. In the case of a 3-d system of coupled chains, this singularity occurs at a finite value of the scaled cut-off and the corresponding temperature determines the critical temperature T_c . Considering now a system in which inter-chain scattering and inter-chain hopping are present simultaneously the contribution of the diagrams in the high-temperature region $T > t$ is the same as for

$t=0$, and the scaling equations (12.17) and (12.18) can be used. If the critical temperature obtained from these equations satisfies the condition $T_c > t$, the hopping does not contribute to the 3-d ordering and the analysis in §§ 12.2 and 12.3 is valid. Only a charge-density wave state can arise in this system. If, however, no singularity occurs until the scaled cut-off reaches a value of the order of t , the behaviour changes dramatically. Once the cut-off is smaller than t , the zero-sound channel is no longer logarithmic, and only the Cooper-pair diagrams contribute to the Lie equations, as is the case in real 3-d systems. The scaling equations are easily obtained and have the form

$$\frac{dg_{1\lambda\mu}}{dx} = \frac{1}{x} \left\{ \frac{1}{\pi v_F} g_{1\lambda\mu} g_{2\lambda\mu} + \dots \right\} \quad (12.50)$$

and

$$\frac{dg_{2\lambda\mu}}{dx} = \frac{1}{x} \left\{ \frac{1}{2\pi v_F} (g_{1\lambda\mu}^2 + g_{2\lambda\mu}^2) + \dots \right\}. \quad (12.51)$$

These equations are equivalent to the parquet equations of Gorkov and Dzyaloshinsky (1974); they were also obtained by Prigodin and Firsov (1977). When solving the problem with $T_c < t$, the scaling has to be performed in two steps. First, eqns. (12.17) and (12.18) must be used until the new cut-off is scaled to t , when the couplings take on the values $g_{1\lambda\mu}(t/E_0)$ and $g_{2\lambda\mu}(t/E_0)$. Then, starting with these values, eqns. (12.50) and (12.51) have to be used in the further scaling. The procedure is somewhat similar to the two-cut-off problem discussed in § 11.2.

Depending on the initial conditions, either $g_{1\lambda\mu} + g_{2\lambda\mu}$ or $-g_{1\lambda\mu} + g_{2\lambda\mu}$ will diverge first. These are just the combinations which appear in the Lie equations (12.29)–(12.34) for the singlet- and triplet-superconductor responses respectively. Accordingly the system will have a superconducting phase transition with singlet or triplet Cooper pairs.

Horovitz (1976) and later Prigodin and Firsov (1977) pointed out that, in contrast to the situation discussed in connection with eqn. (12.49), the zero-sound channel is not sensitive to the hopping if the dispersion relation has the symmetry property

$$\varepsilon(k, q) - \varepsilon_F = -[\varepsilon(k - k_0, q - q_0) - \varepsilon_F] \quad (12.52)$$

for a particular value of (k_0, q_0) and the zero sound bubble is calculated with these external momenta. The nearest-neighbour, tight-binding approximation (12.48) satisfies this relation, with $k_0 = 2k_F$ and $q_0 = (\pi/a, \pi/a)$. Since the zero-sound channel is again logarithmic for all temperatures, the scaling equations are the same as for $t=0$, and the charge-density wave response function with wave-vector (k_0, q_0) is singular. In the ordered phase the charge-density waves on the neighbouring chains are in opposite phase.

Klemm and Gutfreund (1976) approached the problem of 3-d ordering due to inter-chain hopping in a different way. As a first step they studied the effect of inter-chain hopping in a perturbational calculation, i.e. the response functions were calculated with a strictly one-dimensional energy spectrum to fourth order in the hopping Hamiltonian. The inter-chain couplings $g_{1\lambda\mu}$ and $g_{2\lambda\mu}$ were neglected. They concluded from this calculation that the most important contribution to the response functions comes from the “pair self-avoiding random walk” processes. The

hopping of an electron creates a disturbance which propagates along the chain with the velocity characteristic for the spin-density modes of the bosonized Hamiltonian. This disturbance causes another particle—electron or hole, depending on whether the transition is to a superconducting or a density wave state—to hop to the same adjacent chain. The second hopping takes place before the first particle can propagate to another chain. The important processes are those in which the pairs never return to the same chain.

The response functions were then calculated in a pair approximation, considering the propagation of pairs between the chains, by using the bosonization transformation. After a rather lengthy calculation they found that a superconducting or density-wave state appears, depending on whether $g_1 - 2g_2 > 0$ or $g_1 - 2g_2 < 0$. This demarcation between the superconducting and density-wave state is the same as for the single-chain problem. Thus one can say that the effect of inter-chain hopping is to stabilize, at a finite temperature, that state which would be obtained as a ground state of the single-chain problem.

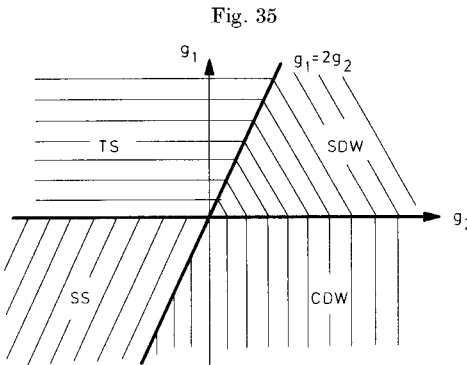
Further clarification is necessary for $g_1 > 0$, for which both the singlet- and triplet-superconductor responses and the charge-density and spin-density wave responses are singular for $g_1 - 2g_2 > 0$ and $g_1 - 2g_2 < 0$ respectively. This region was studied by Suzumura and Fukuyama (1978) in greater detail. In a mean-field theory of the pair hopping, they found that the critical temperature of triplet-superconductivity is higher than that of singlet-superconductivity if $g_1 - 2g_2 > 0$. Similarly, for $g_1 - 2g_2 < 0$ the critical temperature of the spin-density wave state lies higher than that of the charge-density wave state. The results are summarized in fig. 35, which shows the type of ordering found when the coupling between the chain is due to inter-chain hopping only. This phase diagram is very similar to the one shown in fig. 13, which was obtained for a strictly one-dimensional system.

12.6. Quasi-1-d fermion model with strong on-site interaction

The 1-d fermion model with strong on-site interaction has been considered in §11.4. This model can also be extended to a set of coupled chains by assigning a chain index λ to the creation and annihilation operators:

$$\begin{aligned}
 H = & U \sum_{\lambda i} c_{\lambda i\uparrow}^+ c_{\lambda i\uparrow} c_{\lambda i\downarrow}^+ c_{\lambda i\downarrow} \\
 & + t_{\parallel} \sum_{\lambda i\sigma} [c_{\lambda i\sigma}^+ c_{\lambda i+1\sigma} + c_{\lambda i+1\sigma}^+ c_{\lambda i\sigma}] \\
 & + t_{\perp} \sum_{\lambda\lambda' i\sigma} c_{\lambda i\sigma}^+ c_{\lambda' i\sigma} \\
 & + V_{\parallel} \sum_{\lambda i\sigma\sigma'} c_{\lambda i\sigma}^+ c_{\lambda i\sigma} c_{\lambda i+1\sigma'}^+ c_{\lambda i+1\sigma'} \\
 & + V_{\perp} \sum_{\lambda\lambda' i\sigma\sigma'} c_{\lambda i\sigma}^+ c_{\lambda i\sigma} c_{\lambda' i\sigma'}^+ c_{\lambda' i\sigma'}, \tag{12.53}
 \end{aligned}$$

where λ and λ' are first-neighbour chains and nearest-neighbour interaction has been assumed. If the on-site interaction U is the largest energy in the problem, this Hamiltonian has been shown by Emery (1976 b) to be equivalent to the problem of



Type of ordered state for a system of chains, with intra-chain backward and forward scattering, coupled by inter-chain hopping.

interacting spin- $\frac{1}{2}$ chains in the same way as eqn. (11.59) is equivalent to eqn. (11.66). In this way is obtained

$$\begin{aligned}
 H = & \frac{4t_{\parallel}^2}{|U|} \sum_{\lambda i} [S_{\lambda i}^z S_{\lambda i+1}^z - \frac{1}{2}(S_{\lambda i}^+ S_{\lambda i+1}^- + S_{\lambda i}^- S_{\lambda i+1}^+)] \\
 & + \frac{4t_{\perp}^2}{|U|} \sum_{\lambda \lambda' i} [S_{\lambda i}^z S_{\lambda' i}^z - \frac{1}{2}(S_{\lambda i}^+ S_{\lambda' i}^- + S_{\lambda i}^- S_{\lambda' i}^+)] \\
 & + 4V_{\parallel} \sum_{\lambda i} S_{\lambda i}^z S_{\lambda i+1}^z + 4V_{\perp} \sum_{\lambda \lambda' i} S_{\lambda i}^z S_{\lambda' i}^z \\
 & + 4(V_{\parallel} + zV_{\perp}) \sum_{\lambda i} S_{\lambda i}^z,
 \end{aligned} \tag{12.54}$$

where z is the number of nearest-neighbour chains.

Emery (1976 b) and Fowler (1978) studied this model by taking over results from the literature on the Heisenberg model. They concluded that $U < 0$ allows only a charge-density wave or superconducting state, whereas for $U > 0$ a transverse or longitudinal spin-density wave state can be formed, as in the single-chain problem. It follows from the relationship between the spin operators and the fermion operators, which is valid for $U < 0$ and is given by eqns. (11.61), (11.62) and (11.65), that ordering in the z direction corresponds to the formation of a charge-density wave, whereas ordering in either the x or y direction corresponds to superconductivity in the fermion problem. Without inter-chain hopping ($t_{\perp} = 0$), the chains are coupled by the z components of the spin and only a charge-density wave state can be stabilized, in agreement with the discussion in § 12.2. Taking into account the inter-chain hopping, superconductivity could be favoured.

§ 13. CONCLUDING REMARKS

In this paper the properties of the 1-d Fermi gas model has been reviewed. It has been shown that, depending on the values of the coupling constants, the behaviour of the system can be quite different. Coulomb coupling between the chains favours the appearance of a charge-density wave state. If the coupling between the chains is due predominantly to inter-chain hopping, the type of order that occurs is the same as the type of order that would set in at $T = 0$ in a single chain. The corresponding phase diagram is given in § 8.1. The question concerning the application of these results to

real systems is what the values of the couplings could be, but unfortunately the answer is far from certain. As an example, consider TTF-TCNQ (tetrathiafulvalene-tetracyanoquinodimethane), a typical representative of quasi-1-d conductors which has been studied extensively.

There are at present two schools of thought, advocating conflicting views. The Pennsylvania group (Heeger and Garito 1975) believe that the on-site Coulomb interaction is reduced by screening and, due to the strong polarizability of molecules to such a small value, that its effect is minor compared to that of the electron-electron interaction. Their interpretation of the properties of TTF-TCNQ is based on a Fröhlich Hamiltonian, neglecting completely the electron-electron interaction. Contrary to this view, the IBM group (Torrance *et al.* 1977) claim that the effective Coulomb interaction is comparable to, or larger than, the bandwidth and is more important than the electron-phonon coupling. This assertion is based on the interpretation of the optical absorption spectrum (Torrance *et al.* 1975), of the enhancement of the magnetic susceptibility, of the enhancement of the N.M.R. relaxation rate T_1^{-1} (Jérôme and Weger 1977) and of the $4k_F$ scattering (Pouget *et al.* 1976, Kagoshima *et al.* 1976) discussed in § 4.3. The latter can be observed only if the Coulomb interaction is strongly repulsive.

Other charge-transfer salts have different ratios of effective Coulomb interaction to bandwidth. In NMP-TCNQ (*N*-methylphenazinium-tetracyanoquinodimethane) Epstein *et al.* (1972) found $t_{\parallel} = 2.1 \times 10^{-2}$ eV and $U = 0.17$ eV, thus $U/4t_{\parallel} \approx 2$, whereas in HMTSF-TCNQ (hexamethylenetetraselenofulvalene-tetracyanoquinodimethane) $U/4t_{\parallel}$ is considerably smaller than unity (Jérôme and Weger 1977). It is interesting to attempt to situate the various systems in the space of couplings, as Jérôme and Weger (1977) did, and to interpret all the properties in an interacting Fermi gas model. It seems that if this is done many of the physically most interesting systems fall into the strong-coupling regime where the results described in this paper are not easily applicable.

The Fermi gas model as presented here is interesting in its own right, apart from its possible relevance to real systems. As a model system it shows particular dimensionality effects. How to obtain a good description of its behaviour is an interesting theoretical problem. Furthermore, as has been emphasized in this review, the model is related to a large number of other models. Although in most cases the relationship is only approximate, and it is hard to estimate to what extent results obtained for one model can be extended to the others, it is hoped that further study of the related models will contribute to a better understanding of the behaviour of the Fermi gas model.

ACKNOWLEDGMENTS

It would be impossible to list all colleagues with whom I had fruitful discussion which helped to develop my ideas on the subject. I specifically acknowledge Dr. A. Zawadowski and Professor L. P. Gorkov, I. E. Dzyaloshinsky and P. Nozières for invaluable discussions. I am most indebted to Drs. N. Menyhárd, L. Mihály and G. Szabó with whom I worked at various stages.

Note added in proof—The relationship between the 1-d Fermi gas model and the bosonized model has been analysed further recently. Grinstein, Minnhagen and Rosengren (to be published) have shown that the fermion model can be bosonized in

the way it is done in the Luther-Emery model, if the backward scattering term

$$g_{1\perp} \sum_{\alpha} \int dx dx' \psi_{1\alpha}^+(x) \psi_{2\alpha}(x) u(x-x') \psi_{2,-\alpha}^+(x) \psi_{-,\alpha}(x'),$$

where ψ_1 and ψ_2 are the field operators for the right- and left-going particles and $u(x-x')$ is the interaction potential, is replaced by

$$g_{1\perp} \sum_{\alpha} \int dx dx' \psi_{1\alpha}^+(x) \psi_{1,-\alpha}(x) u(x-x') \psi_{2,-\alpha}^+(x) \psi_{2\alpha}(x'),$$

and a momentum transfer cut-off is used for the interaction. This type of scattering corresponds, in fact, to forward scattering of particles with spin-flip.

Similarly, it was shown by Rezayi, Sak and Sólyom (to be published) that using the interaction

$$\begin{aligned} & \frac{1}{4} g_3 \sum_{\alpha\beta\gamma\delta} (\delta_{\alpha\gamma}\delta_{\beta\delta} - \delta_{\alpha\delta}\delta_{\beta\gamma}) \int \int dx dx' \\ & \times [\psi_{1\alpha}^+(x) \psi_{1\beta}^+(x) u(x-x') \psi_{2\gamma}(x') \psi_{2\delta}(x')] \\ & + [\psi_{2\alpha}^+(x) \psi_{2\beta}^+(x) u(x-x') \psi_{1\gamma}(x') \psi_{1\delta}(x')] \end{aligned}$$

instead of the usual Umklapp term and modifying the g_4 -type interactions correspondingly, the charge- and spin-density degrees of freedom separate, as in the bosonized model. This indicates that the choice of cut-off in the Luther-Emery model is quite close, although not exactly equivalent, to the momentum transfer cut-off in the interactions given above.

The renormalization group calculation has been reanalysed in the three loop order by Rezayi, Sak and Talukdar (to be published), using spin-flip forward scattering instead of the usual backward scattering. In contrast to Ting's result, they have found that $g_1 - 2g_2$ is scale invariant in the absence of Umklapp processes and also the scaling equation for g_1 differs in the fourth order term, having fixed points at $g_1^* = 0$ and $-\infty$ only.

REFERENCES

- ABRIKOSOV, A. A., 1965, *Physics*, **2**, 5.
 ABRIKOSOV, A. A., and MIGDAL, A. A., 1970, *J. low Temp. Phys.*, **3**, 519.
 ABRIKOSOV, A. A., and RYZHKIN, I. A., 1978, *Adv. Phys.*, **27**, 147.
 ANDERSON, P. W., 1970, *J. Phys. C*, **3**, 2346.
 ANDERSON, P. W., YUVAL, G., and HAMANN, D. R., 1970, *Phys. Rev. B*, **1**, 4464.
 BARIĆIĆ, S., 1978, *J. Phys. Colloque*, C2, **39**, 262.
 BAXTER, R. J., 1971, *Phys. Rev. Lett.*, **26**, 834. 1972, *Ann. Phys.*, **70**, 193.
 BEREZINSKY, V. L., 1970, *Zh. eksp. teor. Fiz.*, **59**, 907 (English translation: 1971, *Soviet Phys. JETP*, **32**, 493); 1973, *Zh. eksp. teor. Fiz.*, **65**, 1251.
 BERGCAN, E., COOPER, L. N., and STÖLAN, B., 1978 (in the press).
 BJELIŠ, A., ŠAUB, K., and BARIĆIĆ, S., 1974, *Nuovo Cim. B*, **23**, 102.
 BJORKEN, J. D., and DRELL, S. D., 1965, *Relativistic Quantum Fields* (New York: McGraw-Hill).
 BOGORILOBOV, N. N., and SHIRKOV, D. V., 1959, *Introduction to the Theory of Quantized Fields* (London: Interscience Publishers, Inc.)
 BRAZOVSKY, S. A., and DZYALOSHINSKY, I. E., 1976, *Zh. eksp. teor. Fiz.*, **71**, 2338.
 BRAZOVSKY, S. A., DZYALOSHINSKY, I. E., and OBUKHOV, S. P., 1977, *Zh. eksp. teor. Fiz.*, **72**, 1550.
 BRÉZIN, E., LE GUILLOU, J.-C., and ZINN-JUSTIN, J., 1973, *Phys. Rev. D*, **8**, 434.
 BYCHKOV, Yu. A., GORKOV, L. P., and DZYALOSHINSKY, I. E., 1966, *Zh. eksp. teor. Fiz.*, **50**, 738 (English translation: 1966, *Soviet Phys. JETP*, **23**, 489).
 CHUI, S.-T., and LEE, P. A., 1975, *Phys. Rev. Lett.*, **35**, 315.
 CHUI, S.-T., RICE, T. M., and VARMA, C. M., 1974, *Solid St. Commun.*, **15**, 155.
 CHUI, S.-T., and WEEKS, J. D., 1976, *Phys. Rev. B*, **14**, 4978.
 COLEMAN, S., 1975, *Phys. Rev. D*, **11**, 2088.

- DASHEN, R. F., HASLACHER, B., and NEVEU, A., 1975, *Phys. Rev. D*, **11**, 3424.
- DIATLOV, I. T., SUDAKOV, V. V., and TER-MARTIROSIAN, K. A., 1957, *Zh. éksp. teor. Fiz.*, **32**, 767 (English translation: 1957, *Soviet Phys. JETP*, **5**, 631).
- DI CASTRO, C., 1972, *Lett. nuovo Cim.*, **5**, 69.
- DIETERICH, W., 1974, *Z. Phys.*, **270**, 239.
- DZYALOSHINSKY, I. E., and KAC, E. I., 1968, *Zh. éksp. teor. Fiz.*, **55**, 338.
- DZYALOSHINSKY, I. E., and LARKIN, A. I., 1971, *Zh. éksp. teor. Fiz.*, **61**, 791; 1973, *Ibid.*, **65**, 411 (English translation: 1974, *Soviet Phys. JETP*, **38**, 202).
- EFEKTOV, K. V., and LARKIN, A. I., 1975, *Zh. éksp. teor. Fiz.*, **69**, 764 (English translation: 1976, *Soviet Phys. JETP*, **42**, 390).
- EMERY, V. J., 1976 a, *Phys. Rev. Lett.*, **37**, 107; 1976 b, *Phys. Rev. B*, **14**, 2989.
- EMERY, V. J., LUTHER, A., and PESCHEL, I., 1976, *Phys. Rev. B*, **13**, 1272.
- EPSTEIN, A. J., ETEMAD, S., GARITO, A. F., and HEEGER, A. J., 1972, *Phys. Rev. B*, **5**, 952.
- EVERTS, H. U., and KOCH, W., 1977, *Z. Phys. B*, **28**, 117.
- EVERTS, H. U., and SCHULZ, H., 1974, *Solid St. Commun.*, **15**, 1413.
- FINKELSTEIN, A. M., 1977, *Pisma Zh. éksp. teor. Fiz.*, **25**, 83.
- FOGEDBY, H. C., 1976, *J. Phys. C*, **9**, 3757.
- FORGÁCS, G., SÓLYOM, J., and ZAWADOWSKI, A., 1978, *Phase Transitions in Condensed Matter*, edited by M. Matyás (Prague: Czechoslovak Academy of Sciences).
- FOWLER, M., 1976, *Solid St. Commun.*, **18**, 241; 1978, *Phys. Rev. B*, **17**, 2989.
- FOWLER, M., and ZAWADOWSKI, A., 1971, *Solid St. Commun.*, **9**, 471.
- FRÖHLICH, H., 1954, *Proc. R. Soc. A*, **223**, 296.
- FUKUYAMA, H., RICE, T. M., VARMA, C. M., and HALPERIN, B. I., 1974 a, *Phys. Rev. B*, **5**, 3775.
- FUKUYAMA, H., RICE, T. M., and VARMA, C. M., 1974 b, *Phys. Rev. Lett.*, **33**, 305.
- GINZBURG, S. L., 1974, *Zh. éksp. teor. Fiz.*, **66**, 647.
- GORKOV, L. P., and DZYALOSHINSKY, I. E., 1973, *Pisma Zh. éksp. teor. Fiz.*, **18**, 686; 1974, *Zh. éksp. teor. Fiz.*, **67**, 397 (English translation: 1975, *Soviet Phys. JETP*, **40**, 198).
- GÖTZE, W., and WÖLFE, P., 1972, *Phys. Rev. B*, **6**, 1226.
- GREST, G. S., 1976, *Phys. Rev. B*, **14**, 5114.
- GREST, G. S., ABRAHAMS, E., CHUI, S.-T., LEE, P. A., and ZAWADOWSKI, A., 1976, *Phys. Rev. B*, **14**, 1225.
- GRINSTEIN, G., MINNHAGEN, P., and ROSENGREN, A., 1978, *Phys. Rev. B*, **18**, 1356.
- GRÜNER, G., and ZAWADOWSKI, A., 1974, *Rep. Prog. Phys.*, **37**, 1497.
- GURGENISHVILI, G. E., NERSESYAN, A. A., and CHOBANYAN, L. A., 1977, *Zh. éksp. teor. Fiz.*, **73**, 279.
- GUTFREUND, H., and HUBERMAN, B. A., 1977, *J. Phys. C*, **10**, L225.
- GUTFREUND, H., and KLEMM, R. A., 1976, *Phys. Rev. B*, **14**, 1073.
- GUTFREUND, H., and SCHICK, M., 1968, *Phys. Rev.*, **168**, 418.
- HAUGE, E. H., and HEMMER, P. C., 1971, *Physica norv.*, **5**, 209.
- HEEGER, A. J., and GARITO, A. F., 1975, *Low-Dimensional Cooperative Phenomena*, edited by H. J. Keller (New York: Plenum Press).
- HEIDENREICH, R., SCHROER, B., SEILER, R., and UHLENBROCK, D., 1975, *Phys. Lett. A*, **54**, 119.
- HOROVITZ, B., 1976, *Solid St. Commun.*, **19**, 1001.
- HOROVITZ, B., GUTFREUND, H., and WEGER, M., 1975, *Phys. Rev. B*, **12**, 3174.
- HOROVITZ, B., WEGER, M., and GUTFREUND, H., 1974, *Phys. Rev. B*, **9**, 1246.
- HUBBARD, J., 1963, *Proc. R. Soc. A*, **276**, 238.
- JÉRÔME, D., and WEGER, M., 1977, *Chemistry and Physics of One-Dimensional Metals*, edited by H. J. Keller (New York: Plenum Press).
- JOHNSON, J. D., KRINSKY, S., and MCCOY, B. M., 1973, *Phys. Rev. A*, **8**, 2526.
- JOSÉ, J. V., KADANOFF, L. P., KIRKPATRICK, S., and NELSON, D. R., 1977, *Phys. Rev. B*, **16**, 1217.
- KAGOSHIMA, S., ISHIGURO, T., and ANZAI, H., 1976, *J. phys. Soc. Japan*, **41**, 2061.
- KELLER, H. J. (editor), 1975, *Low-Dimensional Cooperative Phenomena* (New York: Plenum Press); 1977, *Chemistry and Physics of One-Dimensional Metals* (New York: Plenum Press).
- KIMURA, M., 1973, *Prog. theor. Phys., Osaka*, **49**, 697; 1975, *Ibid.*, **53**, 955.
- KLEMM, R. A., and GUTFREUND, H., 1976, *Phys. Rev. B*, **14**, 1086.
- KLEMM, R. A., and LARKIN, A. I., 1978, (in the press).
- KLEMM, R. A., LEE, P. A., and RICE, T. M., 1977, *Lecture Notes in Physics*, Vol. 65, edited by L. Pál, G. Grüner, A. Jánossy and J. Sólyom (Berlin: Springer-Verlag).
- KNOPS, H. J. F., 1977, *Phys. Rev. Lett.*, **39**, 766.
- KOSTERLITZ, J. M., 1974, *J. Phys. C*, **7**, 1046; 1977, *Ibid.*, **10**, 3753.
- KOSTERLITZ, J. M., and THOULESS, D. J., 1973, *J. Phys. C*, **6**, 1181.
- LEE, P. A., 1975, *Phys. Rev. Lett.*, **34**, 1247.
- LEE, P. A., RICE, T. M., and KLEMM, R. A., 1977, *Phys. Rev. B*, **15**, 2984.
- LEUNG, M. C., 1975, *Phys. Rev. B*, **11**, 4272.
- LIEB, E. H., and WU, F. Y., 1968, *Phys. Rev. Lett.*, **20**, 1445.
- LUKIN, V. P., 1978, *Zh. éksp. teor. Fiz.*, **74**, 1093.

- LUTHER, A., 1976, *Phys. Rev. B*, **14**, 2153; 1977, *Ibid.*, **15**, 403.
 LUTHER, A., and EMERY, V. J., 1974, *Phys. Rev. Lett.*, **33**, 589.
 LUTHER, A., and PESCHEL, I., 1974 a, *Phys. Rev. B*, **9**, 2911; 1974 b, *Phys. Rev. Lett.*, **32**, 992; 1975, *Phys. Rev. B*, **12**, 3908.
 LUTHER, A., and SCALAPINO, D. J., 1977, *Phys. Rev. B*, **16**, 1153.
 LÜTTINGER, J. M., 1963, *J. math. Phys.*, **4**, 1154.
 MATTIS, D. C., 1974 a, *J. math. Phys.*, **15**, 609; 1974 b, *Phys. Rev. Lett.*, **32**, 714.
 MATTIS, D. C., and LIEB, E. H., 1965, *J. math. Phys.*, **6**, 304.
 MENYHÁRD, N., 1977 a, *Solid St. Commun.*, **21**, 495; 1977 b, *Lecture Notes on Physics*, Vol. 65, edited by L. Pál, G. Grüner, A. Jánossy and J. Sólyom (Berlin: Springer-Verlag).
 MENYHÁRD, N., and SÓLYOM, J., 1973, *J. low Temp. Phys.*, **12**, 529; 1975, *Ibid.*, **21**, 431.
 MIGDAL, A. A., 1975, *Zh. éksp. teor. Fiz.*, **69**, 1457.
 MIHÁLY, L., and SÓLYOM, J., 1976, *J. low Temp. Phys.*, **24**, 579.
 MOTT, N. F., and TWOSE, W. D., 1961, *Adv. Phys.*, **10**, 107.
 MÜLLER-HARTMANN, E., and ZITTARTZ, J., 1974, *Phys. Rev. Lett.*, **33**, 893; 1975, *Z. Phys. B*, **22**, 59.
 NOZIÈRES, P., GAVORET, J., and ROULET, B., 1969, *Phys. Rev.*, **178**, 1084.
 OBUKHOV, S. P., 1977, *Zh. éksp. teor. Fiz.*, **72**, 1051.
 OHMI, T., NAKAJIMA, K., and TSUNETO, T., 1976, *Prog. theor. Phys., Osaka*, **55**, 1396.
 PÁL, GRÜNER, G., JÁNOSSY, A., and SÓLYOM, J. (editors), 1977, *Organic Conductors and Semiconductors*, Lecture Notes in Physics Vol. 65 (Berlin: Springer-Verlag).
 PEIERLS, R. E., 1955, *Quantum Theory of Solids* (Oxford: Clarendon Press), p. 108.
 POUGET, J. P., KHANNA, S. K., DENOYER, F., COMES, R., GARITO, A. F., and HEEGER, A. J., 1976, *Phys. Rev. Lett.*, **37**, 437.
 PRIGODIN, V. N., and FIRSOV, Yu. A., 1976, *Zh. éksp. teor. Fiz.*, **71**, 2252; 1977, *Pisma Zh. éksp. teor. Fiz.*, **25**, 90.
 RICE, M. J., and STEÄSSLER, S., 1973 a, *Solid St. Commun.*, **13**, 125; 1973 b, *Ibid.*, **13**, 1389.
 ROULET, B., GAVORET, J., and NOZIÈRES, P., 1969, *Phys. Rev.*, **178**, 1072.
 SCALAPINO, D. J., SEARS, M., and FERRELL, R. A., 1972, *Phys. Rev. B*, **6**, 3409.
 SCHLOTTMANN, P., 1977 a, *Phys. Rev. B*, **15**, 465; 1977 b, *Ibid.*, **16**, 2055.
 SCHROER, B., and TROUNG, T., 1977, *Phys. Rev. D*, **15**, 1684.
 SCHULZ, H., 1977, *Z. Phys. B*, **26**, 377.
 SCHUSTER, H. G. (editor), 1975, *One-Dimensional Conductors*, Lecture Notes in Physics Vol. 34 (Berlin: Springer-Verlag).
 SÓLYOM, J., 1973, *J. low Temp. Phys.*, **12**, 547; 1974, *J. Phys. F*, **4**, 2269; 1975, *Solid St. Commun.*, **17**, 63.
 SÓLYOM, J., and SZABÓ, G., 1977, *Lecture Notes on Physics*, Vol. 65, edited by L. Pál, G. Grüner, A. Jánossy and J. Sólyom (Berlin: Springer-Verlag).
 SÓLYOM, J., and ZAWADOWSKI, A., 1974, *J. Phys. F*, **4**, 80.
 STOECKLY, B., and SCALAPINO, D. J., 1975, *Phys. Rev. B*, **11**, 205.
 SUZUMURA, Y., and FUKUYAMA, H., 1978, *J. low Temp. Phys.*, **31**, 273.
 SUZUMURA, Y., and KURIHARA, Y., 1975, *Prog. theor. Phys., Osaka*, **53**, 1233.
 THEUMANN, A., 1967, *J. math. Phys.*, **8**, 2460; 1977, *Phys. Rev. B*, **15**, 4524.
 TING, C. S., 1976, *Phys. Rev. B*, **13**, 4029.
 TOMONAGA, S., 1950, *Prog. theor. Phys., Osaka*, **5**, 349.
 TORRANCE, J. B., SCOTT, B. A., and KAUFMAN, F. B., 1975, *Solid St. Commun.*, **17**, 1369.
 TORRANCE, J. B., TOMKIEWICZ, Y., and SILVERMAN, B. D., 1977, *Phys. Rev. B*, **15**, 4738.
 VILLAIN, J., 1975, *J. Phys., Paris*, **36**, 581.
 WEGNER, F., 1967, *Z. Phys.*, **206**, 465.
 WIEGMANN, P. B., 1978, *J. Phys. C*, **11**, 1583.
 WILSON, K. G., 1975, *Rev. mod. Phys.*, **47**, 773.
 WILSON, K. G., and KOGUT, J., 1974, *Physics Lett. C*, **12**, 75.
 ZITTARTZ, J., 1976 a, *Z. Phys. B*, **23**, 55; 1976 b, *Ibid.*, **23**, 63; 1978, *Z. Phys. B*, **31**, 63.
 ZITTARTZ, J., and HUBERMAN, B. A., 1976, *Solid St. Commun.*, **18**, 1373.